(12) LEVEL II

DTNSRDC/SPD-0833-02

DAVID W. TAYLOR NAVAL SHIP RESEARCH AND DEVELOPMENT CENTER

Bethesda, Md. 20084

ADA087069

ANALYSIS OF WAKE SURVEY AND BOUNDARY LAYER MEASUREMENTS FOR THE R/V ATHENA REPRESENTED BY MODEL 5366 IN THE ANECHOIC WIND TUNNEL

BY

RAE B. HURWITZ
AND
DOUGLAS S. JENKINS

APPROVED FOR PUBLIC RELEASE: DISTRIBUTION UNLIMITED

SHIP PERFORMANCE DEPARTMENT REPORT

ANALYSIS OF WAKE SURVEY AND BOUNDARY LAYER MEASUREMENTS FOR THE R/V ATHENA REPRESENTED BY MODEL 5366 IN THE ANECHOIC WIND TUNNEL

JULY 1980 DTNSRDC/SPD-0833-02

MAJOR DTNSRDC ORGANIZATIONAL COMPONENTS

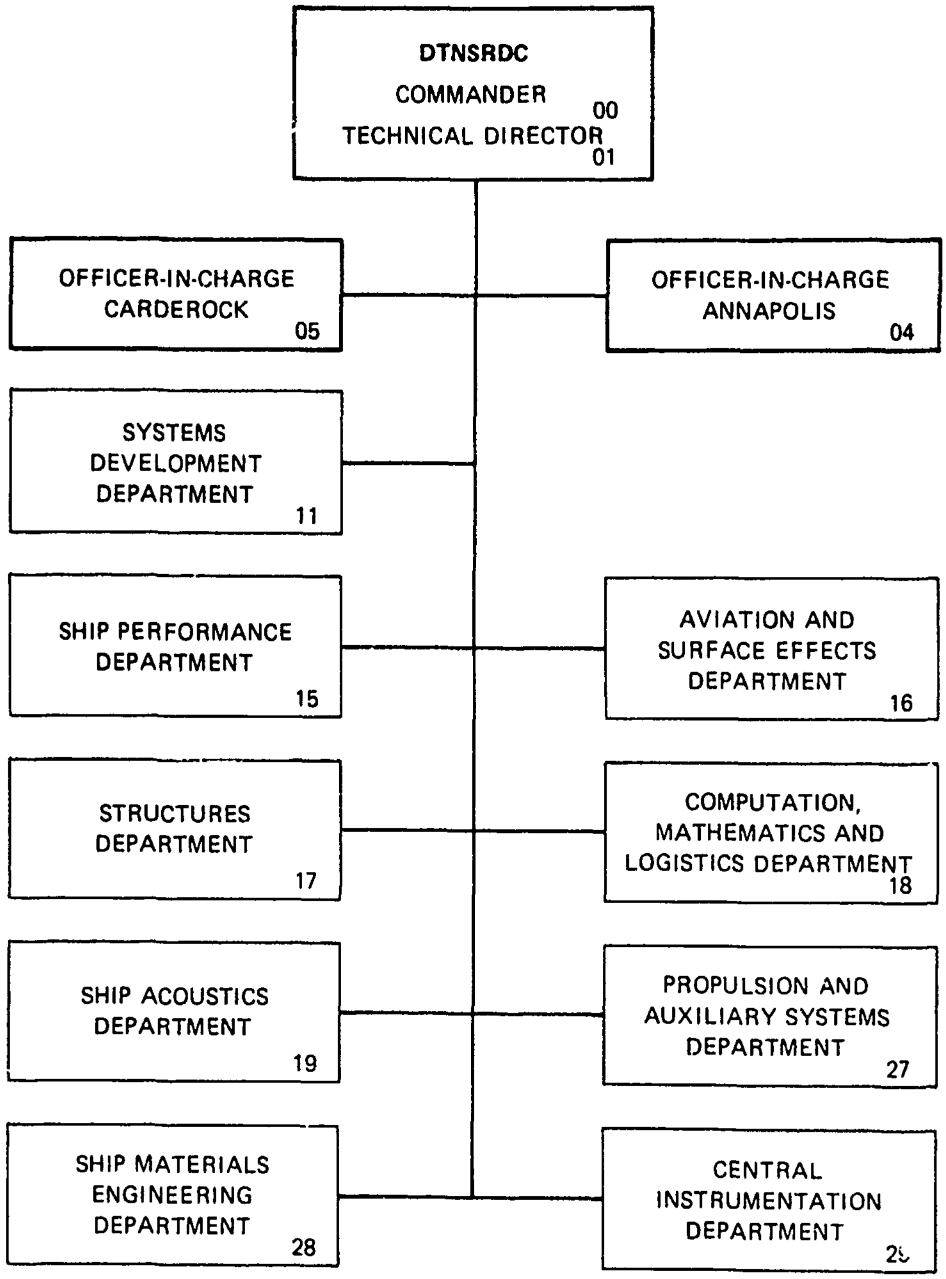

UNCLASSIFIED

SECURITY CLASSIFICATION OF THIS PAGE (When Data Entered)

REPORT DOCUMENTATION PAGE

READ INSTRUCTIONS BEFORE COMPLETING FORM

1. REPORT NUMBER: (14) DTNSRDC/SPD-0833-02

2. GOVT ACCESSION NO.: AD-A087 069

3. RECIPIENT'S CATALOG NUMBER

4. TITLE (and Subtitle): (6) ANALYSIS OF WAKE SURVEY AND BOUNDARY LAYER MEASUREMENTS FOR THE R/V ATHENA REPRESENTED BY MODEL 5366 IN THE ANECHOIC WIND TUNNEL,

5. TYPE OF REPORT & PERIOD COVERED: (9) FINAL rept.,

6. PERFORMING ORG. REPORT NUMBER

7. AUTHOR(s): (10) RAE B./HURWITZ ~~AND~~ DOUGLAS S./JENKINS

8. CONTRACT OR GRANT NUMBER(s): (11) Jul 80

9. PERFORMING ORGANIZATION NAME AND ADDRESS

DAVID W. TAYLOR NAVAL SHIP R&D CENTER
SHIP PERFORMANCE DEPARTMENT
BETHESDA, MARYLAND 20084

10. PROGRAM ELEMENT, PROJECT, TASK AREA & WORK UNIT NUMBERS

Program Element 63508N
Task Area S0379001 Task 19977
Work Unit 1524-641

11. CONTROLLING OFFICE NAME AND ADDRESS

NAVAL SEA SYSTEMS COMMAND (NAVSEA 05R)
WASHINGTON, D. C. 20362

12. REPORT DATE: JULY 1980

13. NUMBER OF PAGES: 78 + xii

14. MONITORING AGENCY NAME & ADDRESS (if different from Controlling Office)

15. SECURITY CLASS. (of this report): UNCLASSIFIED

15a. DECLASSIFICATION/DOWNGRADING SCHEDULE

16. DISTRIBUTION STATEMENT (of this Report)

APPROVED FOR PUBLIC RELEASE: DISTRIBUTION UNLIMITED

17. DISTRIBUTION STATEMENT (of the abstract entered in Block 20, if different from Report)

(12) 93 (16) S0379 (17) S0379001

18. SUPPLEMENTARY NOTES

19. KEY WORDS (Continue on reverse side if necessary and identify by block number)

WAKE SURVEY
BOUNDARY LAYER
WIND TUNNEL
MODEL EXPERIMENTS

20. ABSTRACT (Continue on reverse side if necessary and identify by block number)

The results of wake survey and boundary layer profile measurements ~~are~~ presented for a model representing a twin-screw displacement ship. These measurements were obtained in a wind tunnel using hot wire anemometers. Wake surveys were conducted in the propeller disk and ahead of the propeller plane with and without the propeller operating. Circumferential distributions of the longitudinal, tangential, and radial velocity components at four radial locations and a harmonic analysis of each component are included. The boundary layer profile measurements were obtained at three

DD FORM 1 JAN 73 1473 EDITION OF 1 NOV 65 IS OBSOLETE
S/N 0102-LF-014-6601

Unclassified

SECURITY CLASSIFICATION OF THIS PAGE (When Data Entered)

389694

20.
longitudinal locations in the area of the shafting and struts. A comparison of full-scale, model-scale towing tank, and wind tunnel measurements is presented. Model-scale boundary layer velocity profiles ahead and astern of the propeller plane were smaller than the full-scale profiles. The model wake surveys ahead of the propeller plane showed no significant differences with and without the propeller operating. The data from the wind tunnel wake survey in the propeller plane agreed better with the full-scale data than the towing tank data.

TABLE OF CONTENTS

LIST OF FIGURES

LIST OF FIGURES (continued

LIST OF FIGURES (continued)

LIST OF FIGURES (continued)

Page

LIST OF TABLES

NOTATION

CONVENTIONAL SYMBOL	SYMBOL APPEARING ON PLOTS	DEFINITION
A_N	COS COEF	The cosine coefficient of the $N^{\underline{th}}$ harmonic*
B_N	SIN COEF	The sine coefficient of the $N^{\underline{th}}$ harmonic*
D	---	Propeller diameter
J_V	---	Apparent advance coefficient $J_V = \frac{V}{nD}$ (dimensionless)
L_{WL}		Waterline length
N	N	Harmonic number
n	---	Propeller revolutions
R_n	---	Reynolds number based on length
r/R or x **	Radius or RAD.	Distance (r) from the propeller axis expressed as a ratio of the propeller radius (R)
V	V	Actual model or ship velocity
$V_b(x,\theta)$	---	Resultant inflow velocity to blade for a given point
$\bar{V}_b(x)$	---	Mean resultant inflow velocity to blade for a given radius
$V_r(x,\theta)$	VR	Radial component of the fluid velocity for a given point (positive toward the shaft centerline)
$\bar{V}_r(x)$	---	Mean radial velocity component for a given radius
$V_r(x,\theta)/V$	VR/V	Radial velocity component ratio for a given point
$\bar{V}_r(x)/V$	VRBAR	Mean radial velocity component ratio for a given radius
$V_t(x,\theta)$	VT	Tangential component of the fluid velocity for a given point (positive in a counterclockwise direction looking forward)

*See footnote on the following page

**See footnote on the following page

NOTATION (Continued)

$\bar{V}_t(x)$	---	Mean tangential velocity component for a given radius
$V_t(x,\theta)/V$	VT/V	Tangential velocity component ratio for a given point
$\bar{V}_t(x)/V$	VTBAR	Mean tangential velocity component ratio for a given radius
$(\tilde{V}_t(x)/V)_N$	AMPLITUDE	Amplitude (B_N for single screw symmetric; C_N otherwise) of Nth harmonic of the tangential velocity component ratio for a given radius*
$V_x(x,\theta)$	VX	Longitudinal (normal to the plane of survey) component of the fluid velocity for a given point (positive in the astern direction)
$\bar{V}_x(x)$	---	Mean longitudinal velocity component for a given radius
$V_x(x,\theta)/V$	VX/V	Longitudinal velocity component ratio for a given point
$\bar{V}_x(x)/V$	VXBAR	Mean longitudinal velocity component ratio for a given radius
$(\tilde{V}_x(x)/V)_N$	AMPLITUDE	Amplitude (A_N for single screw symmetric; C_N otherwise) of Nth harmonic of the longitudinal velocity component ratio for a given radius*
x/L_{WL}		Longitudinal position aft of forward perpendicular
ϕ_N	PHASE ANGLE	Phase angle of Nth harmonic*

*The harmonic amplitudes of any circumferential velocity distribution f (θ) are the coefficients of the Fourier Series:

$$f(\theta) = A_o + \sum_{N=1}^{N} A_N \cos(N\theta) + \sum_{N=1}^{N} B_N \sin(N\theta)$$

$$= A_o + \sum_{N=1}^{N} C_N \sin(N\theta + \phi_N)$$

**To avoid confusion it should be noted that subscript x refers to longitudinal component, whereas x as a parameter is used to define a distance (radial or longitudinal).

$1-w(x)$ — 1-WX — Volumetric mean velocity ratio from the hub to a given radius

$$1-w(r/R) = \left[\frac{2 \cdot \int_{r_{hub}/R}^{r/R} (\overline{V}_{x_c}(x)/V) \cdot x \cdot dx}{(r/R)^2 - (r_{hub}/R)^2} \right]$$

where $$\overline{V}_{x_c}(x)/V = \int_0^{2\pi} \left[\frac{V_{x_c}(x,\theta)}{2\,\pi\,V} \right] d\theta$$

and $$V_{x_c}(x,\theta)/V = (V_x(x,\theta)/V) - (V_t(x,\theta)/V) \tan(\beta(x,\theta))$$

$1-w_V(x)$ — 1-WVX — Volumetric mean velocity ratio from the hub to a given radius (without the tangential velocity correction)

$$1-w(r/R) = \left[\frac{2 \cdot \int_{r_{hub}/R}^{r/R} (\overline{V}_x(x)/V) \cdot x \cdot dx}{(r/R)^2 - (r_{hub}/R)^2} \right]$$

$\beta(x,\theta)$ — --- — Advance angle in degrees for a given point

$\overline{\beta}(x)$ — BBAR — Mean advance angle in degrees for a given radius

$+\Delta\beta$ — BPOS — Variation of the maximum advance angle from the mean for a given radius

NOTATION (Continued)

$-\Delta\beta$	BNEG	Variation of the minimum advance angle from the mean for a given radius
θ	Angle in Degrees	Position angle (angular coordinate) in degrees
ν		Kinematic viscosity of fluid medium

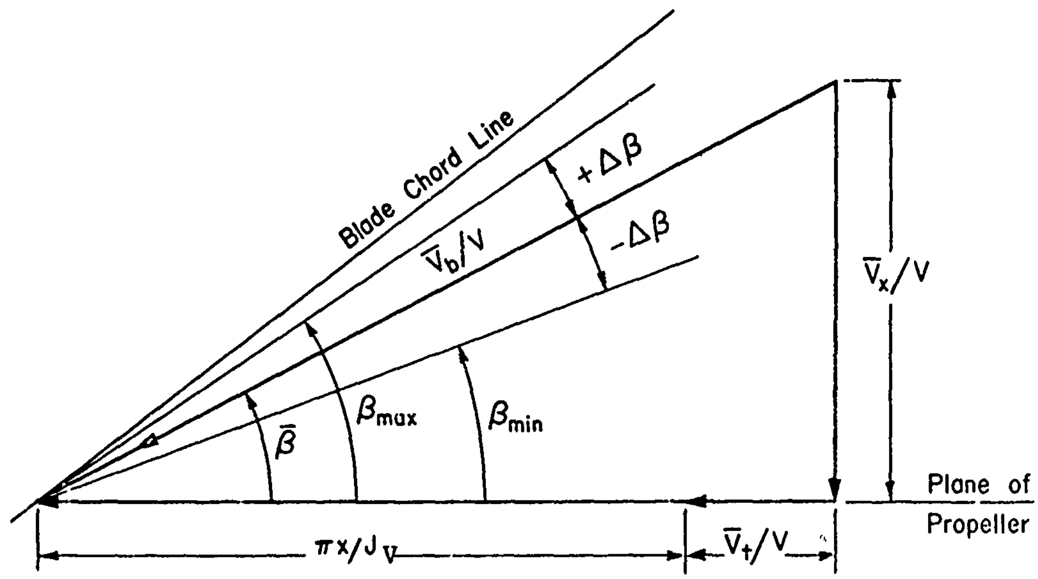

VELOCITY DIAGRAM OF BETA ANGLES

ENGLISH/SI EQUIVALENTS

ENGLISH	SI
1 inch	25.400 millimeter [0.0254 m (meter)]
1 foot	0.3048 m (meter)
1 foot per second	0.3048 m/s (meter per second)
1 knot	0.5144 m/s (meter per second)
1 pound (force)	4.4480 N (Newtons)
1 degree (angle)	0.01745 rad (radians)
1 horsepower	0.7457 kW (kilowatts)
1 long ton	1.016 tonnes, 1.016 metric tons, or 1016 kilograms
1 inch Water (60°F)	248.8 pa (pascals)

ABSTRACT

The results of wake survey and boundary layer profile measurements are presented for a model representing a twin-screw displacement ship. These measurements were obtained in a wind tunnel using hot wire anemometers. Wake surveys were conducted in the propeller disk and ahead of the propeller plane with and without the propeller operating. Circumferential distributions of the longitudinal, tangential, and radial velocity components at four radial locations and a harmonic analysis of each component are included. The boundary layer profile measurements were obtained at three longitudinal locations in the area of the shafting and struts. A comparison of full-scale, model-scale towing tank, and wind tunnel measurements is presented. Model-scale boundary layer velocity profiles ahead and astern of the propeller plane were smaller than the full-scale profiles. The model wake surveys ahead of the propeller plane showed no significant differences with and without the propeller operating. The data from the wind tunnel wake survey in the propeller plane agreed better with the full-scale data than the towing tank data.

ADMINISTRATIVE INFORMATION

Model experiments were performed under the Controllable Pitch Propeller Research Program sponsored by the Naval Sea Systems Command (NAVSEA 05R) and administered by the David W. Taylor Naval Ship R&D Center (DTNSRDC). The project was funded under DTNSRDC Task Area S0379001 and Work Unit 1-1524-641.

INTRODUCTION

As part of the Controllable Pitch Propeller Research Program, the DTNSRDC conducted full-scale wake and boundary layer velocity profile measurements on the high speed transom stern ship, R/V ATHENA. Project goals were to obtain propeller disk velocity component ratios in the wake of a full-scale ship and to determine the effects of propeller induction on the development of the boundary layer. The full-scale wake measurements consisted of the longitudinal, tangential, and radial velocity component ratios ahead of and in the propeller plane. The full-scale boundary layer profile

was obtained at three longitudinal locations in the area of the shafts and struts with and without the propeller operating.

A series of model experiments was instituted to identify the differences between model- and full-scale wake data which would affect the operation of controllable-reversible pitch propellers. Model-scale boundary layer measurements were made to estimate the effects of the hull on the wake distribution.

In an effort to correlate the results of the full-scale measurements, experiments were conducted in the towing tank and wind tunnel at DTNSRDC. Wake survey experiments in the plane of the propeller were conducted in the towing tank with a 1-to-8.25 scale model using five-hole spherical head pitot tubes. Model-scale boundary layer profile measurements and wake surveys in and ahead of the propeller plane were conducted in the Anechoic Flow Facility (AFF) with a 1-to-8.25 scale double model. The double model was constructed so that the effect of the dynamic trim of the ship at 15 knots on the wake could be represented. Although the double model does not allow the effects of the free surface to be accounted for, it does account for the angle of the shafting, including the effects of dynamic trim, to the undisturbed flow. The angle of the shafting to the free stream contributes significantly to the tangential and radial velocity components.

The results of the wake surveys and boundary layer measurements obtained on the double model are reported herein. Full-scale and towing tank data are presented as comparisons with the wind tunnel wake survey and boundary layer measurements. Harmonic analyses of the circumferential distributions of the velocity component ratios obtained from the wind tunnel wake surveys were performed and are reported herein. The results of the towing tank wake surveys will be presented in a separate report.

DESCRIPTION OF EXPERIMENTS

The experimental program reported herein consisted of model-scale boundary layer and wake survey experiments in the Anechoic Flow Facility. The Anechoic Flow Facility enabled measurements to be obtained at model-scale Reynolds numbers with and without the propeller operating. A description and aerodynamic calibration of the Anechoic Flow Facility is given by Brownell[1] and Bowers[2].

Five experiments were performed on a double model in the Anechoic Flow Facility using hot wire anemometers. Table 1 summarizes the experimental program. Experiment 1 consisted of boundary layer profile measurements at six locations on the model corresponding to the locations of the full-scale boundary layer measurements on the R/V ATHENA. Experiments 2 and 3 consisted of velocity measurements of the flow ahead of the propeller plane with and without the propeller operating. These two experiments were designed to measure the effect of the operating propeller on the flow ahead of the propeller disk. Measurements were obtained at the same non-dimensional axial location as those from the full-scale wake survey at the forward rake location, $x/L_{WL} = 0.906$. Experiments 2 and 3 are referred to as the transverse wake surveys. Data were collected in a rectangular grid perpendicular to the waterplane of the model. The hot wire probe was moved in a horizontal direction at various vertical distances above and below the propeller shaft centerline. The results from Experiments 1, 2, and 3 were correlated with the data from the full-scale wake survey.

[1] References are listed on page 17 .

Experiment 4 consisted of measurements of the velocity defect in the propeller plane due to the main vee struts. These measurements were obtained in a rectangular grid perpendicular to the waterplane of the model.

The "rotational" wake survey, Experiment 5, was performed in the propeller plane by rotating the hot wire anemometer to various circumferential positions at four radii from the shaft centerline. The radii at which the measurements were made corresponded exactly to the full-scale and towing tank wake survey radii, allowing a direct one-to-one comparison of the data. These radii were expressed as ratios of the local radius to the propeller radius (r/R). A motor-driven unit which positions the hot wire anemometer at discrete circumferential positions for a particular radial setting was mounted behind the model, with its axis of rotation in line with the propeller shaft.

DESCRIPTION OF EXPERIMENTAL APPARATUS

The wind tunnel experiments were conducted with Model 5366 and Propeller 4712. Model 5366 is a double model of the twin-screw displacement ship, R/V ATHENA. The double model was constructed of fiberglass to a linear ratio of 8.25 with identical top and bottom hulls. The two halves were joined together at a trimmed waterline corresponding to a ship speed of 15 knots. The model was appended with roll fins, shafting, struts, and a centerline skeg. Figure 1 shows model- and full-scale principal dimensions for the R/V ATHENA.

Propeller 4712, a geosim of the R/V ATHENA design propellers, had a stainless steel hub and fiberglass blades. Although the R/V ATHENA was fitted with controllable-reversible pitch propellers, the blades of Propeller 4712 were set at the design pitch. The propeller, propeller

shafting, and its bearings were designed to operate at a rotational rate of 20,000 revolutions per minute and a wind tunnel speed of 61 meters per second. The design of Propeller 4712 is shown in Figure 2 along with Propellers 4710 and 4711 which were used in the towing tank experiments.

Commercially available one-component and three-component hot wire anemometer probes were used to obtain all of the flow measurements in the wind tunnel. The one-component probes measured the boundary layer profiles (Experiment 1), and the three-component probes obtained the wake measurements (Experiments 2 through 5). The one-component probe had a single-sensor wire 1.25 mm in length and 5 μm in diameter held perpendicular to the free stream velocity. The three-component probe had 3 mutually perpendicular wire sensors located within a 3 mm diameter sphere. Each wire sensor was 1.25 mm in length and 5 μm in diameter at an angle of 54.7 degrees to the free stream.

Hot wire probes were probably the best measuring device to use because of their small size and fast response time. Compared to spherical head pitot tubes normally used for wake surveys at DTNSRDC, hot wire probes were more than three times smaller in diameter. The smaller size offered less interference to the local flow. The fast response time allowed a larger quantity of data samples. The pitot tube has a slower response time and smaller sampling rate, and rapid fluctuations in the velocity are not discernable. In addition, the size of the spherical head does not allow the measurement of high velocity gradients which can be measured by the smaller hot wire probes.

The small size of the hot wire probes makes them very susceptable to breakage caused by particles in the fluid medium or by physical mis-

handling. In addition, output voltages are very sensitive to free stream air temperature changes greater than 2.7 degrees Centigrade. Before and after free stream calibrations and constant temperature monitoring were required during each experiment due to this sensitivity. Free stream calibrations were performed at least every three hours. Temperature corrections were applied to the output voltages of the sensors based on these calibrations.

The physical size of the hot wire probe enabled the measurements of boundary layer velocity profiles and the wake ahead of an operating propeller. Scragg and Sandell[3] have shown that hot wire anemometers are at least as accurate as five-hole pitot tubes. The boundary layer measurements were repeatable within $\pm$ 2 percentage points of the free stream velocity. The wake measurements ahead of and in the propeller plane varied within $\pm$ 2-to-5 percentage points for the longitudinal velocity component ratio, $(V_x(x,\theta)/V)$. For wake surveys conducted in the deep water basin at DTNSRDC, the longitudinal velocity component ratios are repeatable within $\pm$ 1 percent, except in areas of high velocity gradients.[4] In these areas, such as behind the shaft struts or at the innermost radii, the five-hole pitot tube has much lower accuracy. In the areas of high velocity gradients, hot wire probes may be an order of magnitude more accurate than the five-hole pitot tubes.

Figure 3 shows the locations where measurements were taken to determine velocities in the boundary layer of the R/V ATHENA and Model 5366. Transverse wake survey and strut wake measurements were taken at the locations presented in Figure 4. The nondimensional radii at which the measurements were made for the rotational wake surveys are shown in Figure 5 and listed in Table 1.

The model was mounted on its side for the boundary layer and rotational wake survey experiments as shown in Figure 6. Figure 7 shows the double model mounted in the horizontal waterplane configuration which was used for the transverse wake surveys and the strut wake measurements.

The boundary layer profile measurements were obtained using a single-sensor hot wire probe. This probe was moved in a horizontal direction by a remotely controlled rack and pinion drive system. This system included a stepping motor having a resolution of 0.02 mm, and was mounted on a vertical strut location in the free stream. The stepping motor was encased in a streamlined piece of aluminum to reduce flow interference. A support arm was attached to the vertical strut and the lower (starboard) shaft tube in order to minimize the relative motion between the double model and the vertical strut. Figures 8 through 10 show the experimental arrangement designed for these experiments. The single-sensor is shown in Figure 11 with a scale in the background.

Two sets of experiments, Experiments 2, 3, and 5, were performed using triple-sensor hot wire probes shown in Figures 12 and 13. The transverse wake survey consisted of measurements of the wake ahead of the propeller plane with and without the propeller operating. Also, measurements of the wake behind the struts were made. Figure 12 presents the experimental set-up for these transverse measurements. The rotational wake survey was conducted in the propeller disk at four radial locations using the motor-drive unit mentioned previously. This motor had a variable rotational speed and an internal triggering system. Measurements were obtained at 128 circumferential locations. Figure 14 shows the experimental set-up for the rotational wake survey.

PRESENTATION AND DISCUSSION OF RESULTS

BOUNDARY LAYER EXPERIMENTS

The boundary layer profile measurements on Model 5366 were obtained at a Reynolds number of 1.68×10^7, based on waterline length, in the wind tunnel at six of the eight locations noted in Figure 3. Measurements, with and without tne propeller operating, were obtained to study the effects of propeller action on the boundary layer. Measurements were made at Locations 1, 2 and 3 without an operating propeller, and at Locations 8, 6, and 7 with the propeller operating. No measurements were taken at Locations 4 and 5 because of the expected similarity with the velocity profiles at Locations 3 and 7, respectively. The full-scale boundary layer measurements, which are presented in this report, were measured at a speed which corresponds to a Reynolds number of 4.10×10^8.

Model-scale boundary layer profiles with and without the propeller operating, are plotted against the full-scale data at the corresponding locations in Figures 15, 16, and 17. These data show the effect of the propeller on the velocity profiles for both scales. The results at Locations 1 and 8 showed a small increase in the velocity profile due to the propeller for both model- and ship-scale. However, at Locations 3 and 7, behind the propeller plane, the velocity defect in the boundary layer was greater due to the operating propeller for both model and ship. For measurements at Locations 2 and 6 for the wind tunnel model, there was no noticeable difference in the data with or without the propeller operating. There were no full-scale measurements at Location 6, shown in Figure 16, due to the failure of that boundary layer probe. A comparison of the boundary layer velocity profiles presented in these figures showed that the model-scale profile is not as fully developed as the full-scale profile at

Locations 1 and 3. This was clearly a consequence of the one decade difference in Reynolds number between model and ship. However, at Location 2, the model- and full-scale profiles were quite similar. Neither profile reached the free stream velocity within the expected range. Further analysis indicated that there were no obvious errors in the collection of the model data. Additional velocity profile measurements were conducted on the model at several positions near Location 2. No unusual flow characteristics were observed and there is still no explanation for this anomaly. The possibility still exists for the full-scale measurements to be in error.

TRANSVERSE WAKE SURVEY EXPERIMENTS

Two wake surveys were conducted to measure the magnitude and direction of the flow forward of the propeller disk. Experiment 2 was performed with the propeller operating and Experiment 3 was conducted without the propeller operating. Measurements were taken at 1.11 propeller diameters forward of the propeller plane, $x/L_{WL} = 0.906$, corresponding to the forward rake location on the R/V ATHENA. Both experiments were performed in the wind tunnel at 38.1 m/s corresponding to a Reynolds number of 1.40×10^7. Measurements were taken at six equally spaced heights of 25.4 millimeters above and below the shaft centerline. The vertical strut, shown in Figure 12, positioned the hot wire probe enabling measurements to be taken at increments of 18 millimeters.

Velocity component ratios from conventional wake surveys done in the towing tank at DTNSRDC are obtained radially and circumferentially in the propeller plane. The wind tunnel data from Experiments 2 and 3 were obtained in a rectangular grid perpendicular to the free stream velocity of the wind tunnel. Computer programs were developed to present the data in a cylindrical coordinate system, which is the coordinate system used in

conventional wake surveys as described by Hadler and Cheng.[5] The longitudinal axis of this system was parallel to the propeller shaft centerline. Once transformed, the data were interpolated to the nondimensional radii corresponding to the full-scale radii at the forward rake location, $x/L_{WL} = 0.906$. The radius ratios of these measurements were 0.417, 0.583, 0.750, 0.917 and 1.083 as listed in Table 1.

The results of the wake survey measurements on the R/V ATHENA and Model 5366 with an operating propeller (Experiment 2) are presented in Figures 18 through 22. The model-scale longitudinal velocity component ratios were three to eight percent lower than the full-scale values. At the two inner radii, 0.417 and 0.583, the full-scale tangential and radial velocity component ratios were slightly lower than the model-scale data between 0 and 180 degrees. There was good agreement with the radial velocity component ratios at the two outer radii, 0.917 and 1.083 from 0 to 180 degrees.

Full-scale data taken on the starboard side as reported by Reed and Day[6] are presented in Figures 23 through 27 along with the model data from Experiment 3. These measurements were obtained forward of the propeller plane without an operating propeller. The full-scale longitudinal velocity component ratios were five-to-ten percent higher than the model-scale. A large degree of scatter was observed in the full-scale longitudinal velocity component ratios. The full-scale tangential velocity component ratios were higher than those for Model 5366 between the angles of 180 and 360 degrees. The full-scale radial velocity component ratios were lower than the model-scale values.

The wake survey data from Experiments 2 and 3 are presented in Appendix A for all radii. Figures showing the effect of the propeller suction on each of the three velocity component ratios for each radius at model-scale, i.e., with and without a propeller turning, are also included in Appendix A.

A harmonic analysis of the circumferential distribution of the longitudinal and tangential velocities was performed. A diagram showing the relationship between the longitudinal and tangential velocity vectors, the advance coefficients and the advance angles is presented on page xii. The mean longitudinal $(\overline{V}_x(x)/V)$, tangential $(\overline{V}_t(x)/V)$, and radial $(\overline{V}_r(x)/V)$ velocity component ratios, and volumetric mean wake velocity ratio $(1-w(x))$ are presented in Appendix A for Experiments 2 and 3. These quantities, except for the radial velocity component ratio, are shown graphically in this appendix. The calculated mean values of the advance angle $(\overline{\beta}(x))$, and the maximum variations thereof, $(+\Delta\beta)$ and $(-\Delta\beta)$, are given graphically and in tabular form in Appendix A. The advance angles were calculated using an advance coefficient, J_V, of 0.739. The harmonic analyses of the circumferential distribution of the longitudinal and tangential velocity component ratios at the experimental and interpolated radii are presented in Appendix A for Experiments 2 and 3.

Wake survey measurements were made on the port side of the double model for Experiments 2 and 3. No significant differences of the velocity component ratios of these two experiments were observed. The small variations shown in Figures A-1 through A-8 were due to the limitations of the numerical interpolation. No model data was available from 260 to 360 degrees because the experimental set-up limited the position of the hot wires

to the outside of the propeller shafting. Consequently, when the data for Experiment 3 was transposed to the starboard side, there was no model data between 0 and 100 degrees. This transposition was required to compare the wind tunnel model data to the full-scale data which was available only on the starboard side of the R/V ATHENA.

A study of the full- and model-scale velocity component ratios presented shows that the data agreement is acceptable. Comparison of the data from the wind tunnel transverse wake surveys reveals that there is little significant difference between measurements made ahead of the propeller plane with and without an operating propeller. Differences in the wake with and without the propeller operating are within experimental accuracy. From these wake survey experiments, the effect of an operating propeller is not measurable at 1.11 diameters forward of the propeller disk.

ROTATIONAL WAKE SURVEY EXPERIMENT

Model-scale wake surveys were performed in the wind tunnel to correlate the data obtained from the full-scale and model-scale towing tank experiments. The wake survey experiment in the towing tank was performed by towing the model at the Froude-scaled speed of the ship. The wind tunnel rotational wake survey was conducted on the double model in the propeller plane at a Reynolds number corresponding to the Froude-scale speed of the towing tank experiment, $R_n = 1.56 \times 10^7$. Measurements made at the same nondimensional radii as used for wake surveys on the R/V ATHENA and the towing tank model, Model 5365, were 0.456, 0.633, 0.781 and 0.963 as listed in Table 1. The results of this wind tunnel experiment are presented in Appendix B for the experimental radii. A harmonic

analysis was performed on the longitudinal and tangential velocity component ratios. The advance angles were calculated using an advance coefficient, J_V, of 0.739. Circumferential mean velocity component ratios, volumetric mean velocities and the advance angles are presented graphically and in tabular form in Appendix B. The harmonic content of the circumferential distribution of the longitudinal and tangential velocity component ratios at the experimental and interpolated radii is presented also in Appendix B.

The data from the wake surveys in the towing tank and wind tunnel are shown in Figures 28 through 31 along with the full-scale data. The velocity component ratios presented in these figures showed that the degree of scatter of the full-scale data was higher than that of the data from the two model experiments. The rotational wake survey data obtained in the wind tunnel showed very little scatter when compared to the towing tank data. The longitudinal velocity component ratios of the wind tunnel Model 5366 were 5-to-10 percent lower than those of the towing tank Model 5365. The tangential velocity component ratios for Model 5366 at radius ratios of 0.456 and 0.781 were 2-to-5 percent higher than those for Model 5365 from 0 to 360 degrees. The radial velocity component ratios of Model 5366 were 2-to-8 percent higher than Model 5365 from 180 to 360 degrees for all four radii. The tangential and radial velocity component ratios for radius ratios of 0.633 and 0.963, were similar at angles between 0 and 180 degrees.

The results from model wake experiments in the wind tunnel and in the towing tank indicated significant differences. The greatest variation in the data was ten percent in the longitudinal velocity component ratio

for the innermost radius. The large values of the towing tank data, which were consistent with other R/V ATHENA model experiments, may be due to the inability of the pitot tube to measure velocities at large flow angles.

At the outer radii, the longitudinal velocity component ratios for the ship were 1-to-2 percent lower than those for the model in the wind tunnel. The peaks of the radial and tangential velocity component ratios at the outer radii were 8-to-10 percent higher for the ship than for the double model. At the two innermost radii, the shift in the radial and tangential velocity component ratios indicated that there was a stronger upflow on the ship than the model, in the region under and outboard of the propeller hub.

Comparison of the full-scale and wind tunnel model wake revealed differences up to 10 percent. The full-scale data showed the largest scatter and the greater deviation from the model-scale wake.

STRUT WAKE EXPERIMENT

The transverse wake survey experimental set-up also enabled measurements to be taken behind the struts with an operating propeller. The purpose of this experiment was to numerically determine the velocity decrement due to the struts with an operating propeller. Finely spaced measurements were taken transversely behind the struts. Measurements were made between the shafting and the hull surface at 57, 76, and 95 millimeters from the shaft centerline. Figure 32 presents the results of this experiment.

For the measurements obtained at 57 millimeters from the shaft centerline, a 5-to-10 percent variation in the longitudinal velocity components was seen in the area immediately behind the struts. This

variation was not observed at the other two locations from the shaft centerline. At the two innermost radii of the rotational wake survey, the longitudinal velocity components showed a 10 percent velocity defect which was consistent with the results from the strut wake experiment.

CONCLUSIONS

Model-scale boundary layer velocity profiles obtained one propeller diameter ahead (Locations 1 and 8) and astern (Locations 3 and 7) of the propeller plane, were 2-to-10 percent smaller than the full-scale profiles. This difference was caused by the one decade reduction of the model-scale Reynolds number, as compared to the full-scale Reynolds number.

However, in the area where the shaft bossing pierced the hull, the model- and full-scale boundary layer profiles coincided. Further investigation on the model-scale data yielded no unusual flow phenomena in this area. It is recommended that additional experiments be conducted to understand this phenomena.

The propeller caused a 1 percent increase in velocity in both the model- and full-scale boundary layers at Locations 1 and 8, one propeller diameter ahead of the disk. At Locations 2 and 6, where the shaft bossing pierced the hull, there was no measurable difference in the data obtained with or without the propeller operating.

Wake survey experiments ahead of the propeller plane were intended to provide a comparison of velocity components with and without the propeller operating. When the scatter in values is taken into consideration, it is not possible to discern any significant difference between the two sets of data. Wake measurements ahead of the propeller plane without the propeller operating showed only a 1 percent radial decrease in the volumetric mean wake as compared to measurements made with the operating propeller.

Behind the struts in the propeller plane, at a r/R of 0.287, a ten percent velocity defect in the longitudinal component was seen when compared to free stream velocity. This agreed well with the results from the rotational wake survey and also the towing tank wake surveys at a similar radius.

Experiment 5, the wake survey conducted in the propeller disk, was performed at the same Reynolds number as those experiments done in the towing tank. The longitudinal velocity components from the wind tunnel experiments agreed better with the full-scale data than with the towing tank data. As mentioned by Reed and Day,[6] the discrepancy between the towing tank and full-scale data may be due to the difference in attitude between the ship and model. The wind tunnel double model was constructed to take into account the dynamic trim of the full-scale ship, so that an error in attitude is unlikely.

Overall, the longitudinal velocity component ratios obtained in the wind tunnel correlated better with the full-scale data at the inner radii. The tangential and radial velocity component ratios were generally higher for Model 5366 than for the towing tank data. The radial and tangential components from both models seemed closer to each other than to the full-scale data.

Hot wire anemometry enabled the measurements of model-scale boundary layer profiles and nominal wakes in the wind tunnel. A hot wire system has not been used in the towing tank to measure boundary layer profiles at DTNSRDC, and a pitot tube system has not been used to obtain data ahead of the operating propeller. It is felt that with further experiments with hot wire anemometry, measurements in the wind tunnel would provide a valuable technique in determining the wake and boundary layer of surface ships.

REFERENCES

1. Brownell, W. F., "An Anechoic Flow Facility Design for the Naval Ship Research and Development Center, Carderock," NSRDC Report 2924 (Sep 1968).

2. Bowers, B. E., "The Anechoic Flow Facility - Aerodynamic Calibration and Evaluation," DTNSRDC Ship Acoustics Department Evaluation Report SAD-48E-1942 (May 1973).

3. Scragg, C. A. and D. A. Sandell, "A Statistical Evaluation of Wake Survey Techniques," International Symposium on Ship Viscous Resistance, SSPA, Goteborg, Sweden, pp.8:1 - 8:14 (1978).

4. Grant, Jerald W. and Alan C. M. Lin, "The Effects of Variations of Several Parameters on the Wake in Way of the Propeller Plane, For Series 60-0.60 C_B Models," NSRDC Research and Development Center, Report 3024 (Jun 1969).

5. Hadler, J. B. and H. M. Cheng, "Analysis of Experimental Wake Data in Way of Propeller Plane of Single- and Twin- Screw Ship Models," Trans. Soc. Naval Arch. and Mar. Eng., Vol. 73, pp. 287-414 (1965).

6. Reed, A. M. and W. G. Day, "Wake Scale Effects on a Twin-Screw Displacement Ship," Twelfth ONR Symposium on Naval Hydromechanics, Washington, D. C. (1978).

SHIP AND MODEL DATA FOR R/V ATHENA
REPRESENTED BY DTNSRDC MODEL 5365 AND 5366

Appendages: Shafts, V-Struts, Rudders, Centerline Skeg, Stabilizer Fins

	Ship	Model
Length Overall	50.3 m	6.10 m
Length on Waterline	47.0 m	5.70 m
Length Between Perpendiculars	46.9 m	5.69 m
Beam (Maximum)	6.68m	0.81 m
Draft (Mean)	1.715m	0.208m
Displacement	266 t	0.463 t
Wetted Surface	317.1m^2	4.66 m^2

Coefficients

Scale Ratio	$\lambda = L_S/L_M$	8.25
Block Coefficient	C_B	0.48
Prismatic Coefficient	C_p	0.63
Length/Beam Ratio	L/B	7.04
Beam/Draft Ratio	B/T	3.89
Displacement/Length Ratio	Δ_L	7.15

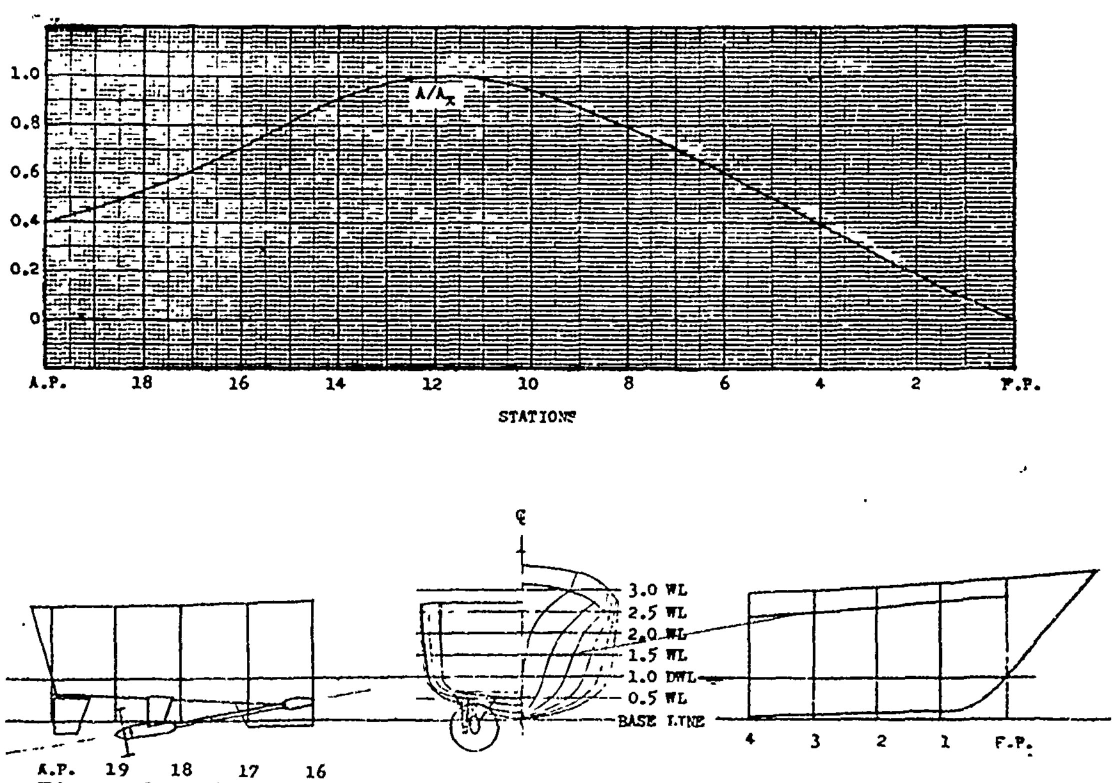

Figure 1 - Ship and Model Data for R/V ATHENA Represented by Models 5365 and 5366

	PROP NO	LINEAR RATIO	DIA MODEL	DIA SHIP	PITCH MODEL AT 70 PCT	PITCH SHIP AT 70 PCT	PITCH RATIO AT 70 PCT	NUMBER OF BLADES	EXP AREA	E.A./D.A.	M.W.R	PROJ AREA	P.A./D.A.	B.T.F	RAKE ANGLE AT TIP	ROTATION	SHIP MODEL	SECTION LENGTH MODEL AT 70 PCT
INCHES MM	4710	8.250	8.727 221.67	72.000 1828.80	9.697 246.30	80.000 2032.00	1.111	4	46.358 29908.6	0.775	0.443	40.100 25871.1	0.670	0.048	0.000	R.H.	4950	4.698 119.33
INCHES MM	4711,12	8.250	8.727 221.67	72.000 1828.80	9.897 246.30	80.000 2032.00	1.111	4	46.358 29908.6	0.775	0.443	40.100 25871.1	0.670	0.048	0.000	L.H.	4950	4.698 119.33

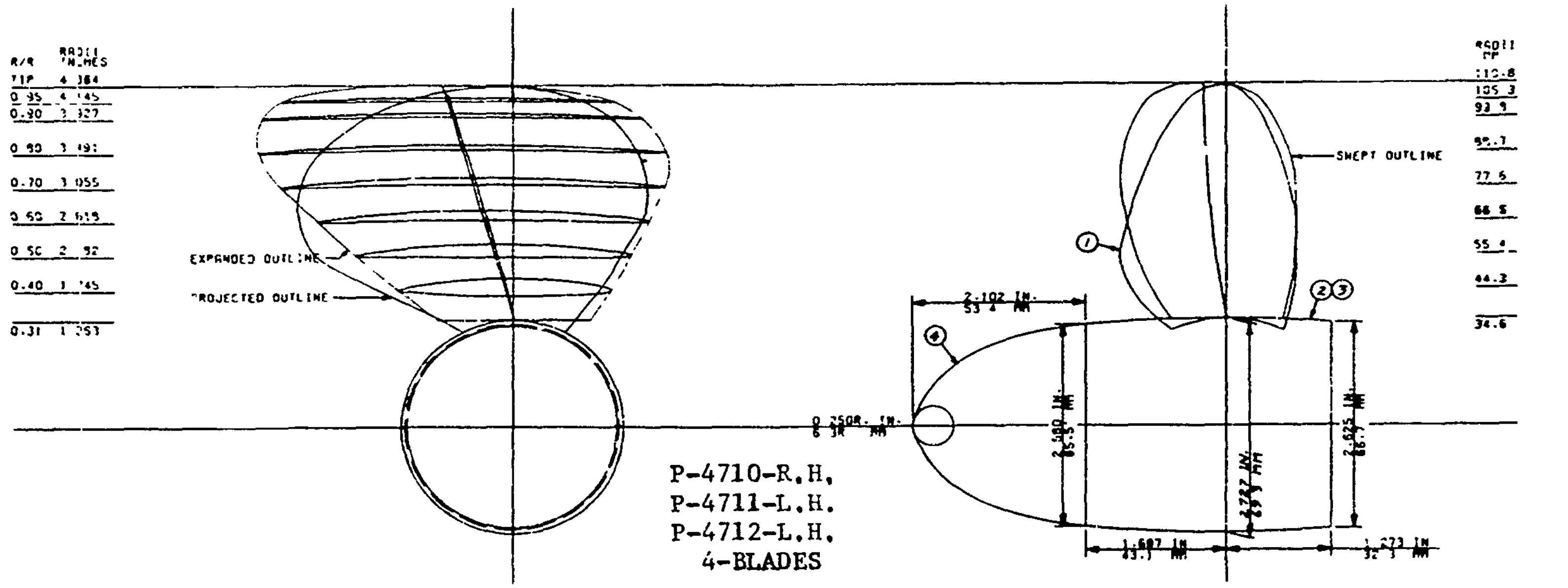

Figure 2 - Controllable-Pitch Propeller Geometry - Propellers 4710, 4711, and 4712

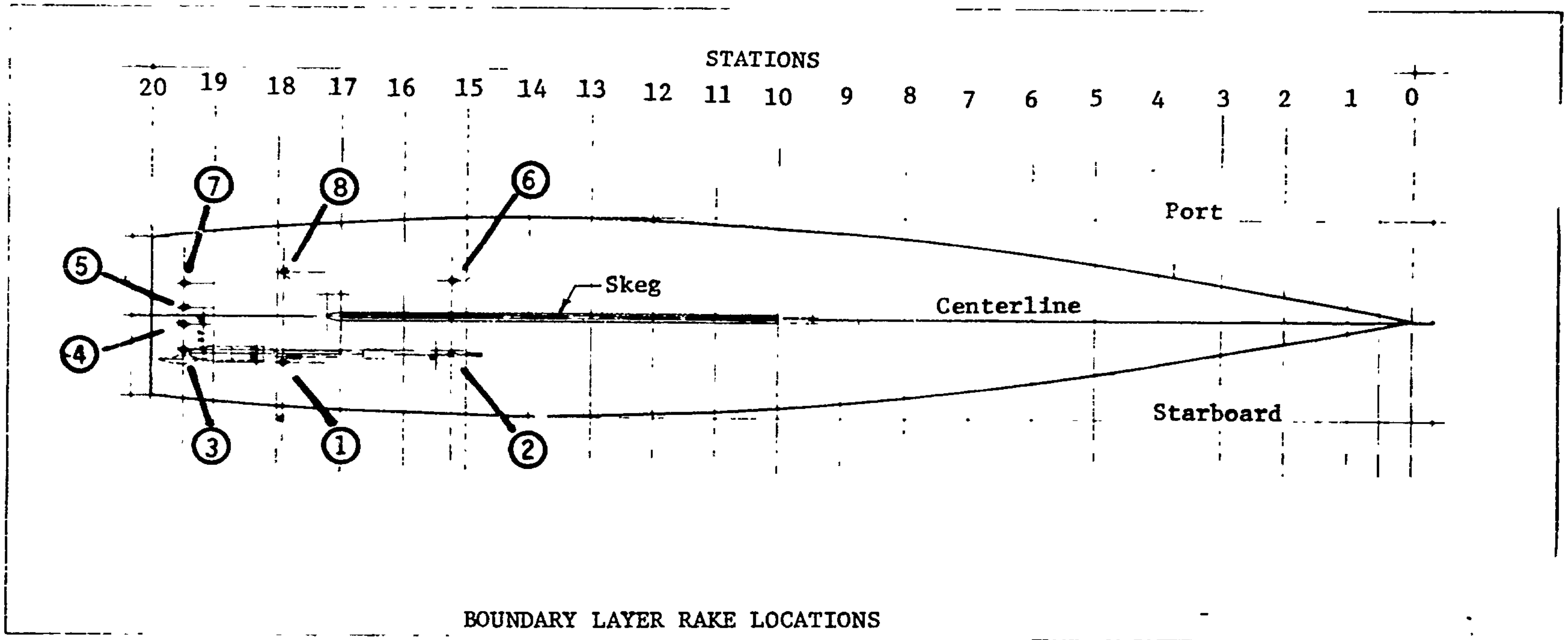

Figure 3 - Plan View of Hull Showing Boundary Layer Rake Locations

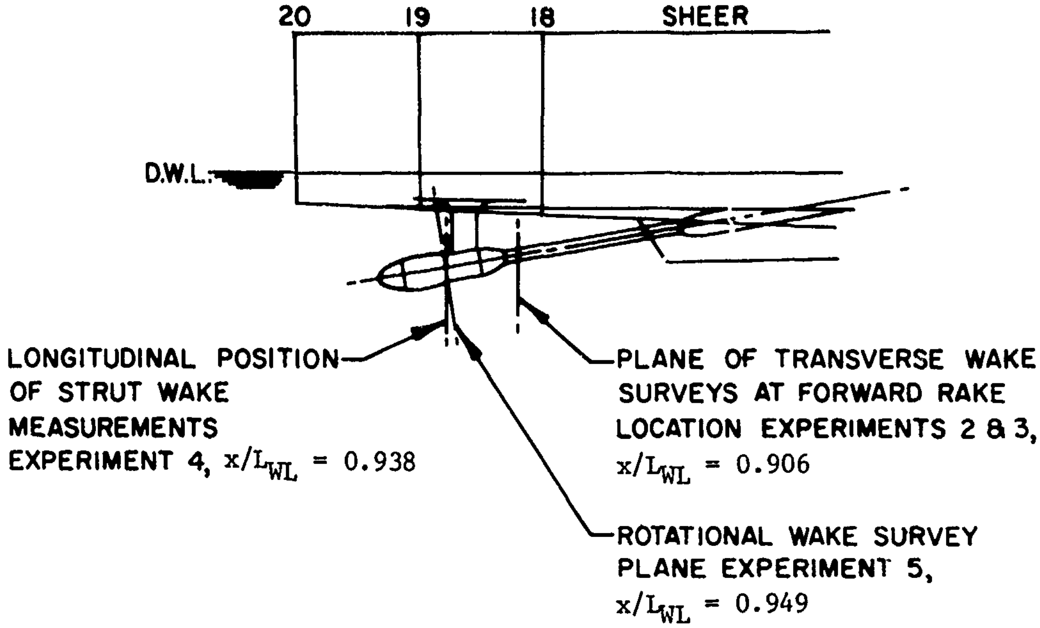

Figure 4a - Longitudinal Locations of Wake Survey and Strut Wake Measurements on Model 5366

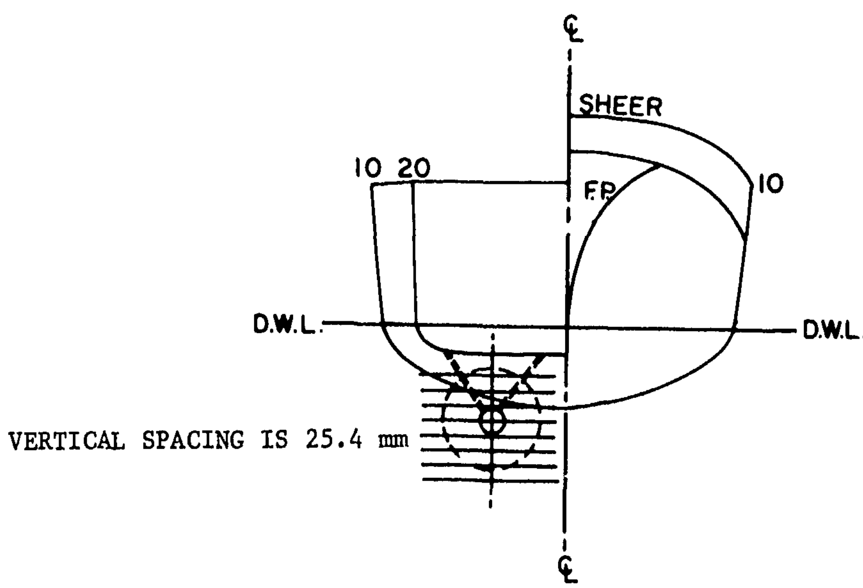

Figure 4b - Transverse Grid Locations of Measurements of Experiments 2 and 3

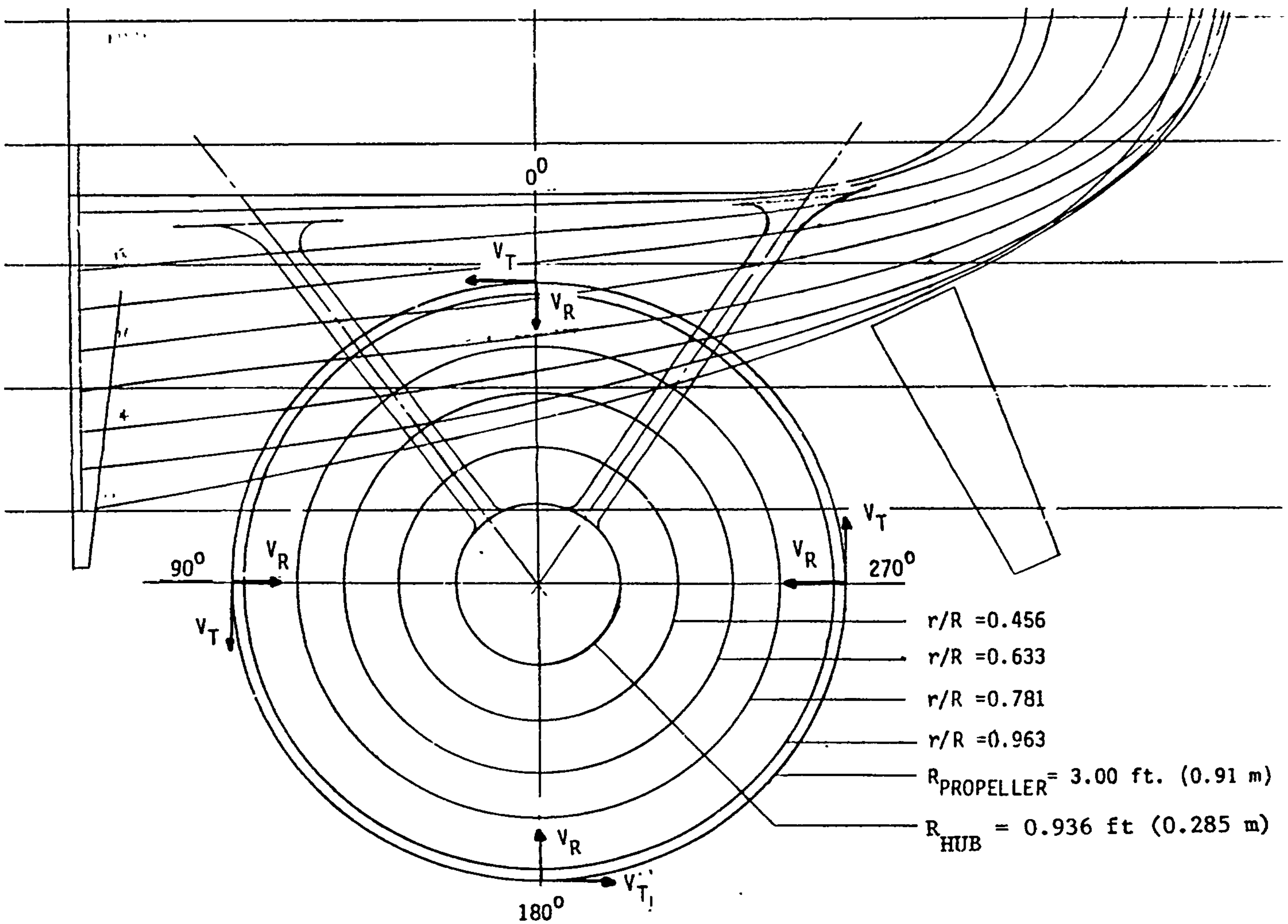

Figure 5 - Afterbody Sections of R/V ATHENA Showing Radii of Wake Measurements

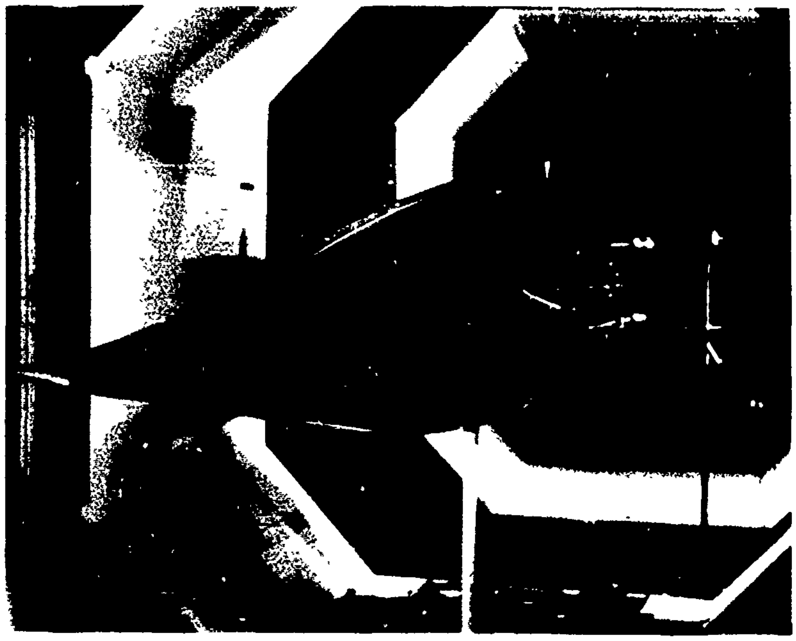

PSD 549-15A

Figure 6 - Double Model Installed in DTNSRDC Wind Tunnel for Boundary Layer and Rotational Wake Survey Experiments

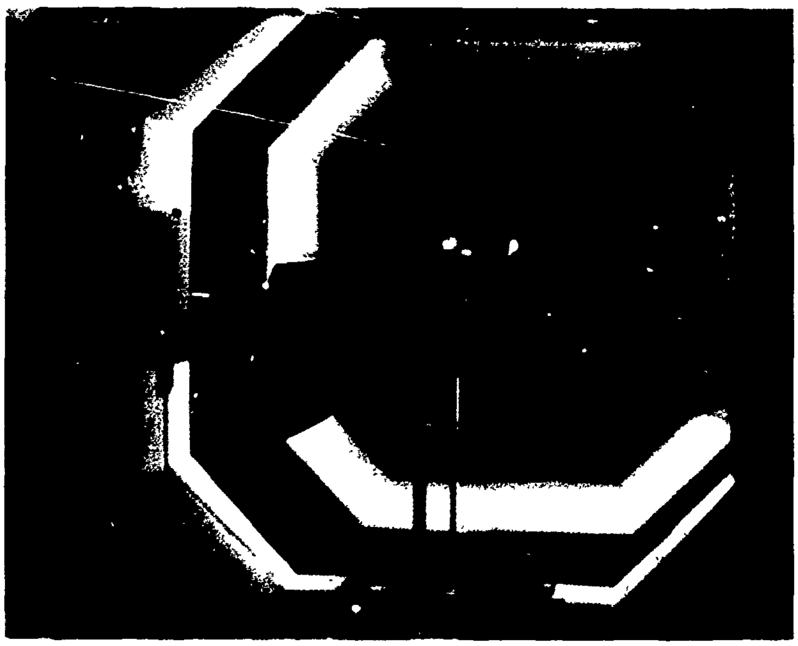

PSD 520-5A

Figure 7 - Double Model Installed in DTNSRDC Wind Tunnel for Transverse Wake Survey Experiments

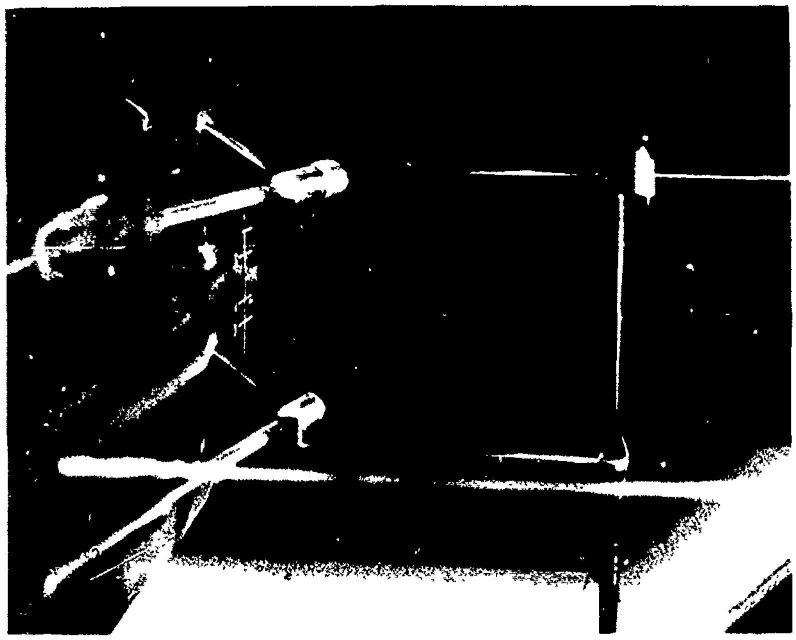

PSD 548-4A

Figure 8 - Experimental Set-Up for Boundary Layer Experiments

P[illegible] 548-6A

Figure 9 - Close-up View of Boundary Layer Rake Locations

PSD 548-18A

Figure 10 - Close-up View of Boundary Layer Probe
with Operating Propeller

PSD 549-11A

Figure 11 - Single Sensor Hot Wire Anemometer Probe
Used for Boundary Layer Profile Measurements

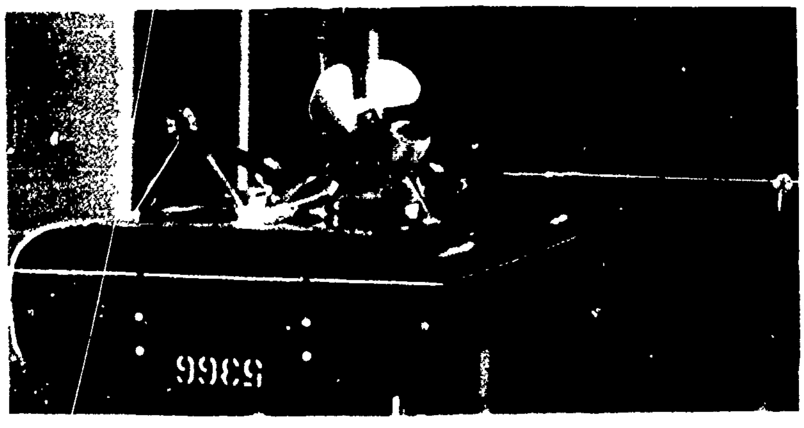

PSD 520-13A

Figure 12 - Experimental Set-Up for Transverse Wake Survey
and Strut Wake Measurements

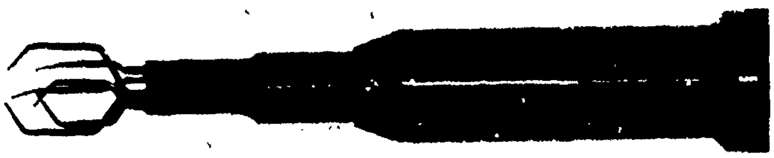

Figure 13 - Triple Sensor Hot Wire Anemometer Probe
Used for Wake Survey Measurements

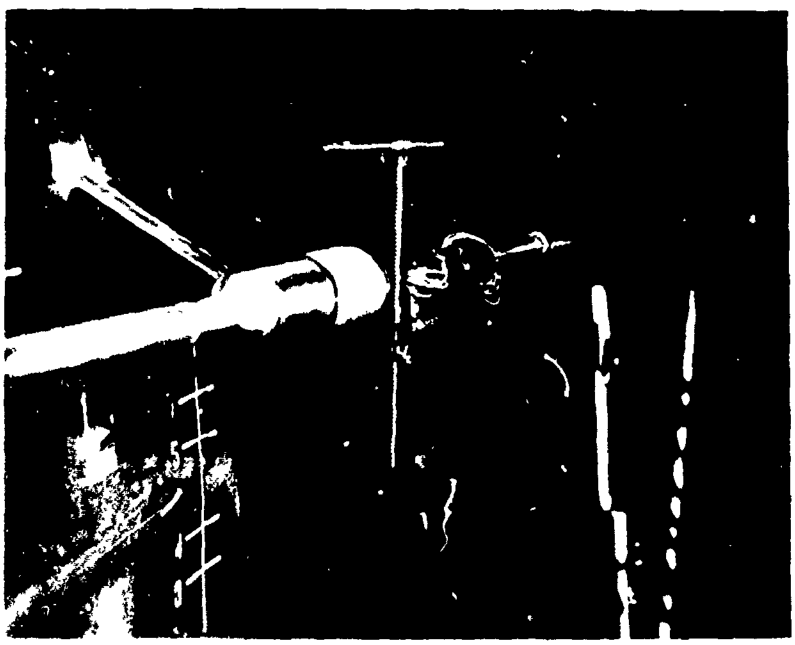

PSD 1009-78-11

Figure 14 - Hot Wire Probe Mounted with Drive Motor
for Rotational Wake Survey Experiment

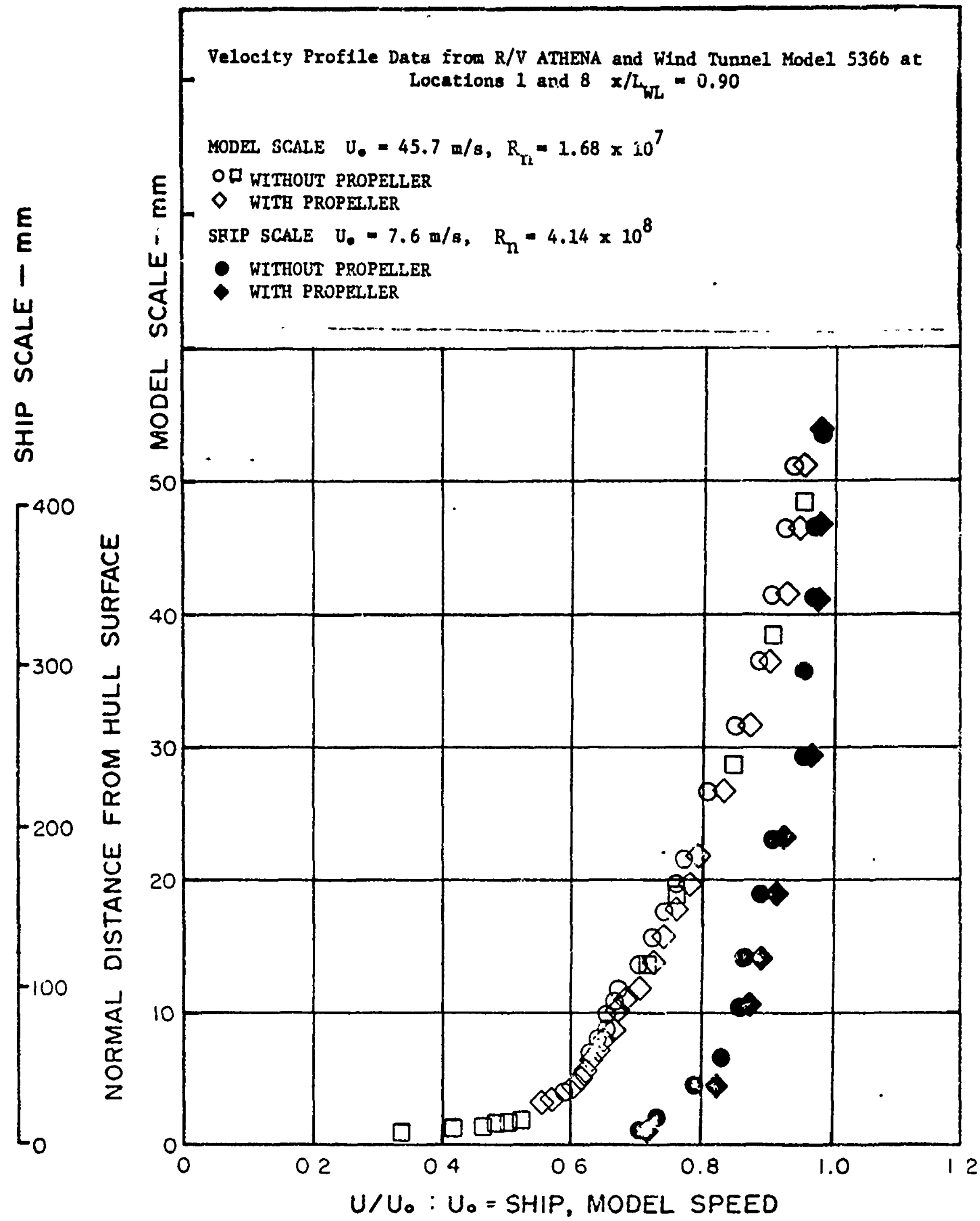

Figure 15 - Measured Boundary Layer Velocity Profiles for R/V ATHENA and Wind Tunnel Model 5366 with and without Propeller at Locations 1 and 8

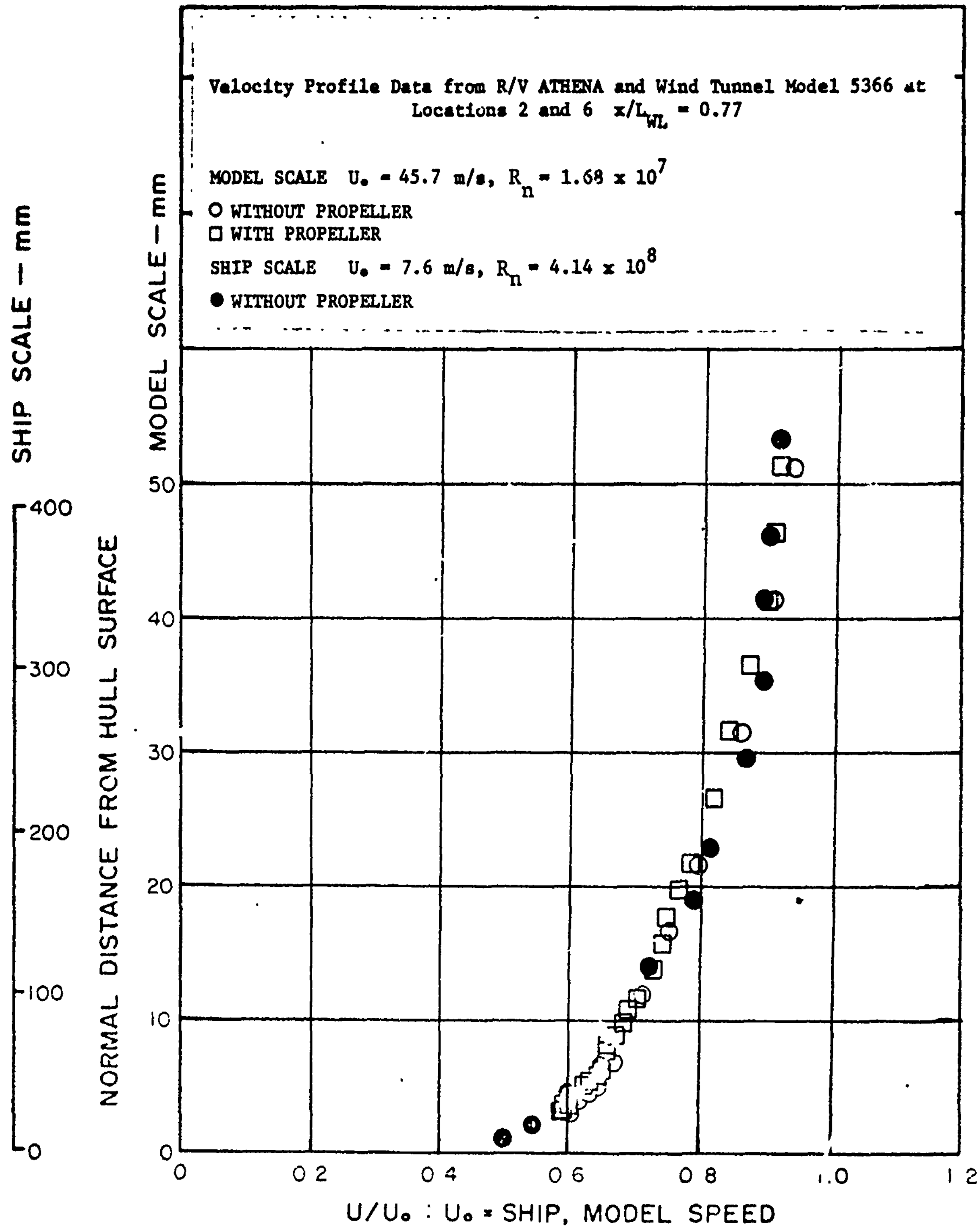

Figure 1ℓ – Measured Boundary Layer Velocity Profiles for R/V ATHENA and Wind Tunnel Model 5366 with and without Propeller at Locations 2 and 6

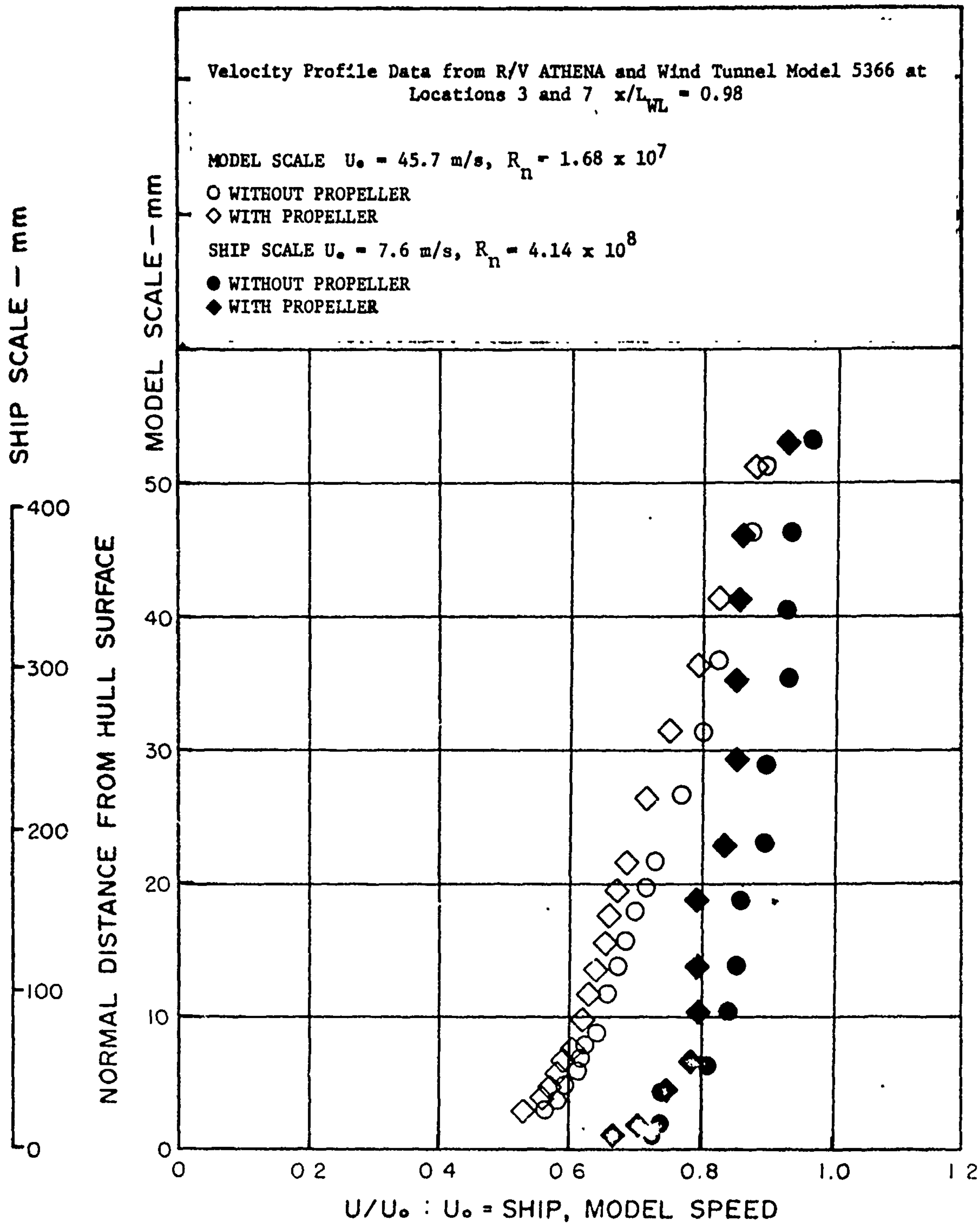

Figure 17 - Measured Boundary Layer Velocity Profiles for R/V ATHENA and Wind Tunnel Model 5366 with and without Propeller at Locations 3 and 7

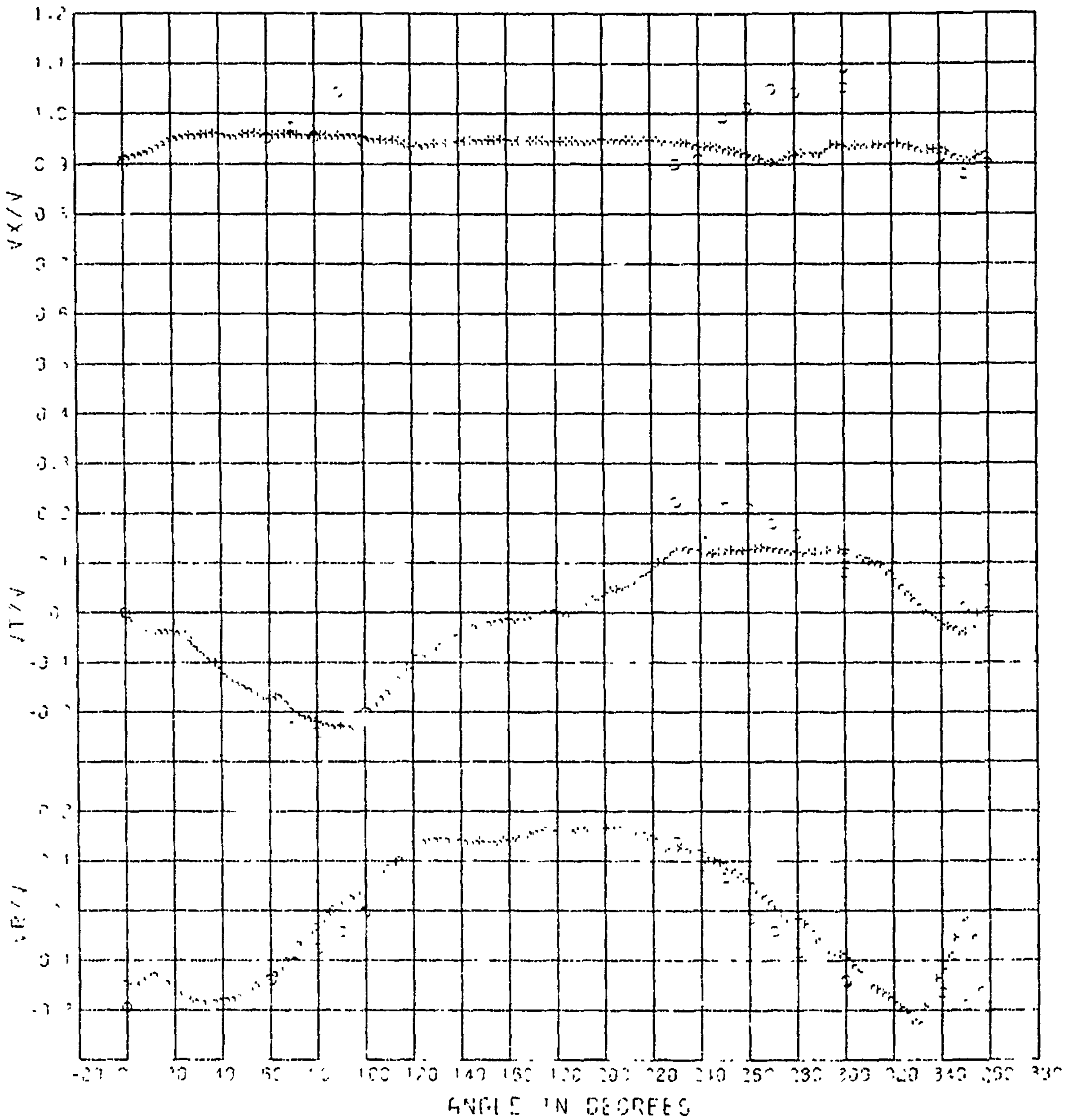

○ FULL SCALE DATA
+ MODEL SCALE DATA - EXPERIMENT 2

Figure 18 - Velocity Component Ratios for R/V ATHENA and Model 5366 at the Forward Rake Location (x/L_{WL} = 0.906) with an Operating Propeller for the 0.417 Radius

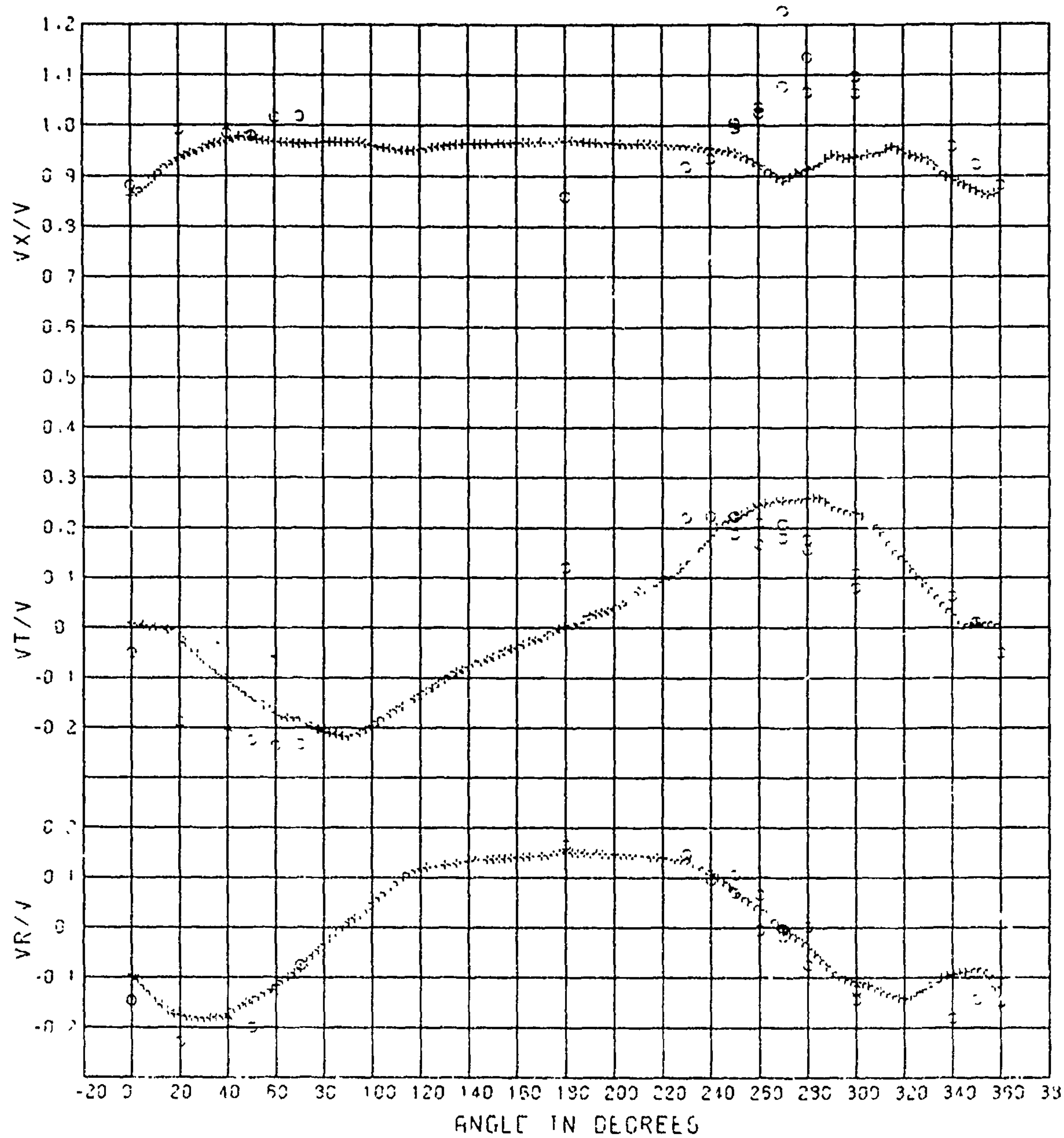

○ FULL SCALE DATA
+ MODEL SCALE DATA -- EXPERIMENT 2

Figure 19 - Velocity Component Ratios for R/V ATHENA and Model 5366 at the Forward Rake Location (x/L_{WL} = 0.906) with an Operating Propeller for the 0.583 Radius

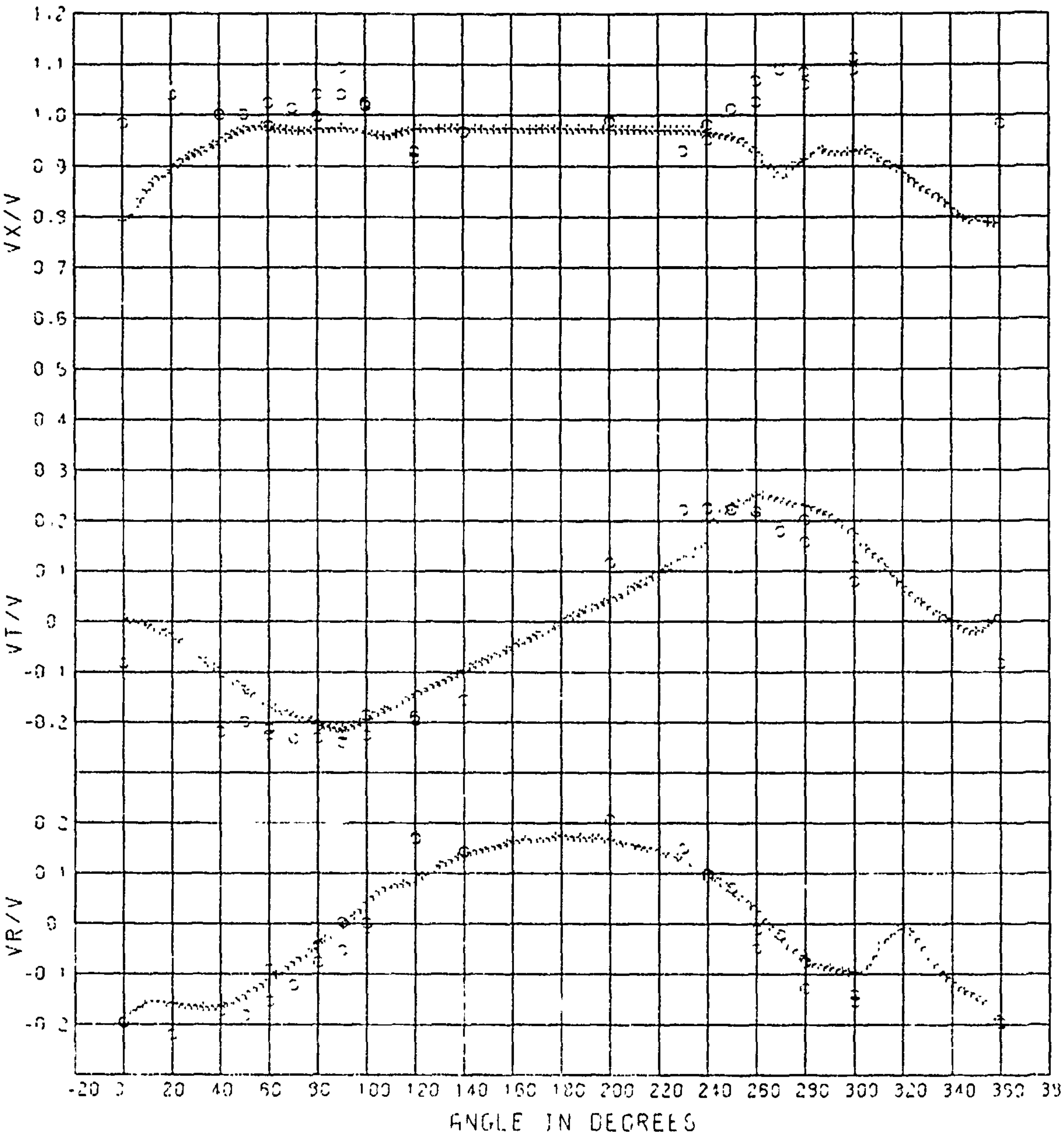

○ FULL SCALE DATA
+ MODEL SCALE DATA - EXPERIMENT 2

Figure 20 - Velocity Component Ratios for R/V ATHENA and Model 5366 at the Forward Rake Location (x/L_{WL} = 0.906\` with an Operating Propeller for the 0.750 Radius

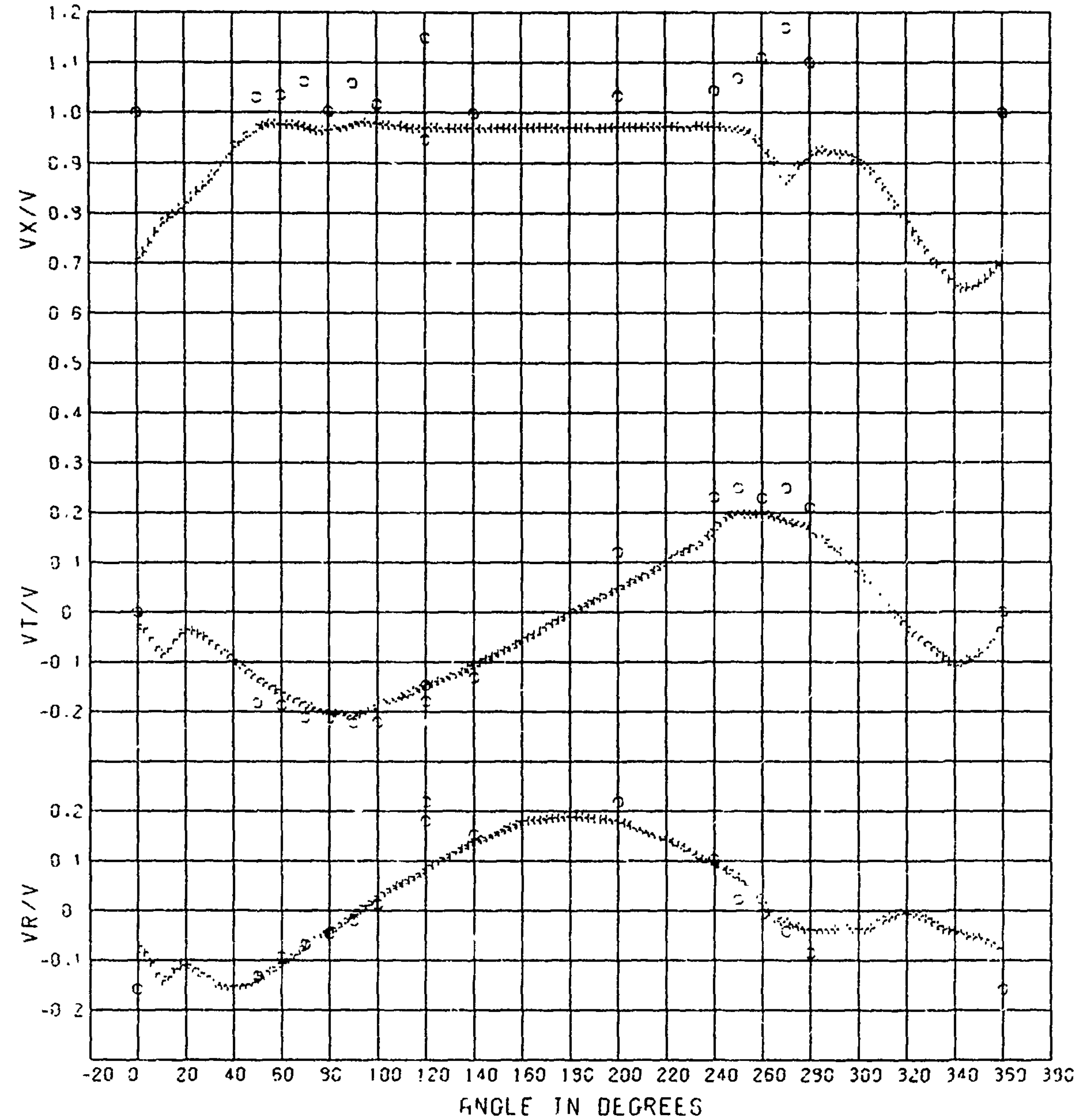

o FULL SCALE DATA
\+ MODEL SCALE DATA - EXPERIMENT 2

Figure 21 - Velocity Component Ratios for R/V ATHENA and Model 5366 at the Forward Rake Location (x/L_{WL} = 0.906) with an Operating Propeller for the 0.917 Radius

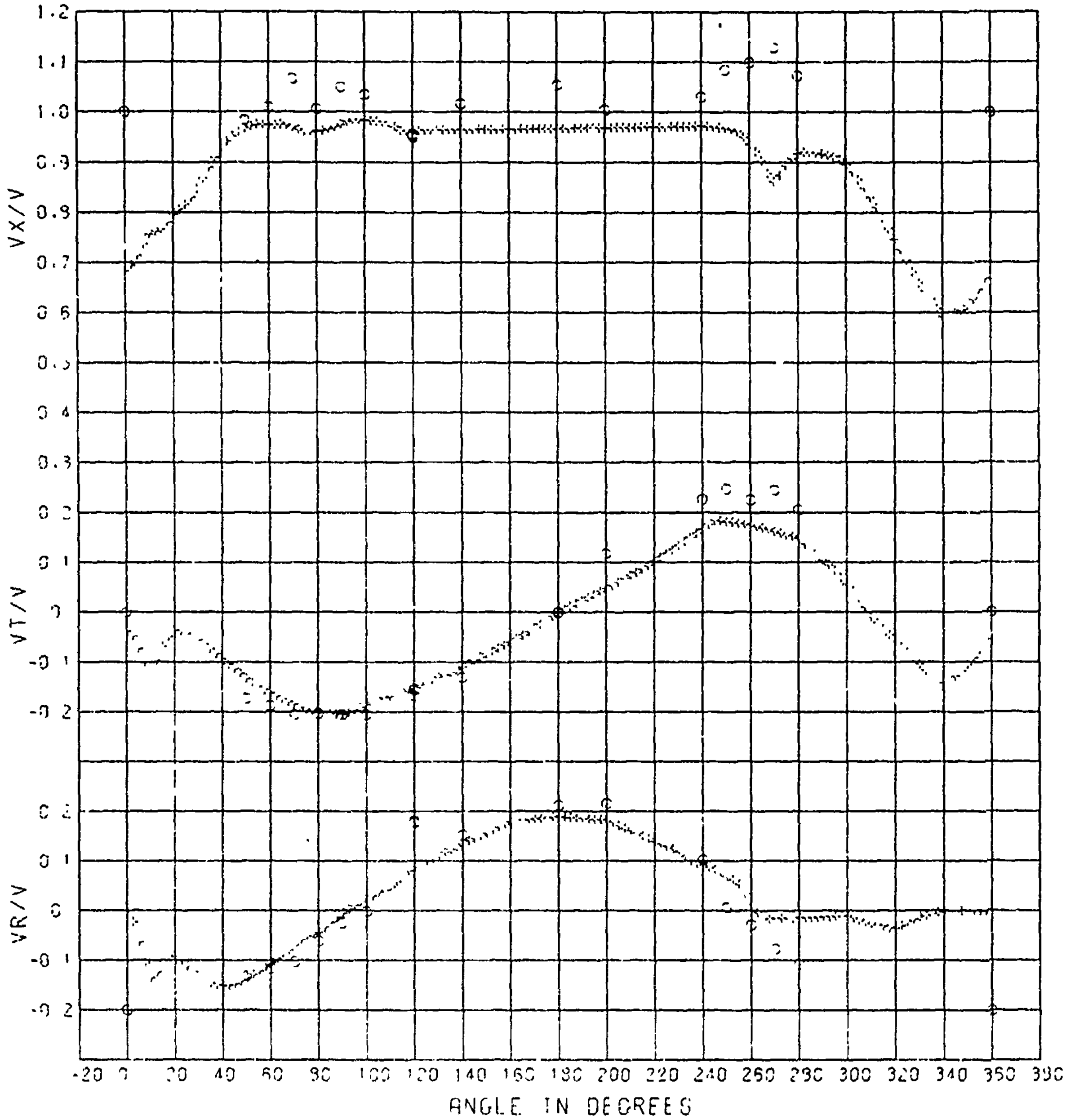

○ FULL SCALE DATA
+ MODEL SCALE DATA - EXPERIMENT 2

Figure 22 - Velocity Component Ratios for R/V ATHENA and Model 5366 at the Forward Rake Location (x/L_{WL} = 0.906) with an Operating Propeller for the 1.083 Radius

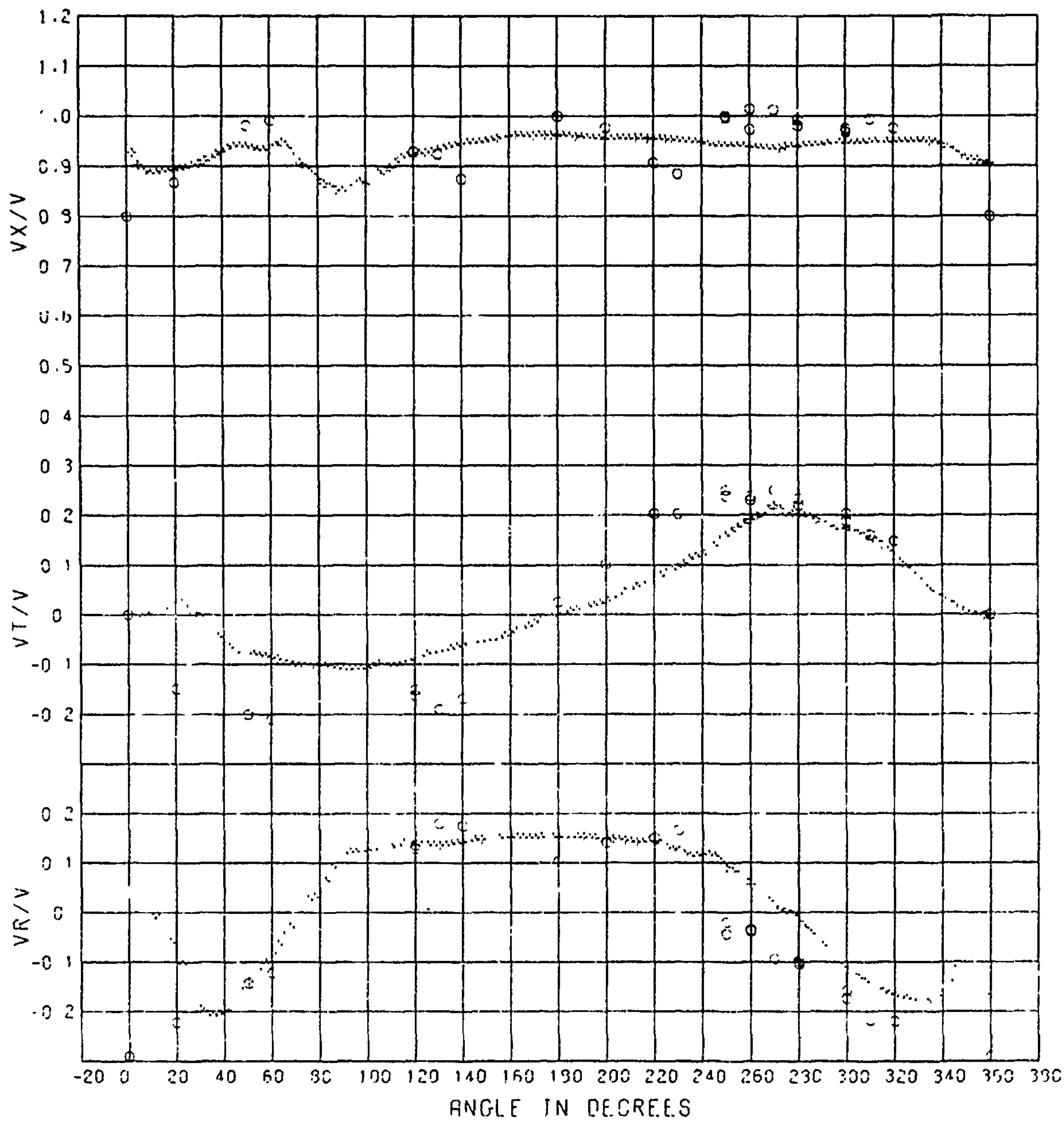

ᶜ FULL SCALE DATA
+ MODEL SCALE DATA - EXPERIMENT 3

Figure 23 - Velocity Component Ratios for R/V ATHENA and Model 5366 at the Forward Rake Location (x/L_{WL} = 0.906) without an Operating Propeller for the 0.417 Radius

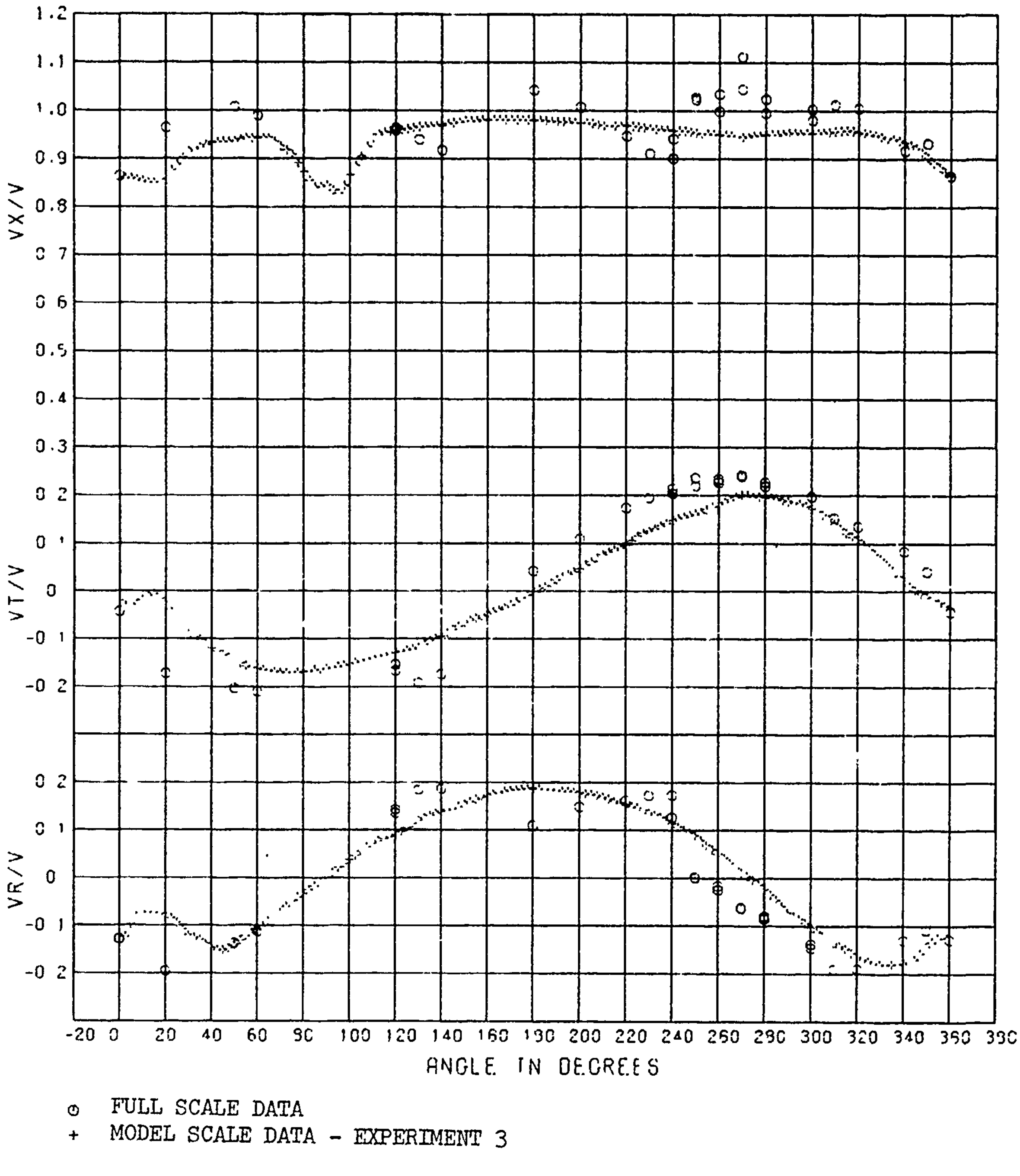

Figure 24 – Velocity Component Ratios for R/V ATHENA and Model 5366 at the Forward Rake Location (x/L_{WL} = 0.906) without an Operating Propeller for the 0.583 Radius

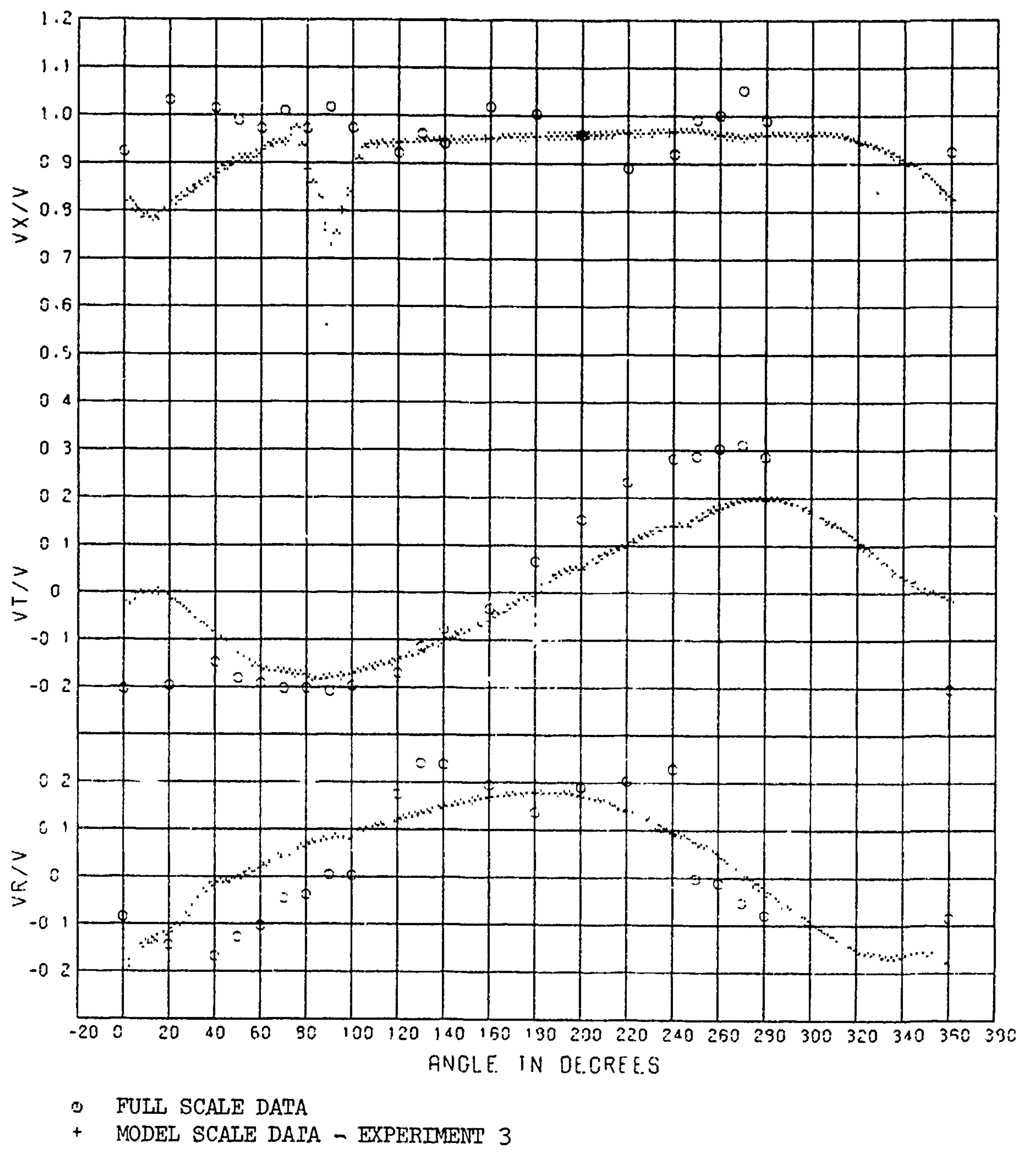

Figure 25 - Velocity Component Ratios for R/V ATHENA and Model 5366 at the Forward Rake Location (x/L_{WL} = 0.906) without an Operating Propeller for the 0.750 Radius

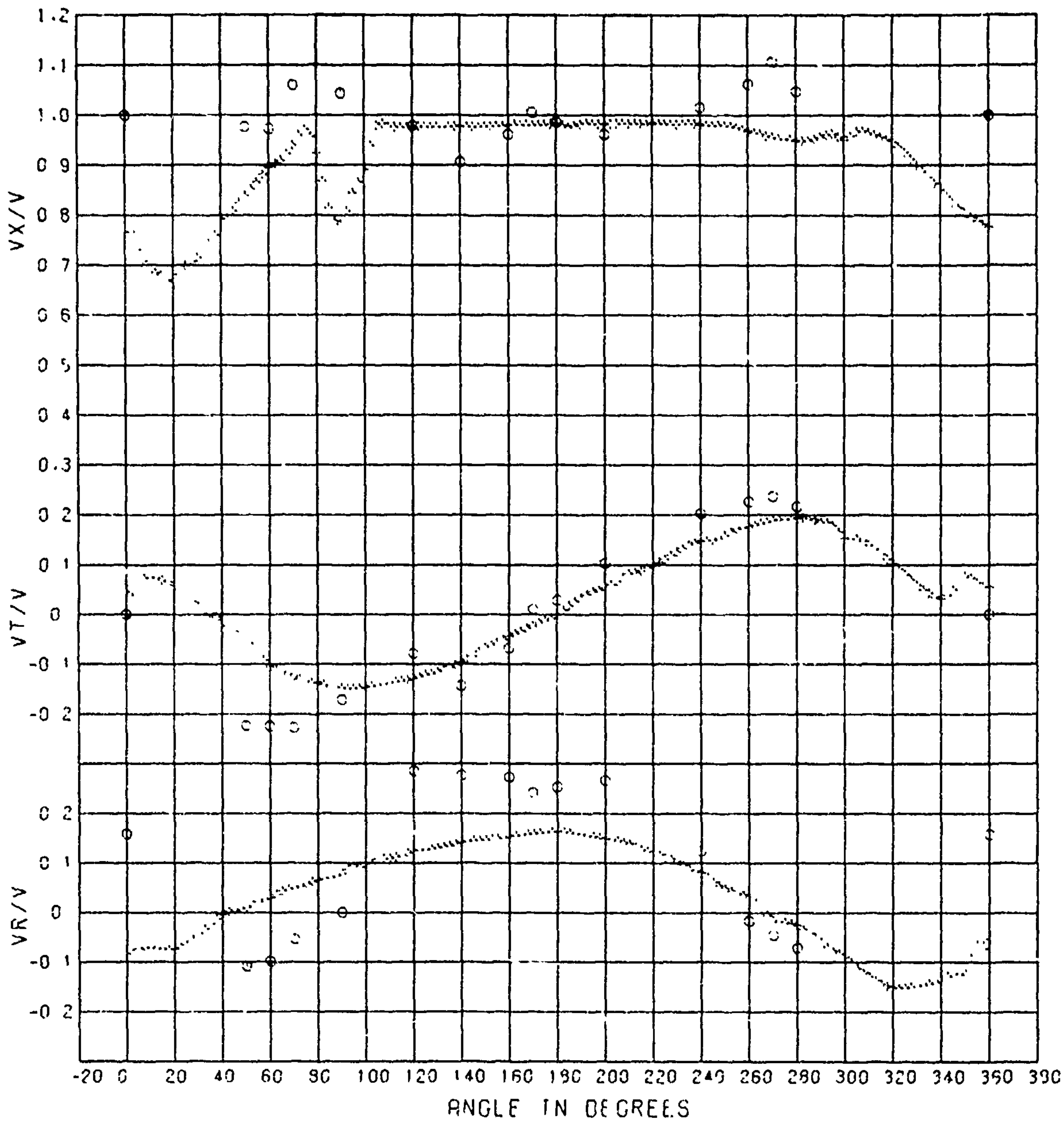

○ FULL SCALE DATA
+ MODEL SCALE DATA - EXPERIMENT 3

Figure 26 - Velocity Component Ratios for R/V ATHENA and Model 5366 at the Forward Rake Location (x/L_{WL} = 0.906) without an Operating Propeller for the 0.917 Radius

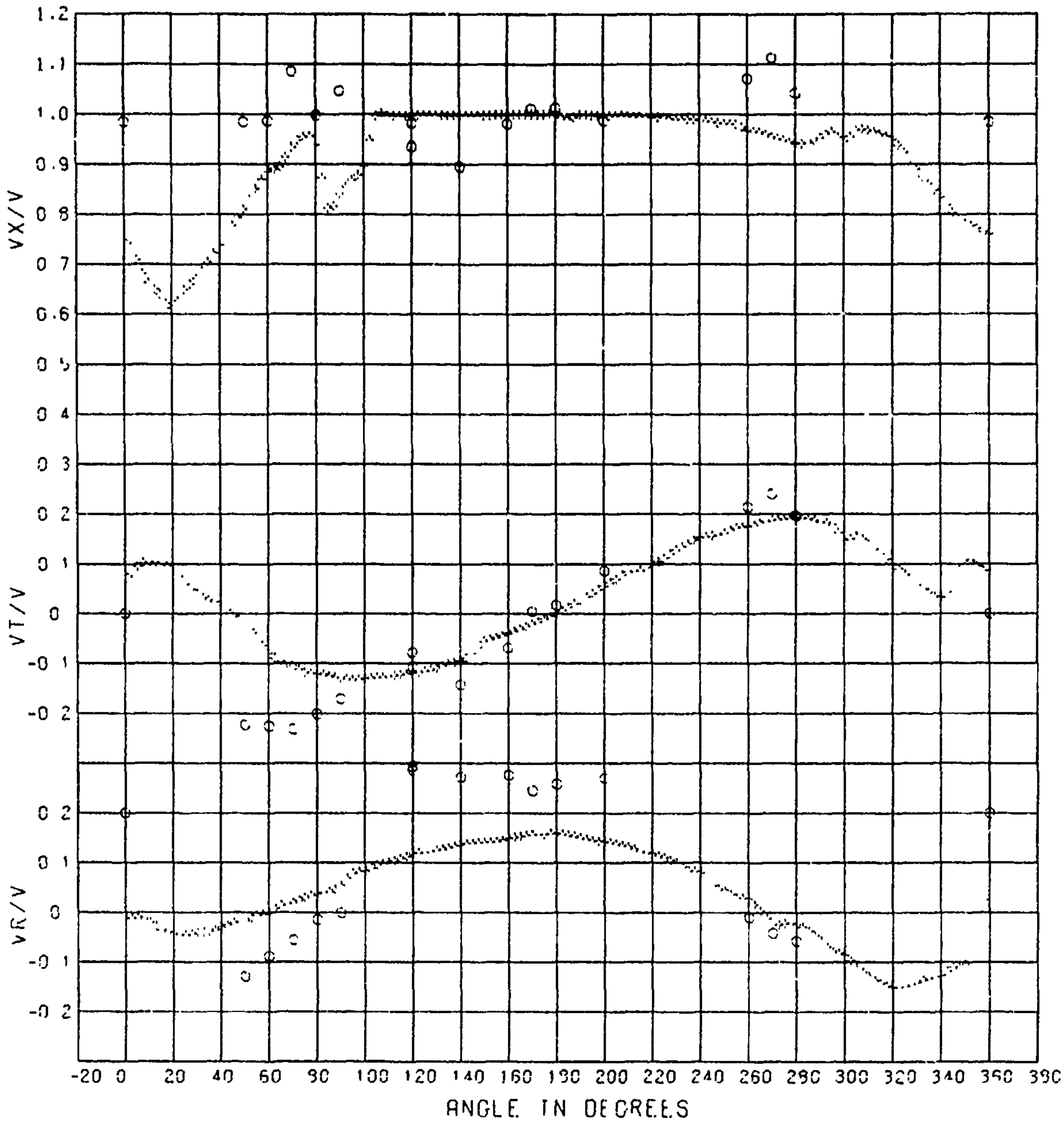

○ FULL SCALE DATA
\+ MODEL SCALE DATA - EXPERIMENT 3

Figure 27 - Velocity Component Ratios for R/V ATHENA and Model 5366 at the Forward Rake Location (x/L_{WL} = 0.906) without an Operating Propeller for the 1.083 Radius

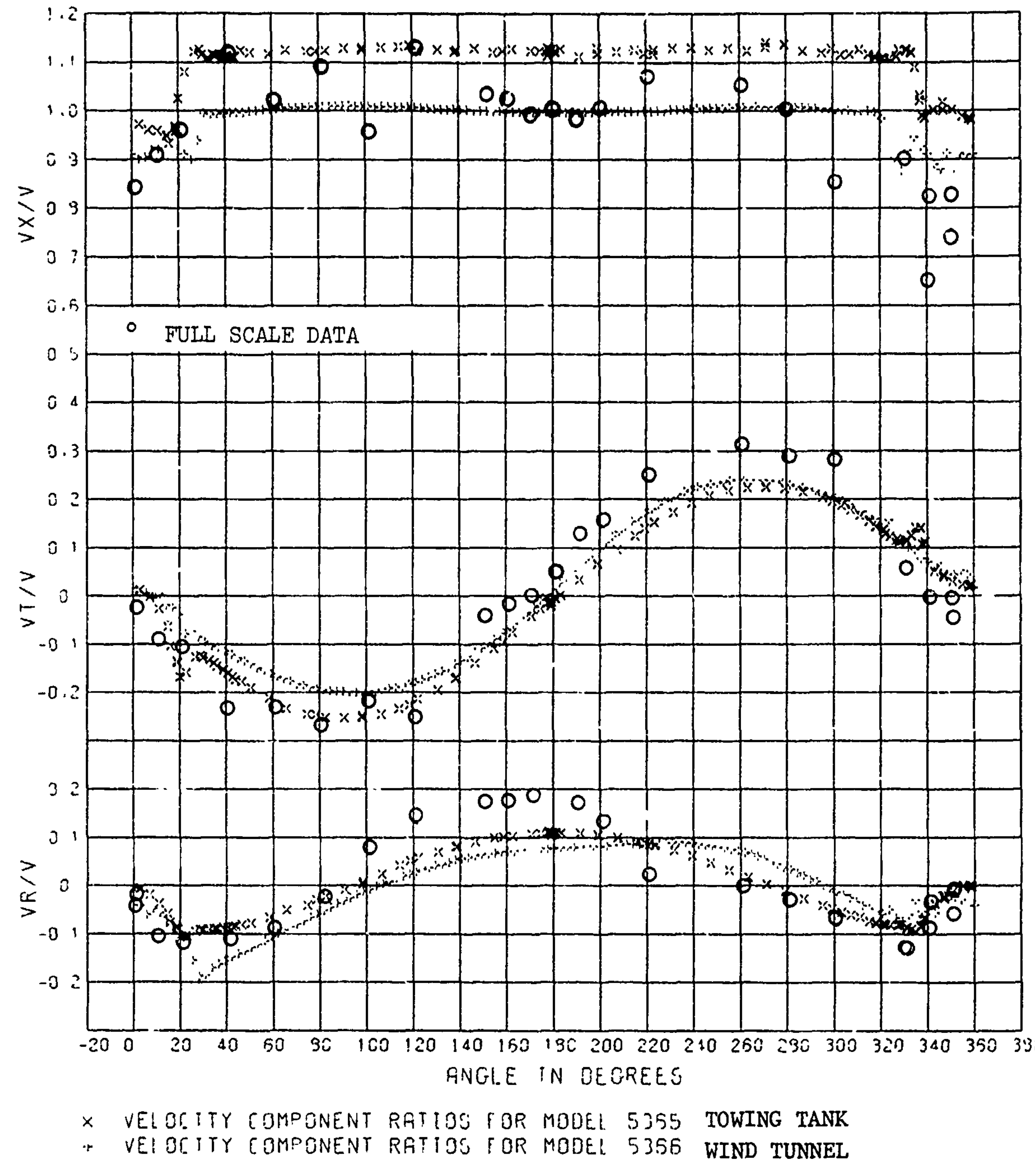

Figure 28 - Composite Plot of Velocity Component Ratios for R/V ATHENA and Models 5365 and 5366 at the Propeller Rake Location (x/L_{WL} = 0.949) for the 0.456 Radius

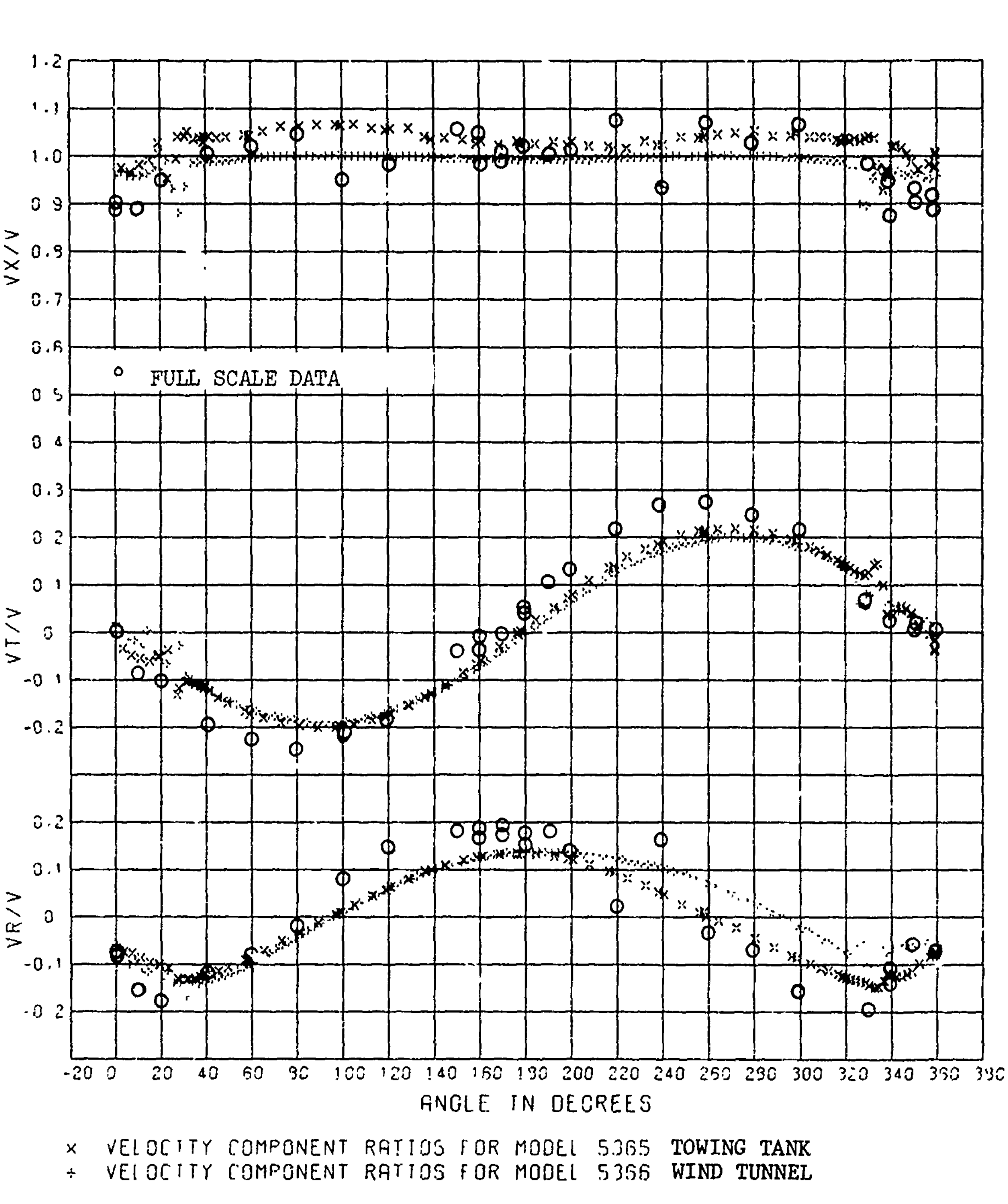

Figure 29 - Composite Plot of Velocity Component Ratios for R/V ATHENA and Models 5365 and 5366 at the Propeller Rake Location ($x/L_{WL} = 0.949$) for the 0.633 Radius

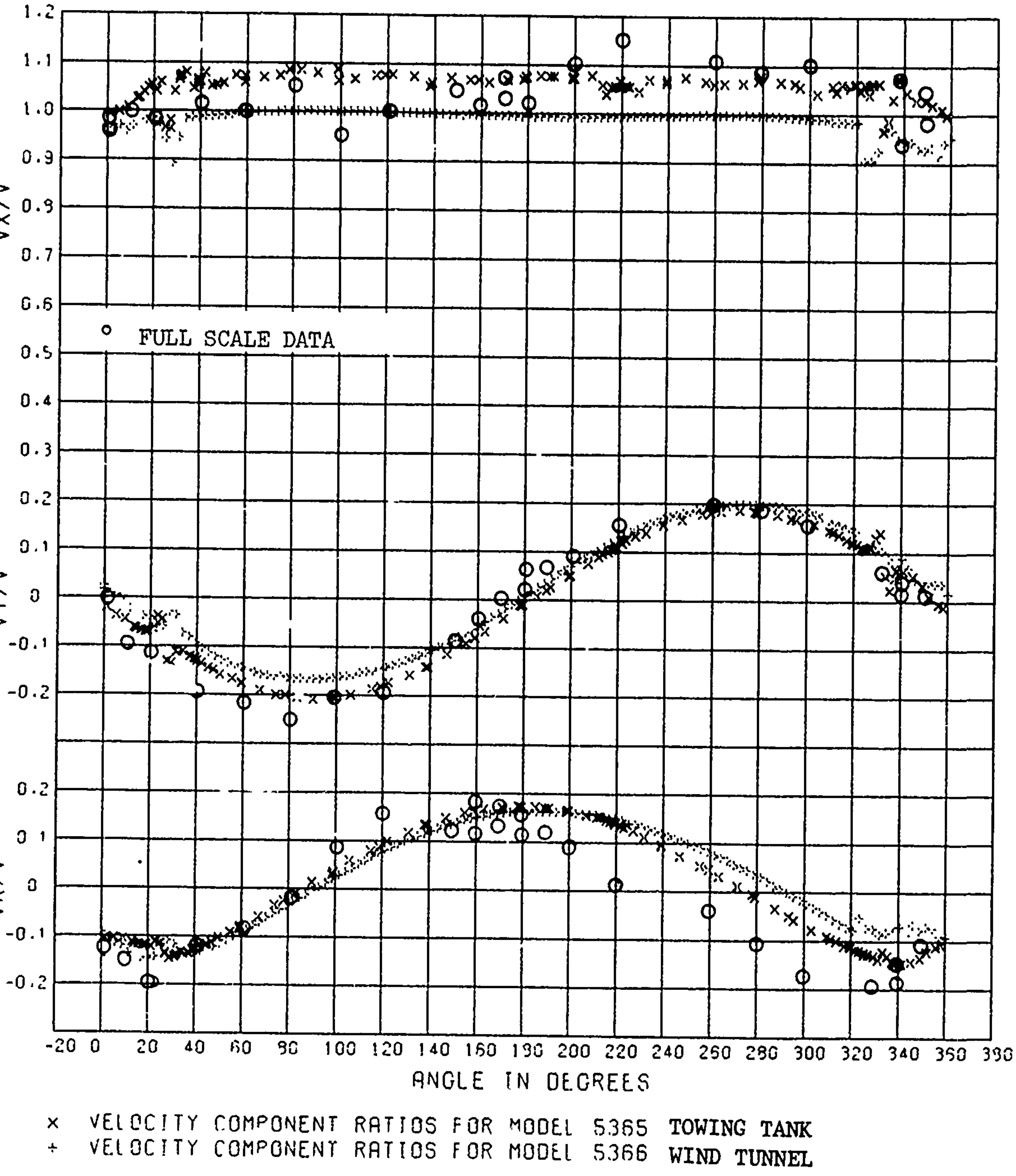

Figure 30 - Composite Plot of Velocity Component Ratios for R/V ATHENA and Models 5365 and 5366 at the Propeller Rake Location (x/L_{WL} = 0.949) for the 0.781 Radius

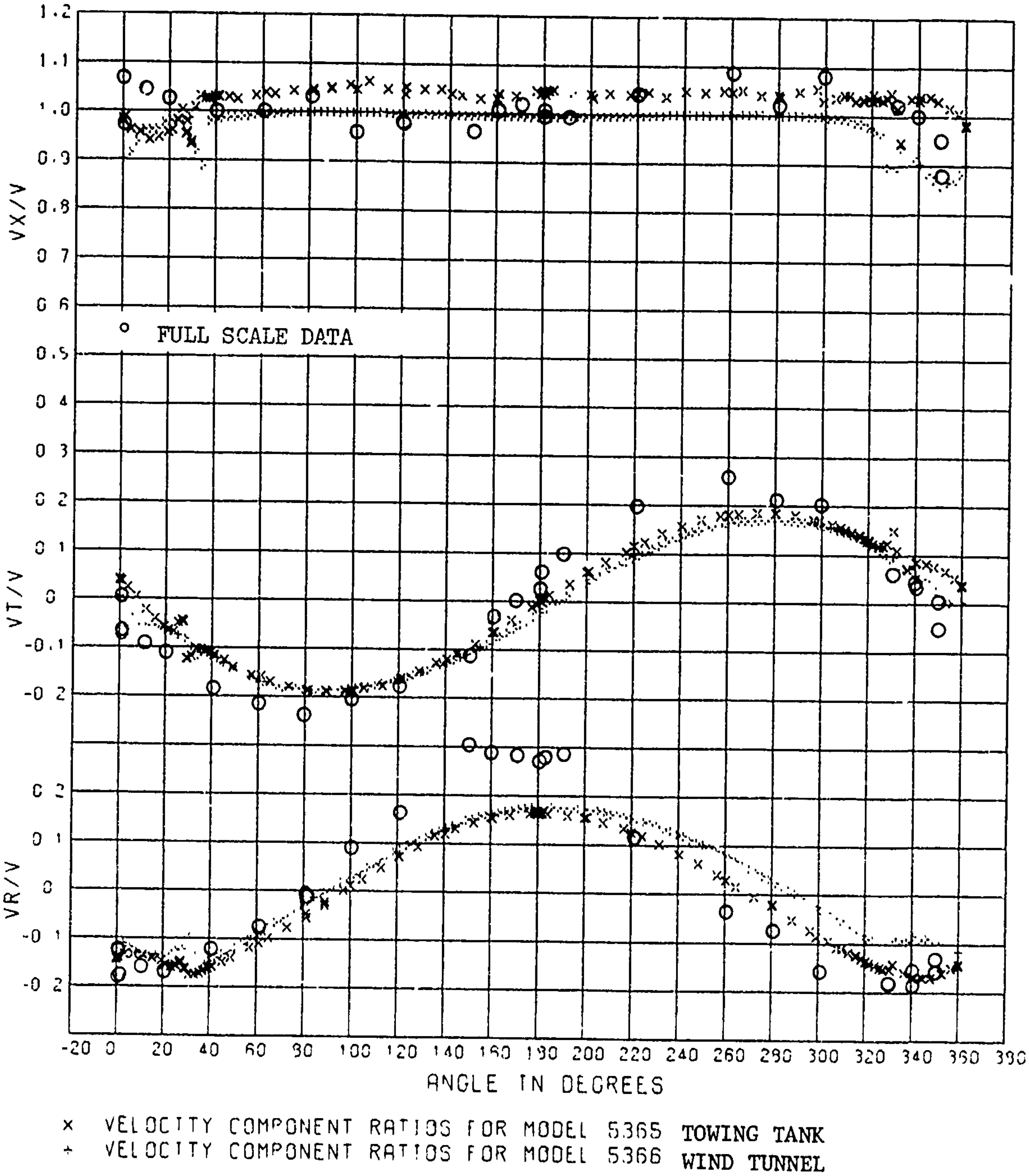

Figure 31 - Composite Plot of Velocity Component Ratios for R/V ATHENA and Models 5365 and 5366 at the Propeller Rake Location (x/L_{WL} = 0.949) for the 0.963 Radius

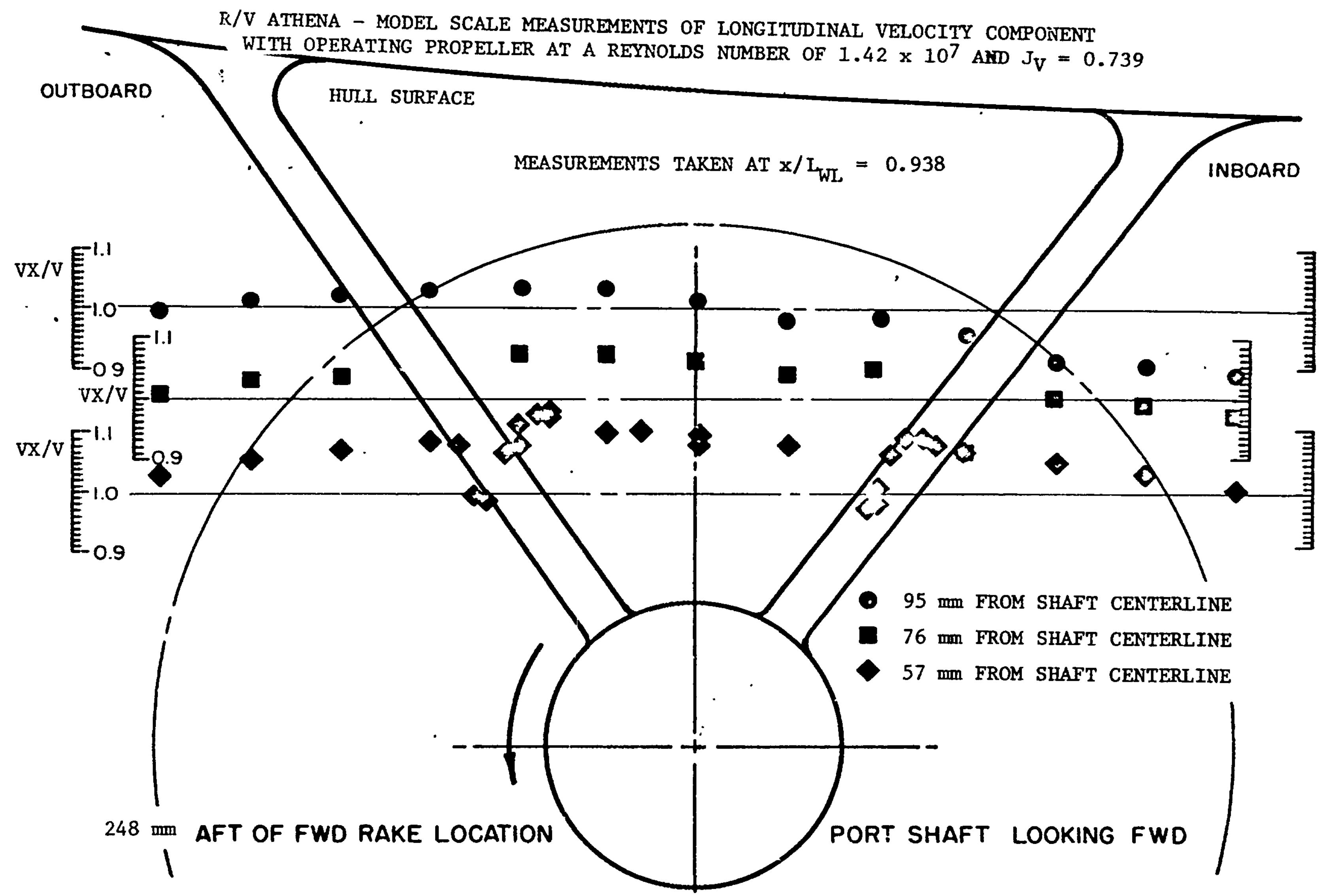

Figure 32 - Strut Wake Measurements at the Location x/L_{WL} = 0.938

TABLE 1

EXPERIMENTAL PROGRAM

Experiment Number	Reynolds Number (based on waterline length)	Description
1	1.68×10^7	Boundary Layer Profile Measurements
2	1.40×10^7	Transverse Wake Survey at Forward Rake Location with Operating Propeller*
3	1.40×10^7	Transverse Wake Survey at Forward Rake Location without Operating Propeller*
4	1.42×10^7	Strut Wake Velocity Defects
5	1.56×10^7	Rotational Wake Survey in Propeller Plane*

*Nondimensional radii of 0.417, 0.583, 0.750, 0.917, and 1.083

**Nondimensional radii of 0.456, 0.633, 0.781, and 0.963

APPENDIX A

VELOCITY COMPONENT RATIOS AND HARMONIC ANALYSIS OF THE TRANSVERSE WAKE SURVEY EXPERIMENTS WITH AND WITHOUT AN OPERATING PROPELLER

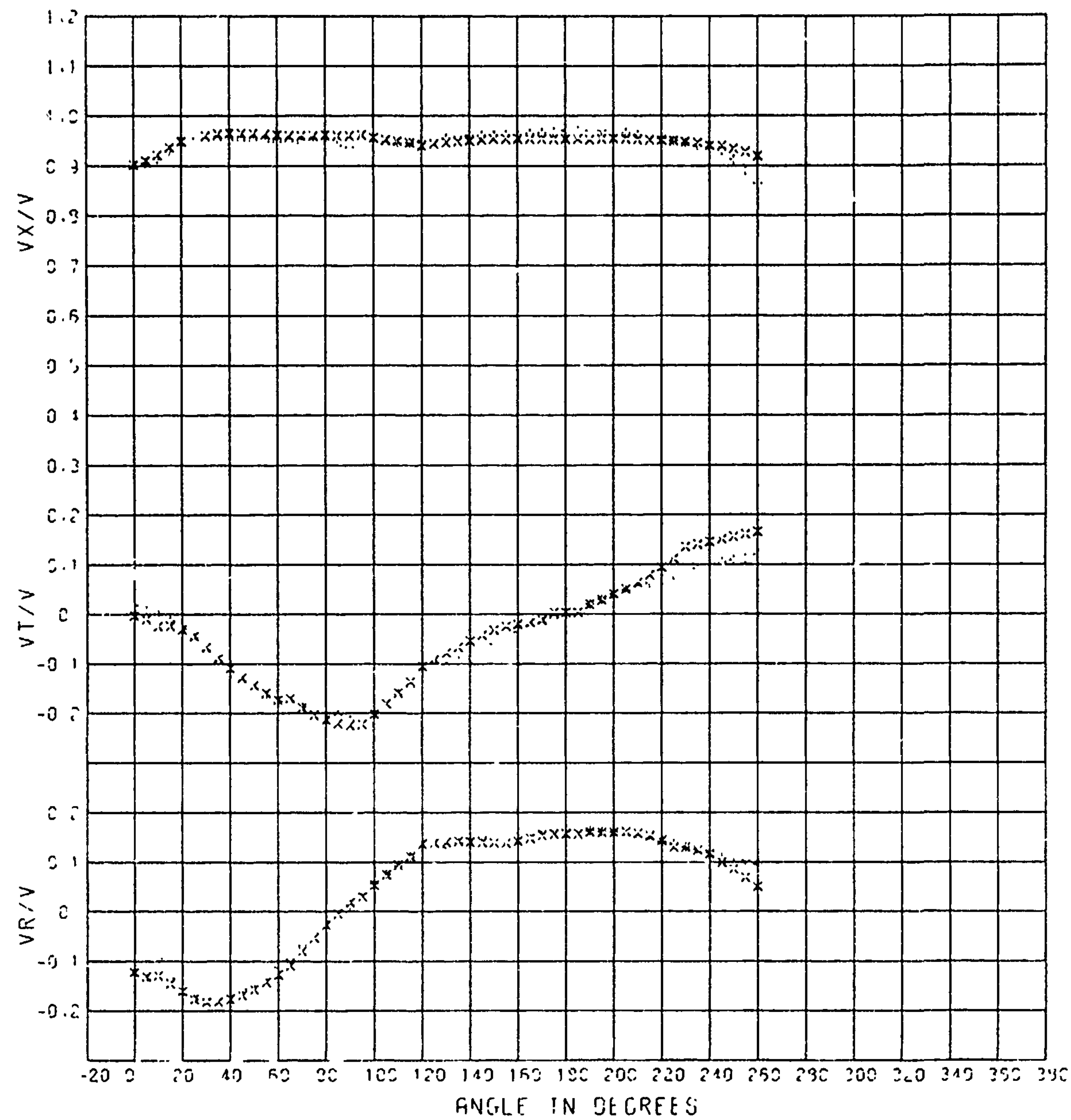

× Model 5366 Transverse Wake Survey Experiment 2 with Propeller
+ Model 5366 Transverse Wake Survey Experiment 3 without Propeller

Figure A-1 - Composite Plot of Velocity Component Ratios from the Transverse Wake Surveys at the Forward Rake Location for the Interpolated Radius of 0.456

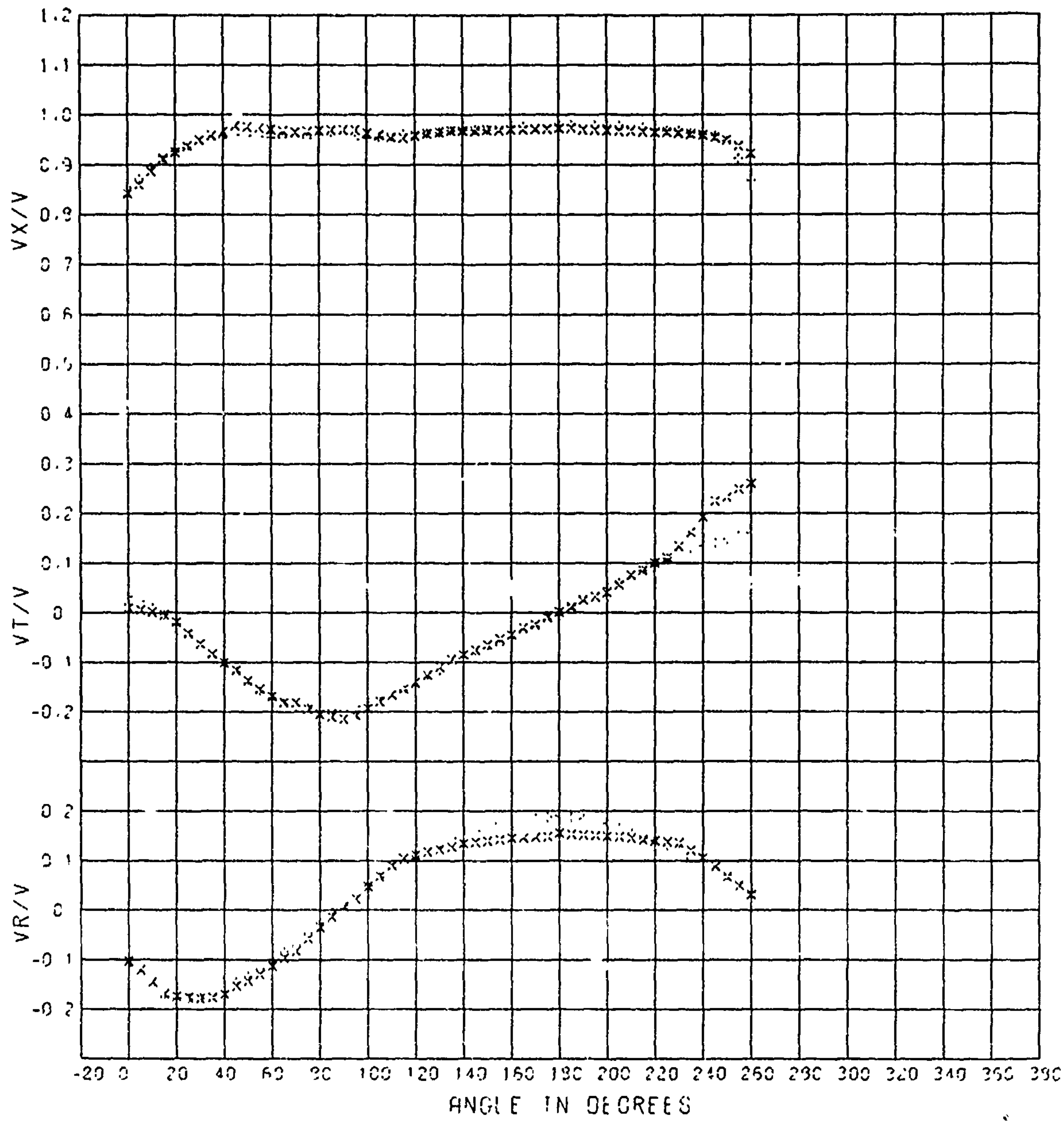

× Model 5366 Transverse Wake Survey Experiment 2 with Propeller
+ Model 5366 Transverse Wake Survey Experiment 3 without Propeller

Figure A-2 - Composite Plot of Velocity Component Ratios from the Transverse Wake Surveys at the Forward Rake Location for the Interpolated Radius of 0.633

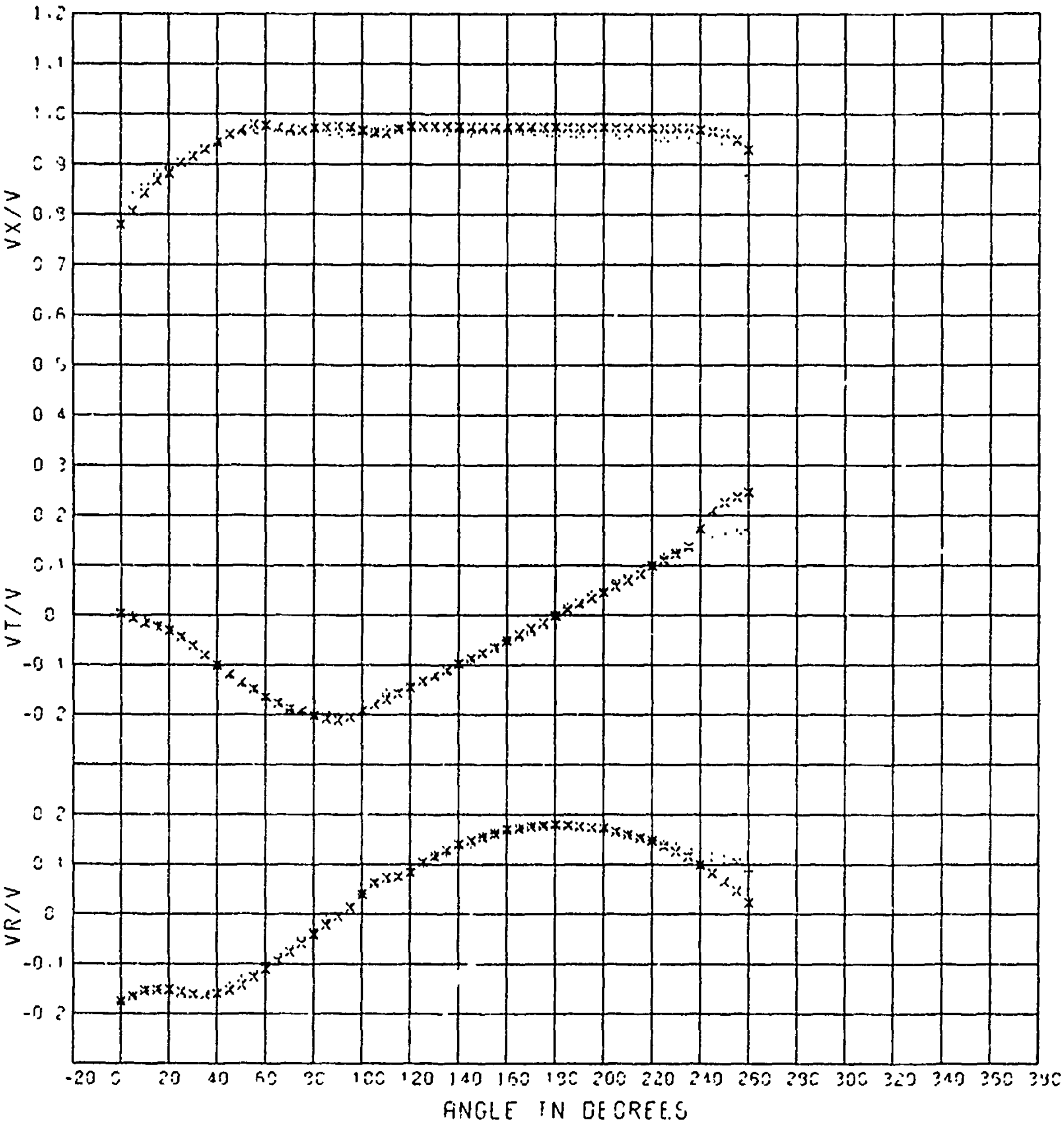

× Model 5366 Transverse Wake Survey Experiment 2 with Propeller
+ Model 5366 Transverse Wake Survey Experiment 3 without Propeller

Figure A-3 - Composite Plot of Velocity Component Ratios from the Transverse Wake Surveys at the Forward Rake Location for the Interpolated Radius of 0.781

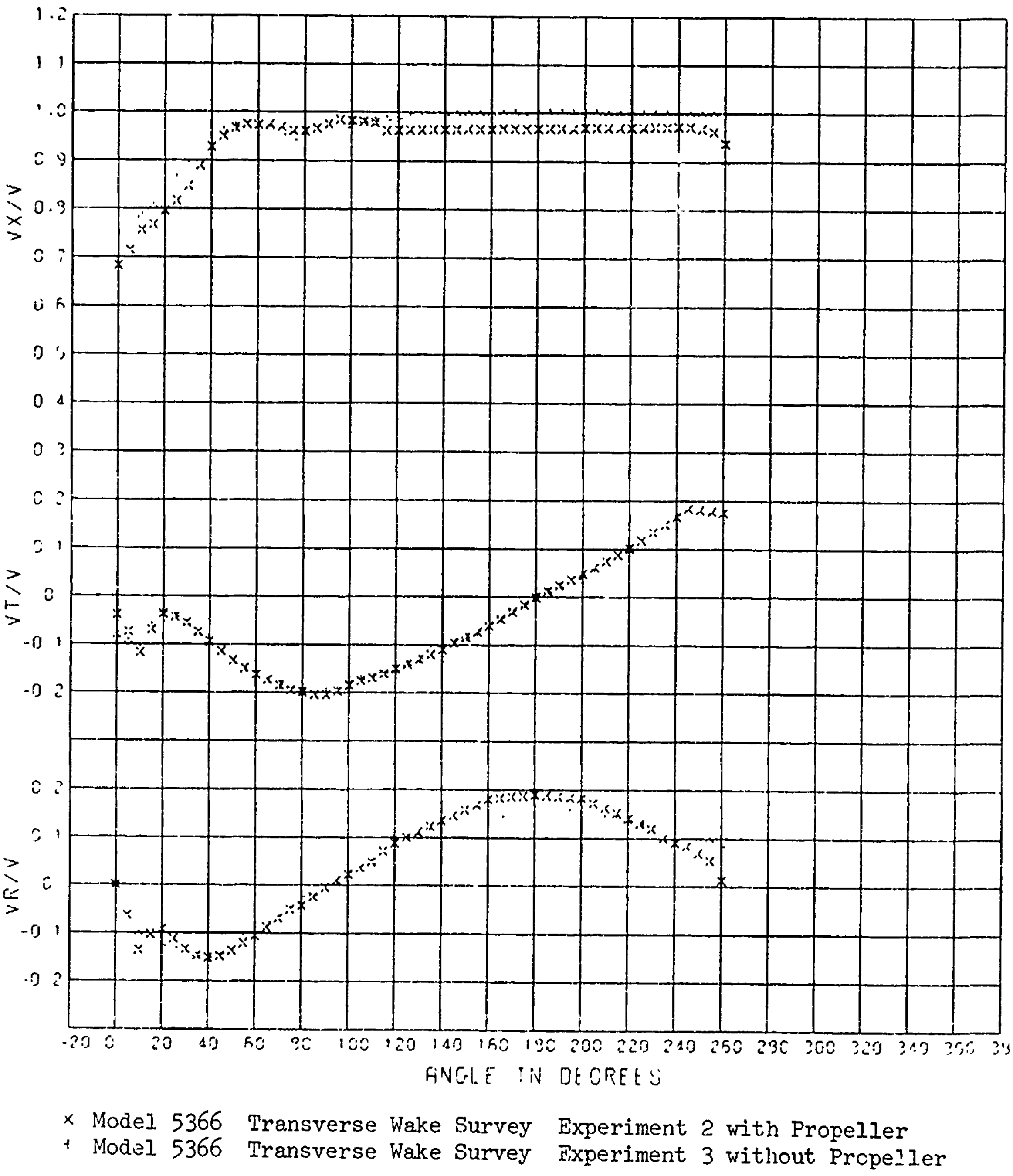

Figure A-4 - Composite Plot of Velocity Component Ratios from the Transverse Wake Surveys at the Forward Rake Location for the Interpolated Radius of 0.963

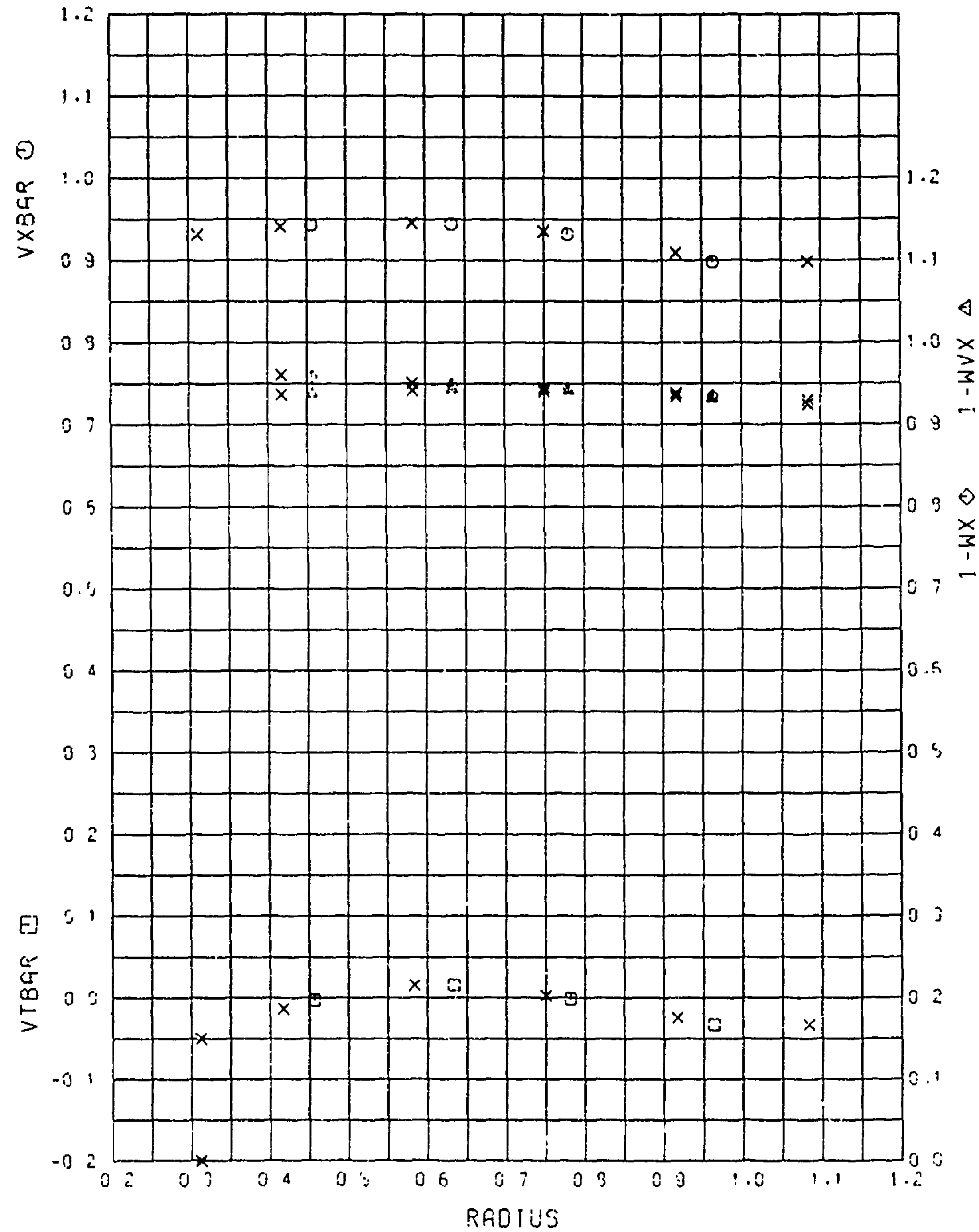

EXPERIMENTAL RADII

INTERPOLATED RADII

Figure A-5 - Radial Distribution of the Mean Velocity Component Ratios from the Transverse Wake Survey at the Forward Rake Location with an Operating Propeller

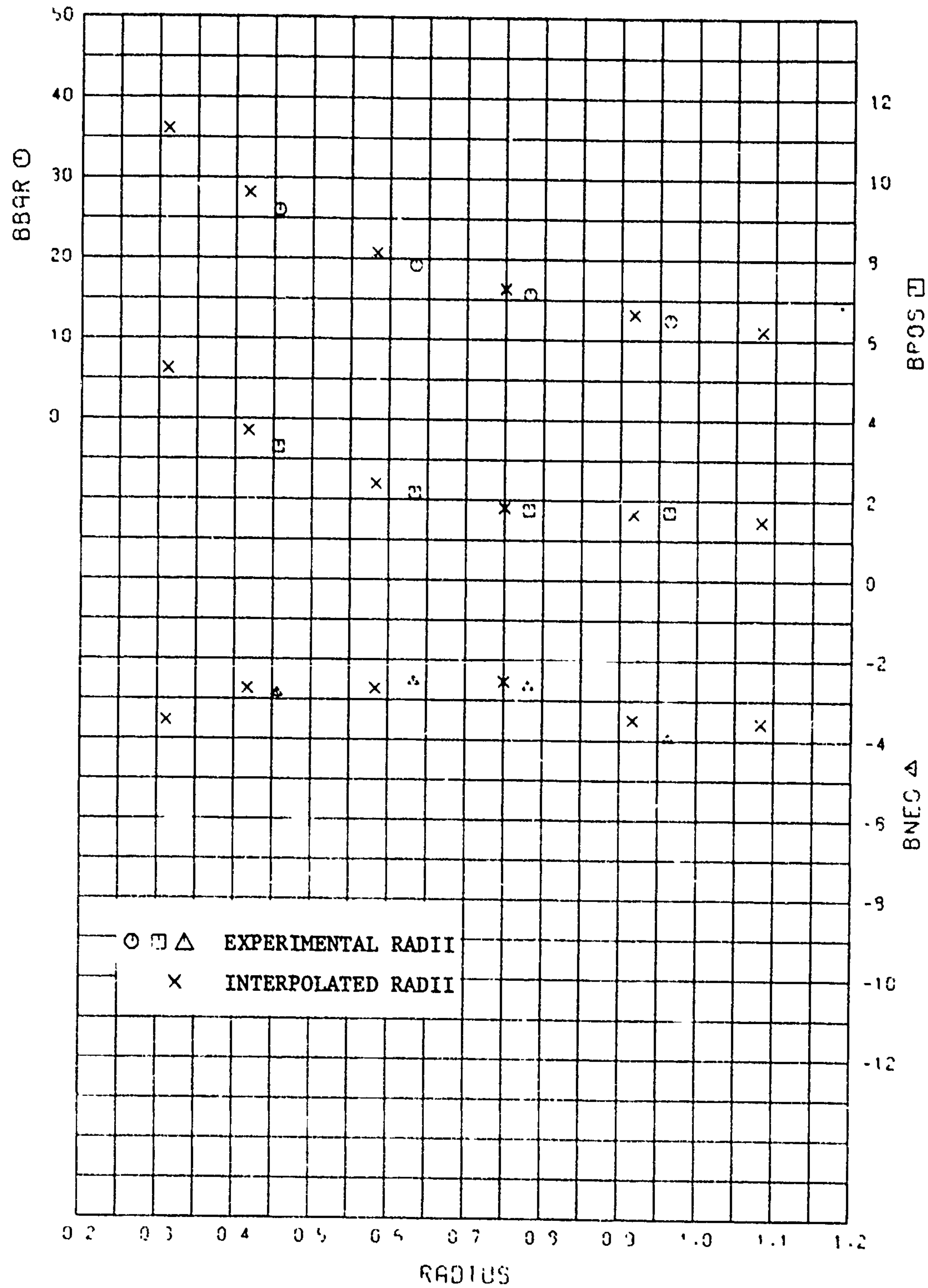

Figure A-6 - Radial Distribution of the Mean Advance Angle and Advance Angle Variations from the Transverse Wake Survey at the Forward Rake Location with an Operating Propeller

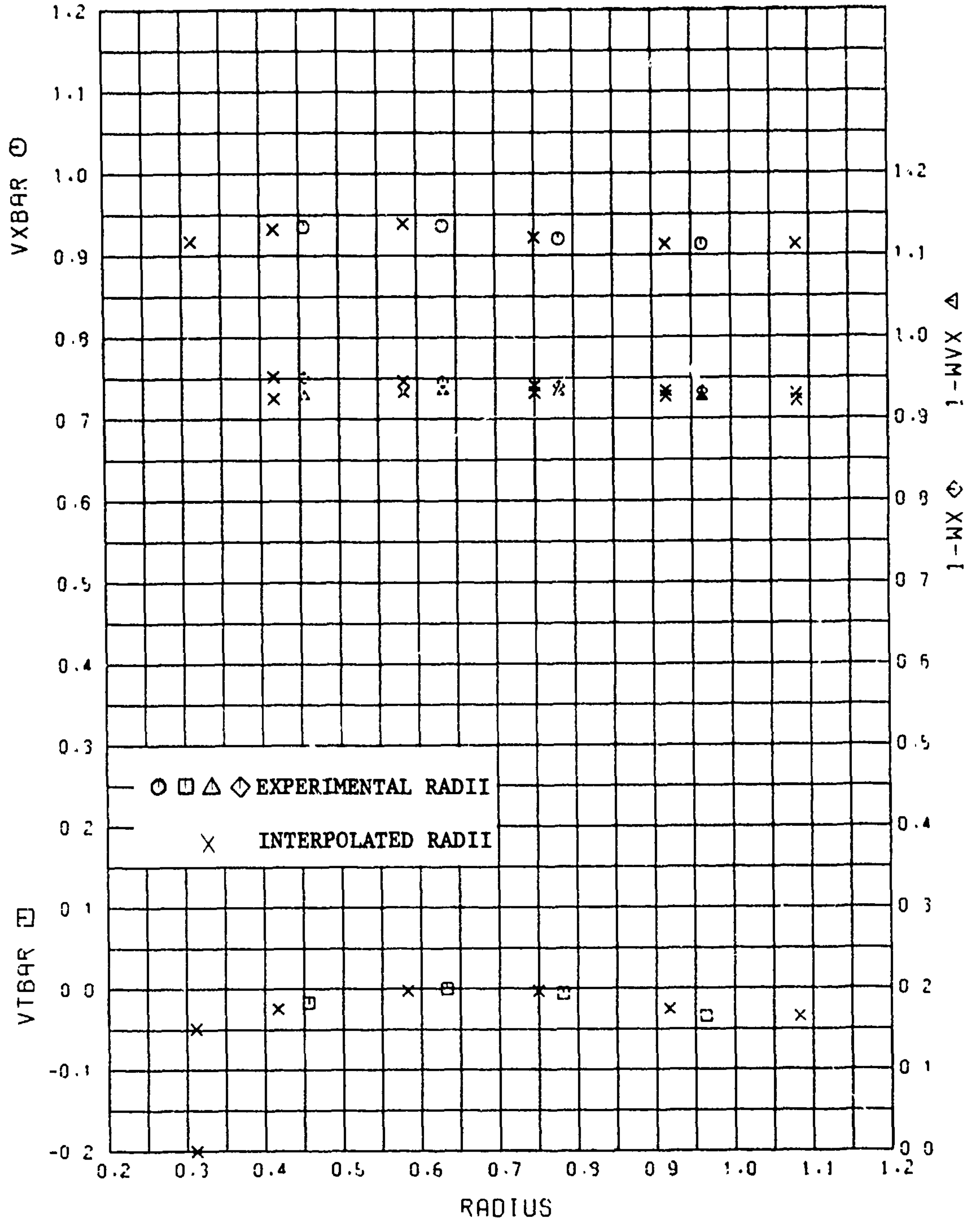

Figure A-7 - Radial Distribution of the Mean Velocity Component Ratios from the Transverse Wake Survey at the Forward Rake Location without an Operating Propeller

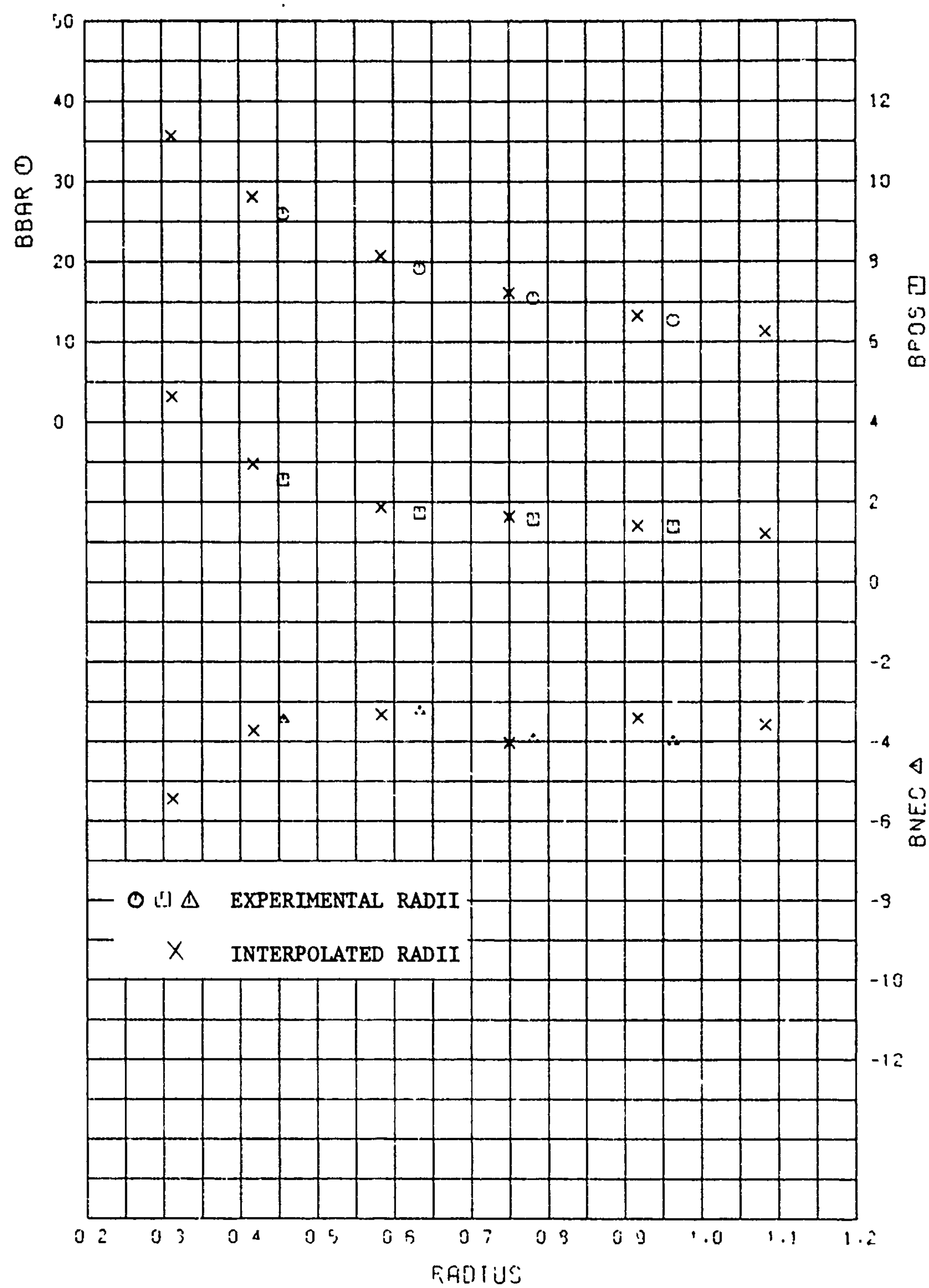

Figure A-8 - Radial Distribution of the Mean Advance Angle and Advance Angle Variations from the Transverse Wake Survey at the Forward Rake Location without an Operating Propeller

TABLE A-1

LISTING OF THE MEAN VELOCITY COMPONENT RATIOS, THE MEAN ADVANCE ANGLES AND OTHER DERIVED QUANTITIES AT THE EXPERIMENTAL AND INTERPOLATED RADII OF THE TRANSVERSE WAKE SURVEY WITH AN OPERATING PROPELLER

RADIUS =	.456	.633	.781	.963	.312	.417	.583	.750	.917	1.083
VXBAR =	.943	.944	.922	.898	.931	.941	.915	.935	.909	.898
VTBAR =	-.003	.016	-.001	-.033	-.050	-.013	.016	.003	-.024	-.033
VRBAR =	.002	.003	.008	.030	.007	.003	.002	.006	.023	.030
1-WVX =	.938	.943	.941	.931	0.000	.937	.932	.911	.934	.924
1-WX =	.959	.949	.945	.935	0.000	.961	.951	.945	.938	.929
BBAR =	25.98	19.22	15.68	12.48	36.11	28.13	20.76	[illegible]	13.20	11.12
BPOS =	3.31	2.17	1.75	1.71	5.26	3.71	2.40	1.81	1.66	1.48
THETA =	92.50	90.00	90.00	95.00	95.00	92.50	90.00	[illegible]	95.00	95.00
BNEG =	-2.85	-2.53	-2.65	-3.95	-3.53	-2.72	-2.71	-2.52	-3.48	-3.56
THETA =	270.00	270.00	357.50	342.50	230.00	270.00	270.00	[illegible]	345.00	342.50

VXBAR IS CIRCUMFERENTIAL MEAN LONGITUDINAL VELOCITY.
VTBAR IS CIRCUMFERENTIAL MEAN TANGENTIAL VELOCITY.
VRBAR IS CIRCUMFERENTIAL MEAN RADIAL VELOCITY.
1-WVX IS VOLUMETRIC MEAN WAKE VELOCITY WITHOUT TANGENTIAL CORRECTION.
1-WX IS VOLUMETRIC MEAN WAKE VELOCITY WITH TANGENTIAL CORRECTION
BBAR IS MEAN ANGLE OF ADVANCE.
BPOS IS VARIATION BETWEEN THE MAXIMUM AND MEAN ADVANCE ANGLES (DELTA BETA PLUS).
BNEG IS VARIATION BETWEEN THE MINIMUM AND MEAN ADVANCE ANGLES (DELTA BETA MINUS).
THETA IS ANGLE IN DEGREES AT WHICH CORRESPONDING BPOS OR BNEG OCCURS.

TABLE A-2

HARMONIC ANALYSES OF LONGITUDINAL VELOCITY COMPONENT RATIOS AT THE EXPERIMENTAL AND INTERPOLATED RADII OF THE TRANSVERSE WAKE SURVEY WITH AN OPERATING PROPELLER

HARMONIC =	1	2	3	4	5	6	7	8
RADIUS = .456								
AMPLITUDE =	.0154	.0061	.0106	.0101	.0076	.0027	.0021	.0019
PHASE ANGLE =	331.2	355.1	247.6	274.3	322.2	291.2	216.4	298.3
RADIUS = .633								
AMPLITUDE =	.0357	.0151	.0192	.0191	.0122	.0033	.0034	.0029
PHASE ANGLE =	299.9	311.8	265.7	277.4	317.2	337.2	224.3	317.3
RADIUS = .781								
AMPLITUDE =	.0674	.0368	.0247	.0217	.0121	.0054	.0029	.0014
PHASE ANGLE =	292.2	302.1	284.1	288.8	335.4	44.8	200.4	293.6
RADIUS = .963								
AMPLITUDE =	.1218	.0820	.0439	.0269	.0163	.0127	.0102	.0041
PHASE ANGLE =	288.7	301.4	302.3	314.4	356.1	79.4	111.3	2.0
RADIUS = .312								
AMPLITUDE =	.0137	.0091	.0012	.0038	.0054	.0017	.0020	.0036
PHASE ANGLE =	2.2	345.4	149.0	51.2	54.6	167.1	113.3	247.9
RADIUS = .417								
AMPLITUDE =	.0139	.0063	.0081	.00[illegible]1	.0060	.0021	.0016	.0020
PHASE ANGLE =	342.1	359.3	242.9	277.6	332.4	279.7	202.4	282.0
RADIUS = .583								
AMPLITUDE =	.0279	.0106	.017[illegible]	.01[illegible]3	.0116	.0034	.0033	.0025
PHASE ANGLE =	305.2	320.1	260.3	275.2	3[illegible].3	320.1	226.1	320.1
RADIUS = .750								
AMPLITUDE =	.0598	.0311	.0229	.0212	.0118	.0046	.0032	.0043
PHASE ANGLE =	293.2	302.9	280.0	285.5	331.2	34.2	215.1	292.6
RADIUS = .917								
AMPLITUDE =	.1064	.0686	.03[illegible]	.0[illegible]0	.0147	.0105	.0069	.0036
PHASE ANGLE =	289.3	301.3	2[illegible]8.9	307.4	351.9	73.5	119.6	[illegible]
RADIUS = 1.083								
AMPLITUDE =	.1218	.0820	.0439	.02[illegible]	.0163	.0127	.0102	.0011
PHASE ANGLE =	288.7	301.4	302.3	314.4	356.1	79.4	111.3	2.0

TABLE A-2 CONTINUED

MODEL 5366 TRANSVERSE WAKE SURVEY EXP 2 WITH PROPELLER

HARMONIC ANALYSES OF LONGITUDINAL VELOCITY COMPONENT RATIOS (VX/V)

HARMONIC =	9	10	11	12	13	14	15	16
RADIUS = .456								
AMPLITUDE =	.0013	.0008	.0009	.0011	.0001	.0004	.0002	.0004
PHASE ANGLE =	324.3	135.5	192.2	251.4	330.3	123.2	225.2	73.6
RADIUS = .633								
AMPLITUDE =	.0041	.0005	.0024	.0025	.0014	.0005	.0009	.0007
PHASE ANGLE =	351.2	104.3	210.4	270.7	302.8	99.6	181.9	222.9
RADIUS = .781								
AMPLITUDE =	.0058	.0008	.0031	.0019	.0027	.0015	.0018	.0018
PHASE ANGLE =	345.4	324.3	213.0	293.6	3.9	103.3	183.5	269.9
RADIUS = .963								
AMPLITUDE =	.0071	.0049	.0021	.0030	.0019	.0019	.0027	.0018
PHASE ANGLE =	6.2	79.0	138.5	298.1	353.0	128.0	199.6	265.8
RADIUS = .312								
AMPLITUDE =	.0028	.0006	.0012	.0021	.0032	.0012	.0005	.0017
PHASE ANGLE =	220.5	214.9	58.9	96.9	74.0	123.4	291.0	17.3
RADIUS = .417								
AMPLITUDE =	.0010	.0007	.0005	.0025	.0006	.0005	.0002	.0006
PHASE ANGLE =	285.8	145.9	167.0	223.5	70.3	124.8	257.3	47.8
RADIUS = .583								
AMPLITUDE =	.0034	.0007	.0020	.0023	.0012	.0003	.0007	.0005
PHASE ANGLE =	350.8	115.5	208.6	266.9	289.0	102.1	183.9	197.7
RADIUS = .750								
AMPLITUDE =	.0055	.0008	.0031	.0019	.0024	.0014	.0016	.0016
PHASE ANGLE =	344.4	308.8	214.6	289.2	.5	101.1	181.8	267.7
RADIUS = .917								
AMPLITUDE =	.0067	.0029	.0020	.0025	.0024	.0019	.0024	.0019
PHASE ANGLE =	358.8	71.6	173.3	299.8	2.2	119.5	194.8	269.4
RADIUS = 1.083								
AMPLITUDE =	.0071	.0049	.0021	.0030	.0019	.0019	.0027	.0018
PHASE ANGLE =	6.2	79.0	138.5	298.1	353.0	128.0	199.6	265.8

TABLE A-3

HARMONIC ANALYSES OF TANGENTIAL VELOCITY COMPONENT RATIOS AT THE EXPERIMENTAL AND INTERPOLATED RADII OF THE TRANSVERSE WAKE SURVEY WITH AN OPERATING PROPELLER

HARMONIC =	1	2	3	4	5	6	7	8
RADIUS = .456								
AMPLITUDE =	.1678	.0129	.0302	.0152	.0074	.0094	.0047	.0011
PHASE ANGLE =	184.7	152.5	8.4	304.9	28.0	47.9	8.5	130.3
RADIUS = .633								
AMPLITUDE =	.2059	.0197	.0364	.0102	.0040	.0083	.0025	.0016
PHASE ANGLE =	179.1	241.2	358.1	6.4	351.0	29.5	46.6	287.6
RADIUS = .781								
AMPLITUDE =	.1850	.0181	.0392	.0124	.0009	.0067	.0035	.0022
PHASE ANGLE =	183.4	306.3	7.5	38.3	305.5	33.0	75.9	236.5
RADIUS = .963								
AMPLITUDE =	.1544	.0459	.0421	.0159	.0061	.0046	.0023	.0013
PHASE ANGLE =	197.6	339.3	8.7	10.7	349.6	70.1	148.4	161.4
RADIUS = .312								
AMPLITUDE =	.1006	.0464	.0293	[illegible]	.0125	.0116	.0084	.0060
PHASE ANGLE =	213.0	84.0	41.9	281.8	53.6	74.1	2.3	134.7
RADIUS = .417								
AMPLITUDE =	.1510	.0173	.0289	.0182	.0085	.0097	.0055	.0021
PHASE ANGLE =	188.5	120.0	15.2	296.3	35.8	54.6	5.6	131.3
RADIUS = .583								
AMPLITUDE =	.2021	.0185	.0349	[illegible]	.0049	.0086	.0027	.0012
PHASE ANGLE =	179.4	227.5	358.3	348.3	1.1	32.5	31.4	295.2
RADIUS = .750								
AMPLITUDE =	.1899	.0160	.0336	.0113	.0009	.0071	.0035	.0022
PHASE ANGLE =	182.1	292.1	6.3	36.9	313.5	31.1	71.0	243.0
RADIUS = .917								
AMPLITUDE =	.1619	.0373	.0415	.0115	.0038	.0049	.0024	.0015
PHASE ANGLE =	192.8	335.8	9.4	22.1	344.9	55.2	116.0	196.2
RADIUS = 1.083								
AMPLITUDE =	.1544	0459	.0421	.0159	.0061	.0046	.0023	.0013
PHASE ANGLE =	197.6	339.3	8.7	10 7	349.6	70.1	148.4	161.4

TABLE A-3 CONTINUED

MODEL 5366 TRANSVERSE WAKE SURVEY EXP 2 WITH PROPELLER

HARMONIC ANALYSES OF TANGENTIAL VELOCITY COMPONENT RATIOS (VT/V)

HARMONIC =	9	10	11	12	13	14	15	16
RADIUS = .456								
AMPLITUDE =	.0039	.0011	.0020	.0024	.0008	.0025	.0013	.0019
PHASE ANGLE =	144.2	104.9	95.9	127.6	116.0	132.4	116.3	126.5
RADIUS = .633								
AMPLITUDE =	.0012	.0017	.0020	.0013	.0020	.0007	.0016	.0011
PHASE ANGLE =	17.9	97.4	317.8	355.5	160.6	121.2	146.6	218.2
RADIUS = .781								
AMPLITUDE =	.0018	.0036	.0012	.0008	.0022	.0011	.0017	.0013
PHASE ANGLE =	356.1	73.6	120.8	47.0	107.4	100.6	55.0	119.8
RADIUS = .963								
AMPLITUDE =	.0045	.0063	.0045	.0047	.0052	.0043	.0026	.0025
PHASE ANGLE =	135.3	136.6	138.4	128.1	138.7	138.2	123.6	119.4
RADIUS = .312								
AMPLITUDE =	.0107	.0020	.0108	[illegible]	.0040	.0056	.0030	[illegible]
PHASE ANGLE =	152.5	65.8	110.9	138.9	32.6	130.5	36.7	100.3
RADIUS = .417								
AMPLITUDE =	.0055	.0011	.0038	.0048	.0011	.0032	.0014	.0028
PHASE ANGLE =	147.9	94.3	108.0	133.4	65.2	132.0	85.9	113.6
RADIUS = .583								
AMPLITUDE =	.0008	.0014	.0018	.0039	.0018	.0010	.0018	.0011
PHASE ANGLE =	69.0	106.6	323.9	9.6	165.0	129.1	150.1	210.3
RADIUS = .750								
AMPLITUDE =	.0020	.0034	.0006	.0039	.0019	.0009	.0015	.0010
PHASE ANGLE =	352.7	69.5	104.7	10.3	109.0	97.6	57.9	128.3
RADIUS = .917								
AMPLITUDE =	.0023	.0049	.0037	.0032	.0041	.0031	.0020	.0022
PHASE ANGLE =	124.6	119.5	135.7	123.5	129.6	132.7	98.1	[illegible]
RADIUS = 1.083								
AMPLITUDE =	.0045	.0063	.0045	.0017	.0052	.0043	.0026	.0025
PHASE ANGLE =	135.3	136.6	138.4	128.1	138.7	138.2	123.6	119.4

TABLE A-4

Listing of the Mean Velocity Component Ratios, the Mean Advance Angles and other Derived Quantities at the Experimental and the Interpolated Radii of the Transverse Wake Survey without an Operating Propeller

RADIUS =	.456	.633	.781	.963	.312	.417	.583	.750	.917	1.083
VXBAR =	.935	.936	.920	.913	.917	.932	.939	.922	.913	.313
VTBAR =	-.017	-.000	-.006	-.034	-.049	-.024	-.032	-.003	-.025	-.034
VRBAR =	.013	.012	.029	.031	.030	.016	.010	.027	.033	.031
1-WVX =	.928	.934	.932	.926	0.000	.925	.933	.932	.927	.922
1-WX =	.951	.946	.940	.933	0.000	.952	.917	.941	.934	.930
BBAR =	25.95	19.19	15.51	12.68	35.68	28.05	20.76	16.15	13.27	11.30
BPOS =	2.56	1.73	1.57	1.39	4.64	2.96	1.87	1.64	1.41	1.21
THETA =	90.00	70.00	75.00	120.00	90.00	90.00	70.00	75.00	107.50	120.00
BNEG =	-3.45	-3.23	-3.94	-3.99	-5.44	-3.72	-3.32	-3.03	-3.40	-3.58
THETA =	275.00	267.50	270.00	340.00	70.00	270.00	265.00	270.00	340.00	340.00

VXBAR IS CIRCUMFERENTIAL MEAN LONGITUDINAL VELOCITY.
VTBAR IS CIRCUMFERENTIAL MEAN TANGENTIAL VELOCITY.
VRBAR IS CIRCUMFERENTIAL MEAN RADIAL VELOCITY.
1-WVX IS VOLUMETRIC MEAN WAKE VELOCITY WITHOUT TANGENTIAL CORRECTION.
1-WX IS VOLUMETRIC MEAN WAKE VELOCITY WITH TANGENTIAL CORRECTION.
BBAR IS MEAN ANGLE OF ADVANCE.
BPOS IS VARIATION BETWEEN THE MAXIMUM AND MEAN ADVANCE ANGLES (DELTA BETA PLUS).
BNEG IS VARIATION BETWEEN THE MINIMUM AND MEAN ADVANCE ANGLES (DELTA BETA MINUS).
THETA IS ANGLE IN DEGREES AT WHICH CORRESPONDING BPOS OR BNEG OCCURS.

TABLE A-5

HARMONIC ANALYSES OF LONGITUDINAL VELOCITY COMPONENT RATIOS AT THE EXPERIMENTAL AND INTERPOLATED RADII OF THE TRANSVERSE WAKE SURVEY WITHOUT AN OPERATING PROPELLER

HARMONIC =	1	2	3	4	5	6	7	8
RADIUS = .456								
AMPLITUDE =	.0287	.0131	.0145	.0191	.0117	.0065	.0034	.0034
PHASE ANGLE =	314.7	69.3	243.7	293.0	348.3	56.4	189.6	283.3
RADIUS = .633								
AMPLITUDE =	.0454	.0109	.0183	.02[illegible]8	.0182	.0089	.0062	.00[illegible]2
PHASE ANGLE =	301.8	10.8	248.5	288.3	343.6	67.0	203.3	292.6
RADIUS = .781								
AMPLITUDE =	.0622	.0231	.0211	.0245	.0201	.0145	.0107	.0139
PHASE ANGLE =	306.1	307.9	275.5	300.1	357.8	85.7	190.6	287.2
RADIUS = .963								
AMPLITUDE =	.1253	.0634	.0362	.0303	.0174	.0188	.0127	.0056
PHASE ANGLE =	288.4	316.7	321.2	316.6	6.5	94.0	148.7	301.9
RADIUS = .312								
AMPLITUDE =	.0262	.0094	.0106	.0123	.0076	.0070	.0051	.0031
PHASE ANGLE =	355.4	101.0	2[illegible]3.1	340.0	55.6	78.0	115.2	172.2
RADIUS = .417								
AMPLITUDE =	.0262	.0128	.0131	.01[illegible]7	.0097	.0063	.0033	.0073
PHASE ANGLE =	323.1	76.3	248.5	299.2	356.4	59.5	176.[illegible]	267.1
RADIUS = .583								
AMPLITUDE =	.0403	.0112	.0176	.02[illegible]3	.0169	.0079	.0051	.0076
PHASE ANGLE =	302.5	35.2	243.7	287.2	342.0	61.0	205.3	293.1
RADIUS = .750								
AMPLITUDE =	.0565	.0183	.0204	.02[illegible]2	.0199	.0134	.010[illegible]	.0138
PHASE ANGLE =	307.9	310.2	267.9	297.5	355.6	83.3	194.5	287.3
RADIUS = .917								
AMPLITUDE =	.1040	.0511	.0302	.0298	.0187	.0181	.0119	.0091
PHASE ANGLE =	292.7	313.5	311.5	312.2	4.7	92.4	162.3	292.3
RADIUS = 1.083								
AMPLITUDE =	.1253	.0634	.0362	.0303	.0174	.0188	.0127	.0056
PHASE ANGLE =	288.4	316.7	321.2	316.6	6.5	94.0	148.7	301.9

TABLE A-5 CONTINUED

MODEL 5366 TRANSVERSE WAKE SURVEY EXP 3 WITHOUT PROPELLER

HARMONIC ANALYSES OF LONGITUDINAL VELOCITY COMPONENT RATIOS (VX,V)

HARMONIC =	9	10	11	12	13	14	15	16
RADIUS = .456								
AMPLITUDE =	.0022	.0023	.0013	.0014	.0013	.0007	.0012	.0017
PHASE ANGLE =	7.7	96.7	130.4	158.7	182.0	249.0	30.4	103.3
RADIUS = .633								
AMPLITUDE =	.0082	.0056	.0027	.0024	.0011	.0018	.0016	.0005
PHASE ANGLE =	9.8	88.1	192.5	281.1	50.4	143.8	206.9	290.8
RADIUS = .781								
AMPLITUDE =	.0141	.0120	.0094	.00[illegible]0	.0083	.0078	.005[illegible]	.0040
PHASE ANGLE =	8.2	88.3	184.2	274.6	6.1	85.5	167.1	261.5
RADIUS = .963								
AMPLITUDE =	.0115	.0124	.0076	.0017	.0047	.0055	.0051	.0015
PHASE ANGLE =	31.8	93.3	162.5	280.8	24.1	105.8	161.2	232.6
RADIUS = .312								
AMPLITUDE =	.0021	.0032	.0057	.0010	.0030	.0049	.0048	.0026
PHASE ANGLE =	205.8	104.8	142.9	197.4	328.7	40.8	75.2	138.0
RADIUS = .417								
AMPLITUDE =	.0010	.0022	.0021	.0019	.0009	.0006	.0019	.0020
PHASE ANGLE =	359.6	100.4	131.9	168.1	206.9	355.8	49.3	111.6
RADIUS = .583								
AMPLITUDE =	.0064	.0041	.0014	.0010	.0010	.0015	.0009	.0004
PHASE ANGLE =	10.1	88.9	191.6	277.6	130.4	184.7	236.1	64.5
RADIUS = .750								
AMPLITUDE =	.0135	.0111	.0080	.00[illegible]4	.0075	.0071	.0050	.0026
PHASE ANGLE =	7.2	88.0	185.7	2[illegible].6	[illegible].2	86.2	169.1	262.7
RADIUS = .917								
AMPLITUDE =	.0129	.0131	.0090	.00[illegible]1	.0068	.0071	.0058	.0027
PHASE ANGLE =	21.4	91.3	172.3	277.0	13.0	93.9	162.4	251.2
RADIUS = 1.083								
AMPLITUDE =	.0115	.0124	.0076	.0017	.0047	.0055	.0051	.0015
PHASE ANGLE =	31.8	93.3	162.5	280.8	24.1	105.8	161.2	232.6

TABLE A-6

HARMONIC ANALYSES OF TANGENTIAL VELOCITY COMPONENT RATIOS AT THE EXPERIMENTAL AND INTERPOLATED RADII OF THE TRANSVERSE WAKE SURVEY WITHOUT AN OPERATING PROPELLER

HARMONIC =	1	2	3	4	5	6	7	8
RADIUS = .456								
AMPLITUDE =	.1472	.0202	.0186	.0100	.0065	.0078	.0057	.0018
PHASE ANGLE =	182.4	108.9	14.2	353.7	25.9	33.3	28.7	69.5
RADIUS = .633								
AMPLITUDE =	.1755	.0108	.0116	.0116	.0077	.0039	.0039	.0042
PHASE ANGLE =	177.8	127.4	3.9	354.7	1.2	29.9	21.8	22.9
RADIUS = .781								
AMPLITUDE =	.1701	.0029	.0175	.0141	.0053	.0036	.0036	.0015
PHASE ANGLE =	181.7	12.5	10.8	357.9	0.5	30.0	59.7	28.8
RADIUS = .963								
AMPLITUDE =	.1432	.0248	.0272	.0156	.0085	.0036	.0055	.0023
PHASE ANGLE =	194.3	342.1	351.8	343.5	332.0	272.9	267.9	288.3
RADIUS = .312								
AMPLITUDE =	.1034	.0286	.0361	.0098	.0080	.0139	.0086	.0072
PHASE ANGLE =	201.5	84.8	21.1	356.3	85.6	34.9	49.0	173.4
RADIUS = .417								
AMPLITUDE =	.1364	.0221	.0223	.0098	.0062	.0092	.0063	.0018
PHASE ANGLE =	185.4	102.7	16.6	354.1	39.7	33.8	33.9	123.9
RADIUS = .583								
AMPLITUDE =	.1713	.0139	.0120	.0110	.0077	.0046	.0043	.0041
PHASE ANGLE =	178.0	124.3	5.3	354.0	3.8	30.9	19.5	25.8
RADIUS = .750								
AMPLITUDE =	.1726	.0022	.0162	.0137	.0056	.0049	.0041	.0020
PHASE ANGLE =	180.5	82.7	12.0	358.5	12.1	32.3	57.3	31.1
RADIUS = .917								
AMPLITUDE =	.1515	.0183	.0242	.0152	.0068	.0021	.0022	.0014
PHASE ANGLE =	189.9	341.8	357.6	348.8	341.7	306.1	277.9	295.3
RADIUS = 1.083								
AMPLITUDE =	.1432	.0248	.0272	.0156	.0085	.0036	.0055	.0023
PHASE ANGLE =	194.3	342.1	351.8	343.5	332.0	272.9	267.9	288.3

TABLE A-6 CONTINUED

MODEL 5366 TRANSVERSE WAKE URVEY EXP 3 WITHOUT PROPELLER

HARMONIC ANALYSES OF TANGENTIAL VELOCITY COMPONENT RATIOS (VT/V)

HARMONIC =	9	10	11	12	13	14	15	16
RADIUS = .456								
AMPLITUDE =	.0034	.0024	.0018	.0014	.0014	.0008	.0010	.0009
PHASE ANGLE =	112.6	117.9	102.9	167.3	157.9	138.2	121.8	152.3
RADIUS = .633								
AMPLITUDE =	.0016	.0030	.0020	.0006	.0020	.0015	.0015	.0007
PHASE ANGLE =	70.2	38.5	55.4	115.1	116.1	126.4	151.1	165.2
RADIUS = .781								
AMPLITUDE =	.0015	.0016	.0005	.0025	.0019	.0012	.0012	.0018
PHASE ANGLE =	162.6	25.0	87.7	[illegible]	112.4	65.5	168.2	65.9
RADIUS = .963								
AMPLITUDE =	.0037	.0017	.0034	.0035	.0036	.0017	.0023	.0025
PHASE ANGLE =	254.0	137.6	130.4	142.0	127.1	151.6	134.3	135.5
RADIUS = .312								
AMPLITUDE =	.0079	.0079	.0040	.0036	.0024	.0015	.0009	.0023
PHASE ANGLE =	142.6	169.6	167.9	151.7	222.8	329.0	10.1	83.5
RADIUS = .417								
AMPLITUDE =	.0043	.0033	.0020	.0019	.0014	.0003	.0007	.0010
PHASE ANGLE =	123.3	141.8	126.1	163.0	178.5	132.6	106.0	128.8
RADIUS = .583								
AMPLITUDE =	.0020	.0028	.0021	.0005	.0019	.0015	.0014	.0009
PHASE ANGLE =	75.7	47.9	60.6	148.5	121.4	132.6	144.2	178.[illegible]
RADIUS = .750								
AMPLITUDE =	.0015	.0019	.0006	.0023	.0018	.0012	.0012	.0016
PHASE ANGLE =	145.2	25.2	61.7	[illegible]	111.2	69.2	187.7	64.1
RADIUS = .917								
AMPLITUDE =	.0027	.0009	.0023	.0032	.0029	.0011	.0017	.0020
PHASE ANGLE =	237.7	116.0	132.1	126.8	123.6	124.9	148.4	110.0
RADIUS = 1 083								
AMPLITUDE =	.0037	.0017	.0034	.0035	.0036	.0017	.0023	.0025
PHASE ANGLE =	254.0	137.6	130.4	142.0	127.1	151.6	134.3	135.5

APPENDIX B

VELOCITY COMPONENT RATIOS AND HARMONIC ANALYSIS OF THE ROTATIONAL WAKE SURVEY

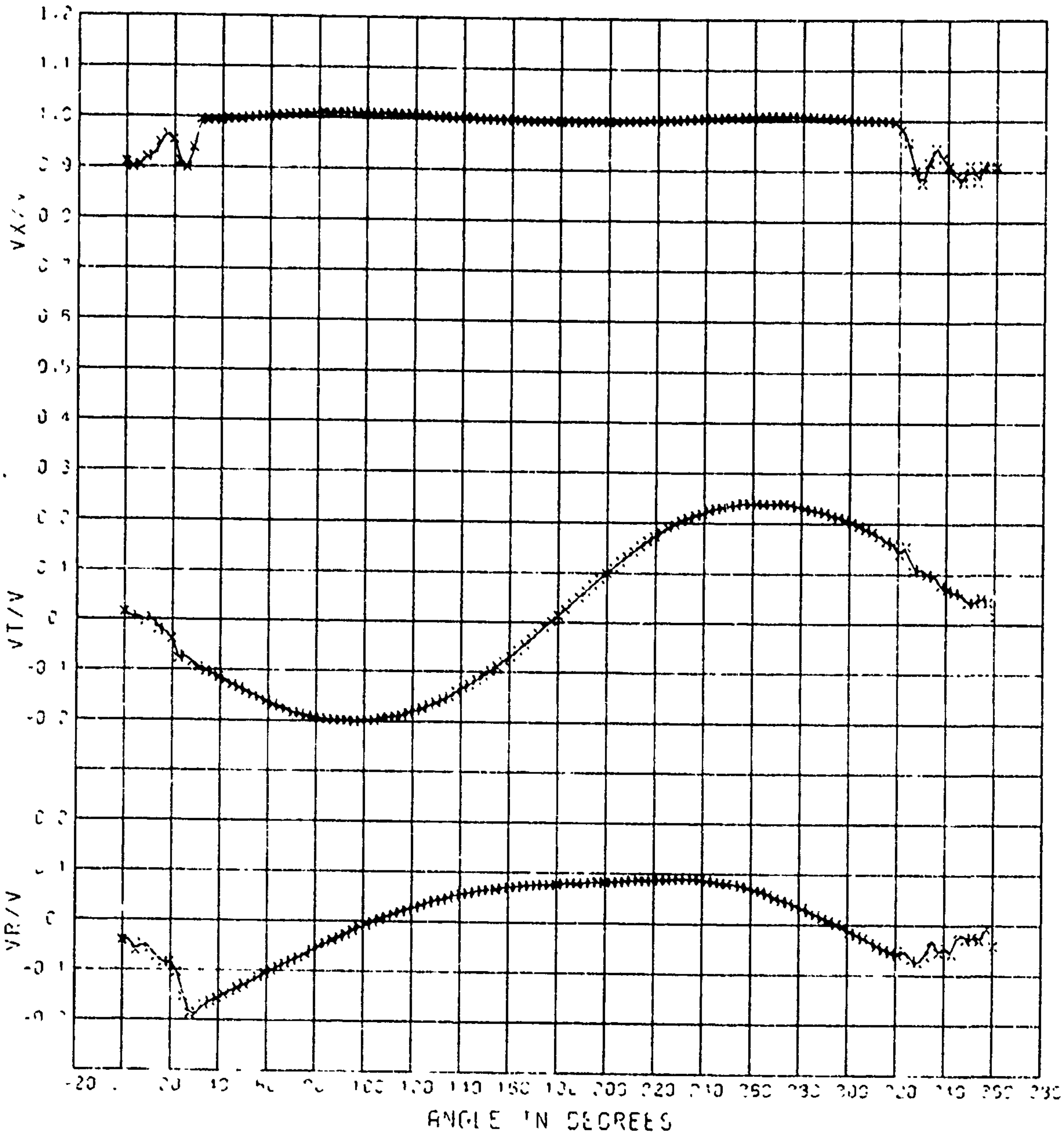

Figure B-1 - Velocity Component Ratios for Model 5366 from the Rotational Wake Survey at the Propeller Rake Location for the 0.456 Radius

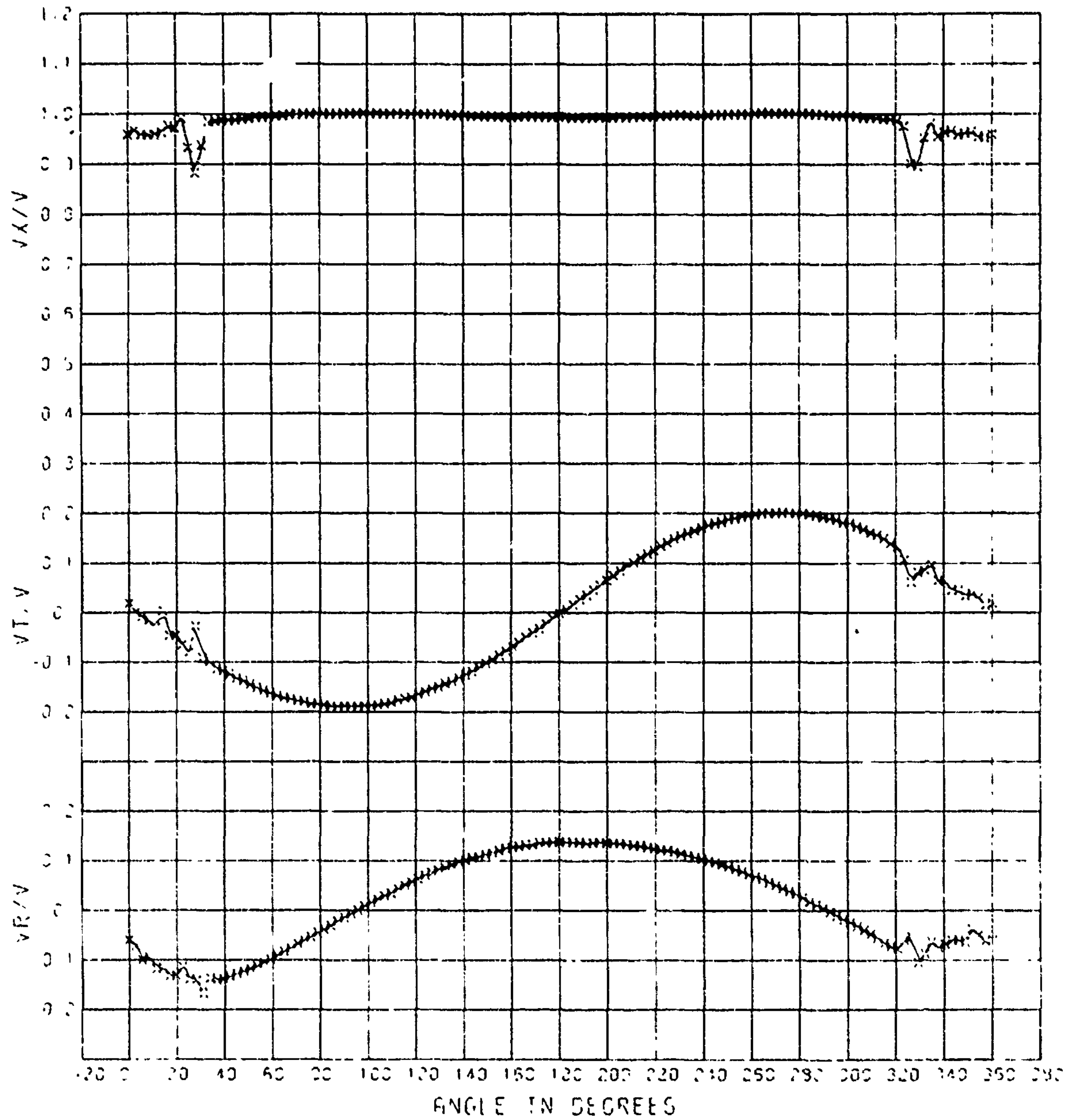

Figure B-2 - Velocity Component Ratios for Model 5366 from the Rotational Wake Survey at the Propeller Rake Location for the 0.633 Radius

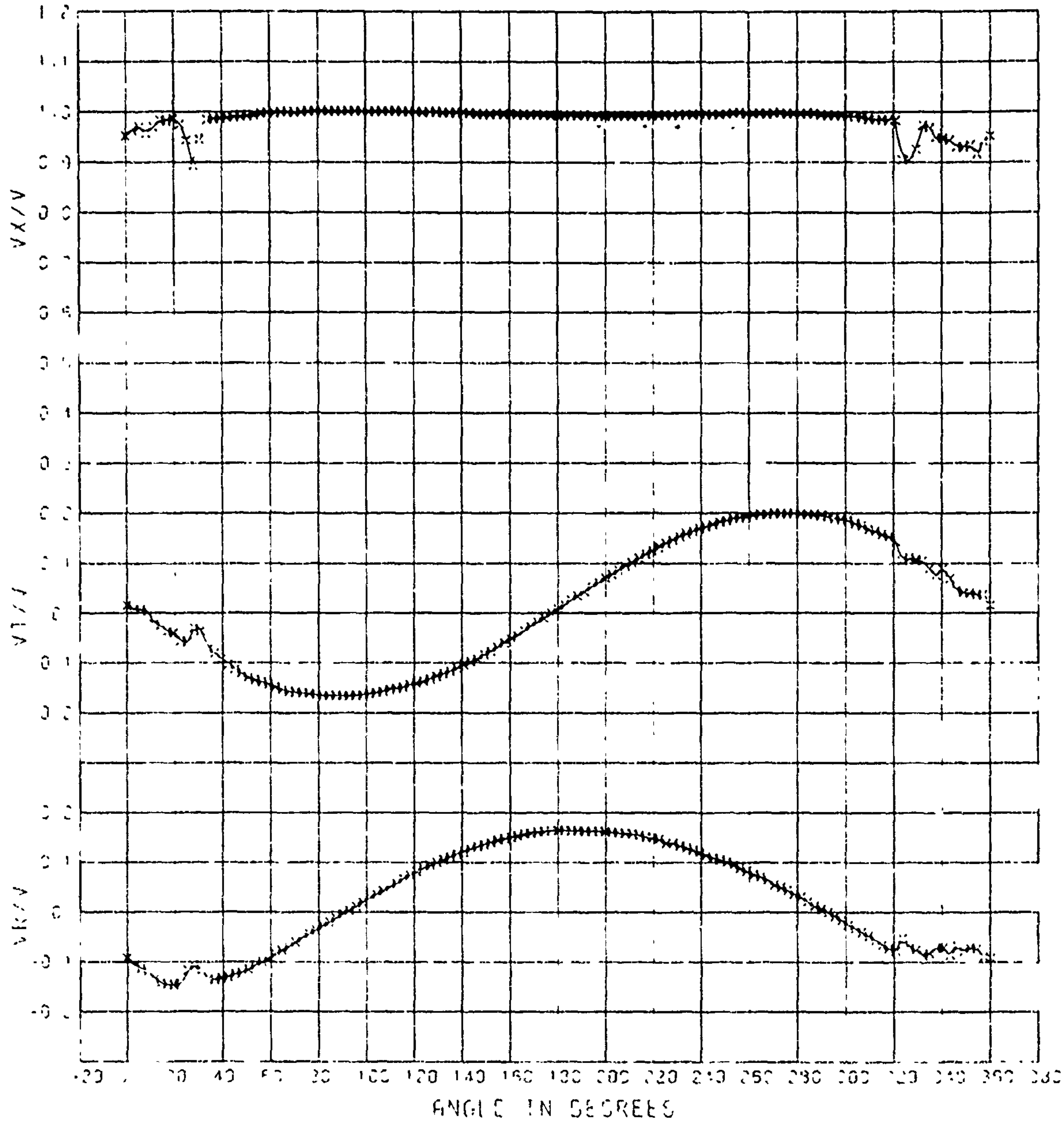

Figure B-3 - Velocity Component Ratios for Model 5366 from the Rotational Wake Survey at the Propeller Rake Location for the 0.781 Radius

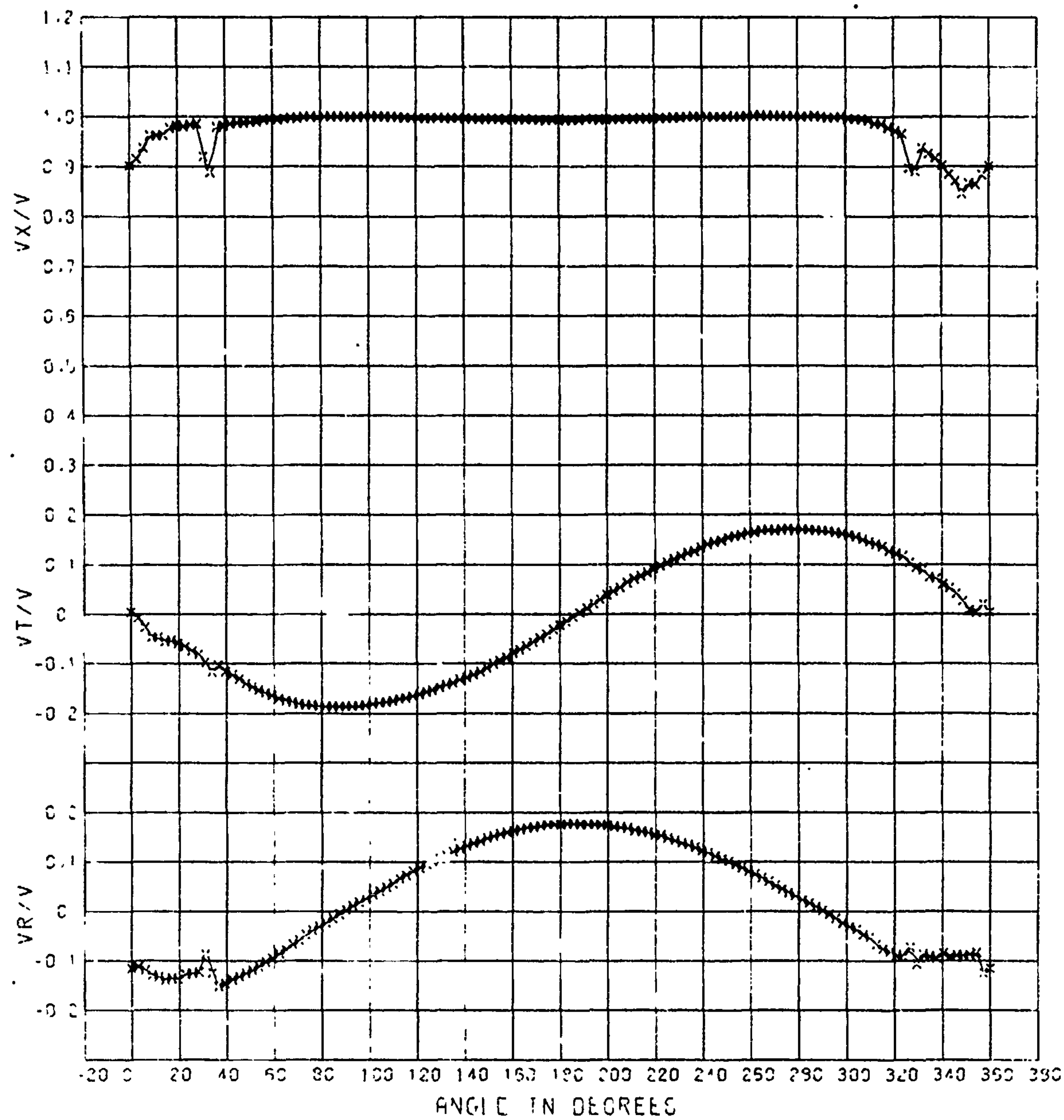

Figure B-4 - Velocity Component Ratios for Model 5366 from the Rotational Wake Survey at the Propeller Rake Location for the 0.963 Radius

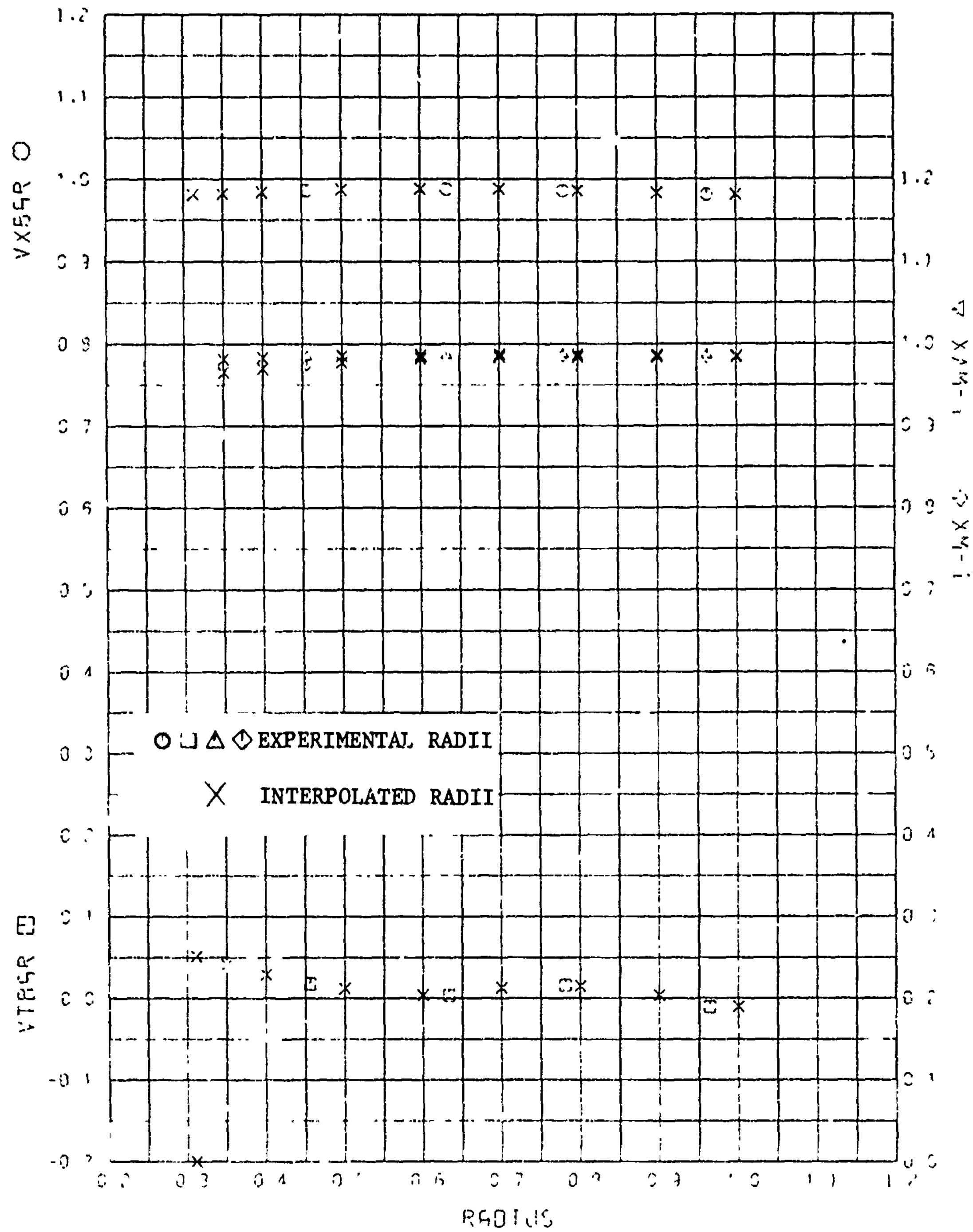

Figure B-5 - Radial Distribution of the Mean Velocity Component Ratios from the Rotational Wake Survey at the Propeller Rake Location

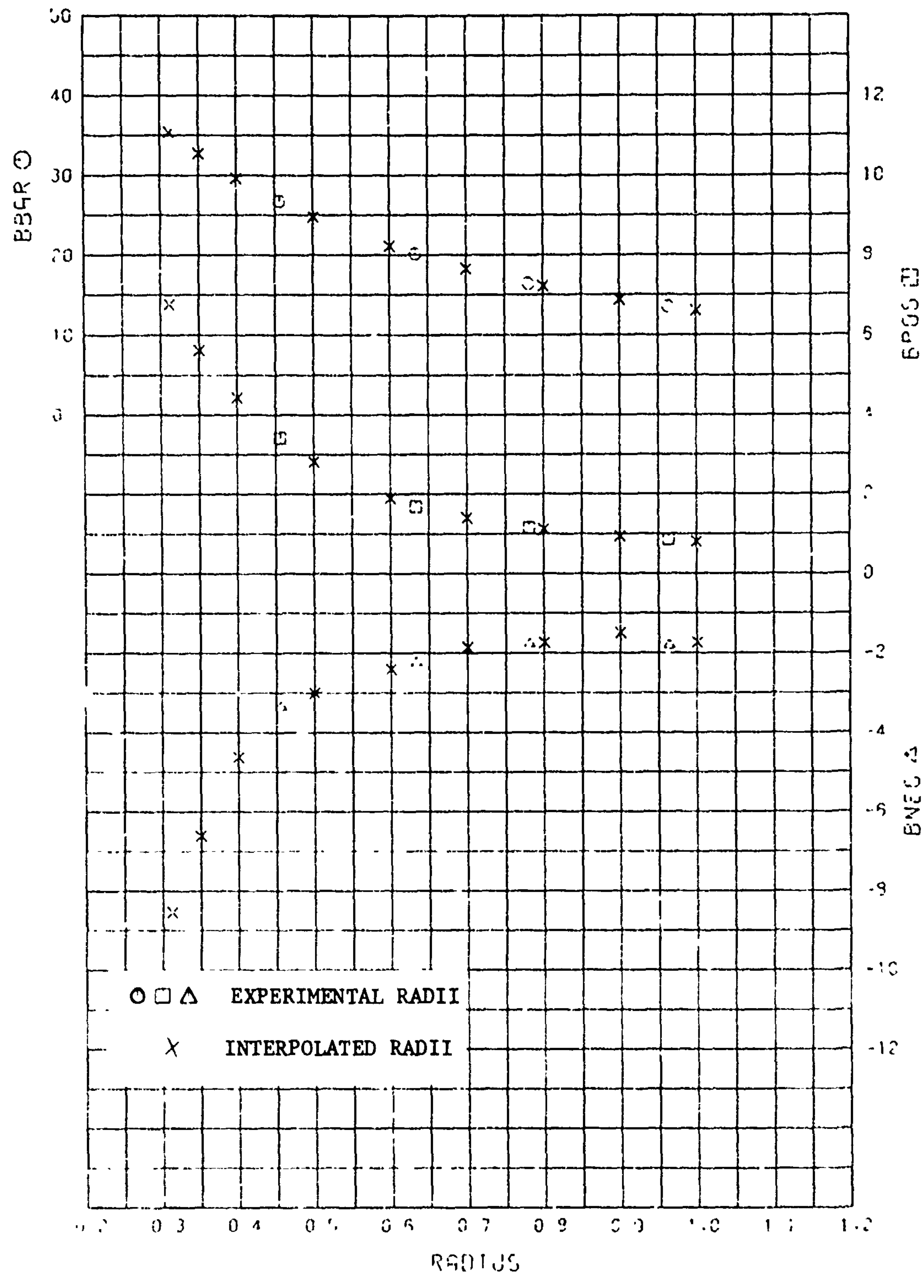

Figure B-6 – Radial Distribution of the Mean Advance Angle and Advance Angle Variations from the Rotational Wake Survey at the Propeller Rake Location

TABLE B-1

LISTING OF THE MEAN VELOCITY COMPONENT RATIOS, THE MEAN ADVANCE ANGLES AND OTHER DERIVED QUANTITIES AT THE EXPERIMENTAL AND INTERPOLATED RADII OF THE ROTATIONAL WAKE SURVEY

RADII	=	.456	.633	.781	.963	.312	.350	.400	.500	.600	.700	.800	.900	1.000
VXBAR	=	.986	.988	.986	.981	.981	.982	.984	.987	.988	.988	.986	.983	.981
VTBAR	=	.018	.004	.016	-.010	.052	.041	.029	.012	.004	.013	.015	.004	-.010
VRBAR	=	.001	.015	.024	.025	-.014	-.010	-.005	.005	.013	.020	.025	.026	.025
1-WVX	=	.984	.986	.987	.986	0.000	.981	.983	.985	.986	.987	.987	.986	.985
1-WX	=	.974	.983	.985	.984	0.000	.965	.970	.977	.982	.984	.984	.984	.984
BBAR	=	26.75	20.14	16.47	13.51	35.42	32.71	29.65	24.79	21.15	18.29	16.10	14.40	13.03
BPOS	=	3.41	1.68	1.16	.85	6.76	5.62	4.43	2.81	1.89	1.40	1.12	.93	.80
THETA	=	92.50	92.50	87.50	82.50	92.50	92.50	92.50	92.50	92.50	92.50	87.50	87.50	82.50
BNEG	=	-3.35	-2.24	-1.77	-1.81	-8.55	-6.61	-4.63	-3.00	-2.40	-1.86	-1.74	-1.50	-1.74
THETA	=	330.00	327.50	325.00	347.50	345.00	345.00	345.00	327.50	327.50	327.50	325.00	347.50	347.50

VXBAR IS CIRCUMFERENTIAL MEAN LONGITUDINAL VELOCITY.
VTBAR IS CIRCUMFERENTIAL MEAN TANGENTIAL VELOCITY.
VRBAR IS CIRCUMFERENTIAL MEAN RADIAL VELOCITY.
1-WVX IS VOLUMETRIC MEAN WAKE VELOCITY WITHOUT TANGENTIAL CORRECTION.
1-WX IS VOLUMETRIC MEAN WAKE VELOCITY WITH TANGENTIAL CORRECTION.
BBAR IS MEAN ANGLE OF ADVANCE.
BPOS IS VARIATION BETWEEN THE MAXIMUM AND MEAN ADVANCE ANGLES (DELTA BETA PLUS).
BNEG IS VARIATION BETWEEN THE MINIMUM AND MEAN ADVANCE ANGLES (DELTA BETA MINUS).
THETA IS ANGLE IN DEGREES AT WHICH CORRESPONDING BPOS OR BNEG OCCURS.

TABLE B-2

HARMONIC ANALYSES OF LONGITUDINAL VELOCITY COMPONENT RATIOS AT THE EXPERIMENTAL RADII OF THE ROTATIONAL WAKE SURVEY

HARMONIC =	1	2	3	4	5	6	7	8
RADIUS = .456								
AMPLITUDE =	.030[illegible]	.0303	.0171	.0098	.0045	.0025	.0035	.0036
PHASE ANGLE =	276.9	277.7	289.9	304.2	329.1	43.6	91.3	108.2
RADIUS = .633								
AMPLITUDE =	.0162	.0148	.0051	.0006	.0035	.0047	.0040	.0027
PHASE ANGLE =	272.7	271.3	283.5	34.6	89.3	96.1	100.8	110.4
RADIUS = .781								
AMPLITUDE =	.0191	.0162	.0072	.0031	.0034	.0040	.0031	.0019
PHASE ANGLE =	283.7	281.1	303.1	350.9	46.5	64.1	61.2	34.3
RADIUS = .963								
AMPLITUDE =	.0294	.0264	.0162	.0113	.0097	.0084	.0069	.0055
PHASE ANGLE =	275.2	284.0	302.2	327.4	352.0	6.1	7.2	353.9
HARMONIC =	9	10	11	12	13	14	15	16
RADIUS = .456								
AMPLITUDE =	.0022	.0003	.0026	.0038	.0041	.0030	.0006	.0019
PHASE ANGLE =	120.7	241.4	299.9	311.7	315.7	318.7	326.6	150.4
RADIUS = .633								
AMPLITUDE =	.0004	.0027	.0045	[illegible]	.0043	.0022	.0004	.0029
PHASE ANGLE =	219.8	278.7	286.7	[illegible]	291.1	289.5	118.2	120.3
RADIUS = .781								
AMPLITUDE =	.0024	.0043	.0053	[illegible]	.0036	.0014	.0016	.0037
PHASE ANGLE =	333.3	316.7	314.5	[illegible]	325.6	340.8	122.2	132.4
RADIUS = .963								
AMPLITUDE =	.0047	.0049	.0047	.0035	.0014	.0013	.0032	.0042
PHASE ANGLE =	327.6	305.7	296.9	288.2	292.6	60.7	83.4	84.3

TABLE B-3

HARMONIC ANALYSES OF LONGITUDINAL VELOCITY COMPONENT RATIOS AT THE INTERPOLATED RADII OF THE ROTATIONAL WAKE SURVEY

HARMONIC =	1	2	3	4	5	6	7	8
RADIUS = .312								
AMPLITUDE =	.0556	.0571	.0388	.0276	.0175	.0087	.0036	.0036
PHASE ANGLE =	282.3	283.0	294.4	305.3	313.8	331.0	28.9	74.0
RADIUS = .350								
AMPLITUDE =	.0476	.0487	.0320	.0220	.0134	.0062	.0031	.0035
PHASE ANGLE =	281.1	281.9	293.5	305.0	315.2	337.6	48.6	86.1
RADIUS = .400								
AMPLITUDE =	.0385	.0392	.0243	.0156	.0087	.0036	.0031	.0035
PHASE ANGLE =	279.3	280.1	292.1	304.5	318.7	356.2	73.4	98.8
RADIUS = .500								
AMPLITUDE =	.0249	.0247	.0127	.0061	.0022	.0030	.0039	.0035
PHASE ANGLE =	275.0	275.6	287.8	304.5	356.5	76.2	98.8	112.6
RADIUS = .600								
AMPLITUDE =	.0174	.0163	.0061	.0009	.0030	.0045	.0041	.0030
PHASE ANGLE =	272.3	271.6	283.1	331.7	86.0	96.2	102.7	113.6
RADIUS = .700								
AMPLITUDE =	.0168	.0146	.0054	.0014	.0033	.0043	.0034	.0018
PHASE ANGLE =	280.5	276.3	295.4	15.6	78.1	87.8	89.3	86.0
RADIUS = .800								
AMPLITUDE =	.0198	.0168	.0079	.0037	.0036	.0041	.0032	.0021
PHASE ANGLE =	283.6	281.9	303.8	346.7	37.5	56.6	53.1	24.8
RADIUS = .900								
AMPLITUDE =	.0249	.0219	.0124	.0078	.0065	.0059	.0049	.0040
PHASE ANGLE =	279.5	284.0	303.7	332.4	2.6	19.7	18.6	359.7
RADIUS = 1.000								
AMPLITUDE =	.0294	.0264	.0162	.0113	.0097	.0084	.0069	.0055
PHASE ANGLE =	275.2	284.0	302.2	327.4	352.0	6.1	7.2	353.9

TABLE B-3 CONTINUED

MODEL 5366 R/V ATHENA DOUBLE MODEL

HARMONIC ANALYSES OF LONGITUDINAL VELOCITY COMPONENT RATIOS (VX/V)

HARMONIC =	9	10	11	12	13	14	15	16
RADIUS = .312								
AMPLITUDE =	.0045	.0037	.0039	.0059	.0066	.0052	.0011	.0033
PHASE ANGLE =	90.6	64.9	23.7	16.1	8.1	358.0	333.4	203.0
RADIUS = .350								
AMPLITUDE =	.0037	.0025	.0028	.0046	.0054	.0044	.0010	.0026
PHASE ANGLE =	97.4	67.6	7.9	2.4	356.6	349.3	330.7	193.5
RADIUS = .400								
AMPLITUDE =	.0029	.0010	.0022	.0038	.0044	.0035	.0008	.0021
PHASE ANGLE =	107.5	73.1	333.2	337.9	337.5	335.6	328.1	175.1
RADIUS = .500								
AMPLITUDE =	.0017	.0011	.0032	.0042	.0042	.0028	.0004	.0020
PHASE ANGLE =	132.3	255.4	288.2	298.8	302.9	306.7	328.2	135.1
RADIUS = .600								
AMPLITUDE =	.0006	.0024	.0043	.0051	.0044	.0024	.0002	.0027
PHASE ANGLE =	174.4	272.0	284.3	289.3	290.8	290.6	105.9	120.7
RADIUS = .700								
AMPLITUDE =	.0011	.0034	.0048	.0052	.0040	.0017	.0010	.0034
PHASE ANGLE =	327.7	305.7	305.2	307.0	311.0	310.4	131.7	132.8
RADIUS = .800								
AMPLITUDE =	.0027	.0045	.0053	.0051	.0035	.0013	.0017	.0037
PHASE ANGLE =	333.3	317.4	315.1	317.0	327.5	348.5	118.8	130.4
RADIUS = .900								
AMPLITUDE =	.0040	.0049	.0051	.0042	.0023	.0012	.0025	.0037
PHASE ANGLE =	330.5	313.9	309.6	309.1	325.2	31.5	97.2	107.6
RADIUS = 1.000								
AMPLITUDE =	.0047	.0049	.0047	.0035	.0014	.0013	.0032	.0042
PHASE ANGLE =	327.6	305.7	296.9	288 2	292.6	60.7	83.4	84.3

TABLE B-4

HARMONIC ANALYSES OF TANGENTIAL VELOCITY COMPONENT RATIOS AT THE EXPERIMENTAL RADII OF THE ROTATIONAL WAKE SURVEY

HARMONIC =	1	2	3	4	5	6	7	8
RADIUS = .456								
AMPLITUDE =	.2202	.0122	.0016	.0027	.0033	.0031	.0026	.0020
PHASE ANGLE =	180.0	350.1	99.7	11.6	46.3	57.2	59.7	57.9
RADIUS = .633								
AMPLITUDE =	.1942	.0036	.0032	.0046	.0038	.0023	.0005	.0012
PHASE ANGLE =	178.6	333.6	13.6	8.7	26.5	42.6	83.7	172.6
RADIUS = .781								
AMPLITUDE =	.1826	.0018	.0023	.0044	.0030	.0004	.0012	.0020
PHASE ANGLE =	178.1	247.1	346.8	343.7	332.3	324.1	191.7	169.7
RADIUS = .963								
AMPLITUDE =	.1797	.0062	.0009	.0028	.0019	.0007	.0006	.0004
PHASE ANGLE =	176.7	202.0	226.8	315.0	290.6	300.1	139.7	161.1

HARMONIC =	9	10	11	12	13	14	15	16
RADIUS = .456								
AMPLITUDE =	.0008	.0003	.0007	.0008	.0010	.0010	.0010	.0009
PHASE ANGLE =	36.7	320.9	282.9	253.7	245.1	233.4	227.8	206.4
RADIUS = .633								
AMPLITUDE =	.0015	.0015	.0009	.0006	.0009	.0014	.0014	.0011
PHASE ANGLE =	204.8	225.9	240.9	309.6	12.4	36.8	59.9	87.2
RADIUS = .781								
AMPLITUDE =	.0020	.0013	.0011	.0014	.0021	.0021	.0016	.0008
PHASE ANGLE =	161.1	138.0	92.9	54.2	35.8	26.0	17.2	15.8
RADIUS = .963								
AMPLITUDE =	.0003	.0003	.0005	.0006	.0009	.0010	.0011	.0014
PHASE ANGLE =	94.4	159.6	144.3	142.6	135.7	106.6	97.5	89.0

TABLE B-5

HARMONIC ANALYSES OF TANGENTIAL VELOCITY COMPONENT RATIOS AT THE INTERPOLATED RADII OF THE ROTATIONAL WAKE SURVEY

HARMONIC =	1	2	3	4	5	6	7	8
RADIUS = .312								
AMPLITUDE =	.2514	.0225	.0066	.0017	.0006	.0025	.0049	.0059
PHASE ANGLE =	181.5	352.5	166.2	245.4	112.9	82.0	62.9	47.7
RADIUS = .350								
AMPLITUDE =	.2423	.0195	.0048	.0009	.0014	.0027	.0042	.0047
PHASE ANGLE =	181.1	352.1	160.2	292.2	65.1	72.7	61.9	48.7
RADIUS = .400								
AMPLITUDE =	.2313	.0158	.0028	.0016	.0024	.0029	.0034	.0033
PHASE ANGLE =	180.6	351.4	144.9	357.8	52.5	64.0	60.7	51.2
RADIUS = .500								
AMPLITUDE =	.2125	.0096	.0017	.0035	.0037	.0030	.0020	.0012
PHASE ANGLE =	179.6	348.5	54.5	13.9	42.4	53.1	59.6	72.0
RADIUS = .600								
AMPLITUDE =	.1980	.0048	.0030	.0045	.0039	.0026	.0008	.0009
PHASE ANGLE =	178.8	340.0	18.7	11.2	31.7	45.3	[illegible]8.5	161.5
RADIUS = .700								
AMPLITUDE =	.1879	.0022	.0029	.0046	.0031	.0011	.0007	.0018
PHASE ANGLE =	178.5	312.7	.8	355.9	359.8	30.9	176.7	170.7
RADIUS = .800								
AMPLITUDE =	.1817	.0021	.0021	.0044	.0030	.0005	.0012	.0019
PHASE ANGLE =	178.0	234.5	343.2	341.1	327.2	305.0	192.0	169.5
RADIUS = .900								
AMPLITUDE =	.1793	.0045	.0010	.0036	.0026	.0008	.0009	.0013
PHASE ANGLE =	177.3	207.0	306.3	327.3	305.6	282.3	181.5	167.8
RADIUS = 1.000								
AMPLITUDE =	.1797	.0062	.0009	.0028	.0019	.0007	.0006	.0004
PHASE ANGLE =	176.7	202.0	226.8	315.0	290.6	300.1	139.7	161.1

TABLE B-5 CONTINUED

MODEL 5366 R/V ATHENA DOUBLE MODEL

HARMONIC ANALYSES OF TANGENTIAL VELOCITY COMPONENT RATIOS (VT/V)

HARMONIC =	9	10	11	12	13	14	15	16
RADIUS = .312								
AMPLITUDE =	.0049	.0040	.0021	.0007	.0025	.0043	.0051	.0040
PHASE ANGLE =	46.5	52.0	43.6	174.7	222.3	232.2	245.1	247.4
RADIUS = .350								
AMPLITUDE =	.0036	.0027	.0013	.0007	.0021	.0033	.0038	.0029
PHASE ANGLE =	44.9	49.1	33.6	203.8	225.8	231.9	243.1	243.1
RADIUS = .400								
AMPLITUDE =	.0022	.0013	.0006	.0007	.0015	.0022	.0024	.0018
PHASE ANGLE =	42.2	40.5	355.3	234.2	232.3	231.8	238.9	233.3
RADIUS = .500								
AMPLITUDE =	.0001	.0008	.0009	.0009	.0006	.0003	.0003	.0006
PHASE ANGLE =	317.8	252.3	263.3	264.3	266.7	248.5	175.7	158.5
RADIUS = .600								
AMPLITUDE =	.0012	.0015	.0011	.0007	.0007	.0011	.0012	.0010
PHASE ANGLE =	210.4	231.8	246.4	291.6	359.2	37.2	66.1	95.8
RADIUS = .700								
AMPLITUDE =	.0018	.0011	.0004	.0009	.0018	.0020	.0015	.0007
PHASE ANGLE =	175.9	176.8	121.0	35.4	27.9	26.8	29.3	43.7
RADIUS = .800								
AMPLITUDE =	.0020	.0013	.0012	.0014	.0020	.0021	.0015	.0008
PHASE ANGLE =	158.8	133.9	92.4	56.9	37.7	27.0	17.1	16.3
RADIUS = .900								
AMPLITUDE =	.0012	.0009	.0010	.0010	.0012	.0013	.0010	.0009
PHASE ANGLE =	146.0	126.9	101.1	78.7	61.0	47.4	42.4	57.2
RADIUS = 1.000								
AMPLITUDE =	.0003	.0003	.0005	.0006	.0009	.0010	.0011	.0014
PHASE ANGLE =	94.4	159.6	144.3	142.6	135.7	106.6	97.5	89.0

DAVID W. TAYLOR NAVAL SHIP RESEARCH
AND DEVELOPMENT CENTER

HEADQUARTERS
BETHESDA, MARYLAND 20084

ANNAPOLIS LABORATORY
ANNAPOLIS, MD 21402

CARDEROCK LABORATORY
BETHESDA, MD 20084

IN REPLY REFER TO:

1524:RBH
5605
21 July 1980

From: Commander, David W. Taylor Naval Ship R&D Center
To: Distribution List

Subj: Forwarding of Technical Report

Ref: (a) Conference at DTNSRDC between NAVSEA (05R) and DTNSRDC (Code 154) on 14 Jul 1977
(b) DTNSRDC ltr 1524:WMB:svc/9245 dtd 22 Jul 1977

Encl: (1) DTNSRDC Ship Performance Department Report DTNSRDC/SPD-0833-02 entitled, "Analysis of Wake Survey and Boundary Layer Measurements for the R/V ATHENA Represented by Model 5366 in the Anechoic Wind Tunnel," by R. Hurwitz and D. Jenkins (July 1980)

1. The results of the model boundary layer and wake survey experiments for the R/V ATHENA are forwarded herewith as enclosure (1) for your information and retention as requested in references (a) and (b).

R. J. Stenson

R. J. STENSON
Acting Head,
Ship Powering Division

1524:RBH
5605
21 July 1980

DISTRIBUTION LIST:
NAVSEA (31 copies)
CHONR (2)
USNA (2)
DTIC (12)
BUSTAND (Klebanoff (1))
US COAST GUARD (3)
U CALIFORNIA, BERKLEY (1)
CIT (4)
MIT (6)
U. MICHIGAN (6)
U. MINNESOTA SAFHL (3)
PENN STATE U., ARL (5)
SIT DAVIDSON LAB (4)
WEBB INST. (2)
BIRD-JOHNSON CO. (2)
HYDRONAUTICS (3)
LIPS (1)

DTNSRDC ISSUES THREE TYPES OF REPORTS

1. DTNSRDC REPORTS, A FORMAL SERIES, CONTAIN INFORMATION OF PERMANENT TECHNICAL VALUE. THEY CARRY A CONSECUTIVE NUMERICAL IDENTIFICATION REGARDLESS OF THEIR CLASSIFICATION OR THE ORIGINATING DEPARTMENT.

2. DEPARTMENTAL REPORTS, A SEMIFORMAL SERIES, CONTAIN INFORMATION OF A PRELIMINARY, TEMPORARY, OR PROPRIETARY NATURE OR OF LIMITED INTEREST OR SIGNIFICANCE. THEY CARRY A DEPARTMENTAL ALPHANUMERICAL IDENTIFICATION.

3. TECHNICAL MEMORANDA, AN INFORMAL SERIES, CONTAIN TECHNICAL DOCUMENTATION OF LIMITED USE AND INTEREST. THEY ARE PRIMARILY WORKING PAPERS INTENDED FOR INTERNAL USE. THEY CARRY AN IDENTIFYING NUMBER WHICH INDICATES THEIR TYPE AND THE NUMERICAL CODE OF THE ORIGINATING DEPARTMENT. ANY DISTRIBUTION OUTSIDE DTNSRDC MUST BE APPROVED BY THE HEAD OF THE ORIGINATING DEPARTMENT ON A CASE-BY-CASE BASIS.